CLIMATE CHANGE IMPACTS ON STREAMFLOW IN THE UPPER NORTH SASKATCHEWAN RIVER BASIN, ALBERTA

MICHAEL W. NEMETH

B.Sc., University of Lethbridge 2008

A Thesis
Submitted to the School of Graduate Studies
of the University of Lethbridge
in Partial Fulfillment of the
Requirements for the Degree

MASTER OF SCIENCE

Department of Geography
University of Lethbridge
LETHBRIDGE, ALBERTA, CANADA

Abstract

This research focuses on the estimation of the impacts of climate change on water yield, streamflow extremes, and the streamflow regimes in the Cline River Watershed, and consequently, water availability for hydropower generation in this area. The Cline River Watershed comprises the flow into Lake Abraham, the reservoir for Bighorn Dam, is part of the upper North Saskatchewan River basin (UNSRB).

This objective was achieved by parameterizing the ACRU agro-hydrological modelling system. After parameterization was complete, ACRU output was calibrated and verified against available observed data, including temperature, snow water equivalent, glacier mass balance, potential evapotranspiration, and streamflow data. After ACRU was properly verified, five selected climate change scenarios to estimate impacts of climate change in this area. Overall water yields are projected to increase over time. A large shift in seasonality is likely the biggest impact climate change will have on water resources in the Cline River Watershed.

Acknowledgements

First and foremost I would like to thank my family; my wife, my daughter, and my parents who have always supported me in my undergraduate and graduate studies; thank you as this wouldn't have been possible without your support.

This research was support by grants held by Dr. Stefan Kienzle from EPCOR and NSERC. Other financial support was provided by the University of Lethbridge. I would like to thank my supervisor Dr. Stefan Kienzle for all of his time and support on this project and patience with me, which truly made the difference to my learning and progress with this research. I would also like to thank my committee members; Dr. Jim Byrne for all his time and guidance with undergraduate and graduate work, Dr. Larry Flanagan for all his time and thoughts that helped me with several vegetation inputs and thesis improvements. As the external examiner, thank you to Dr. Greg Kiker for his thoughts and input which also helped improve this thesis.

I would also like to thank everyone in the Department of Geography that made both my degrees from the University of Lethbridge a success in many ways. Thank you to Ryan MacDonald and Mark Mueller for their help during this project on all the data processing and collection that was done in all the different stages of this project. A special thanks to Ken Perl, Hester Jiskoot, and Craig Coburn for their advice and continued support, and Margaret Cook and Dana Andrei for their administrative support. Thank you to the School of Graduate Studies for their support through the entire length of my program. Thank you to Alison Buckingham from Parks Canada, Mike Seneka, Jon Pedlar, Rick Pickering, Ernst Kerkhoven, and Randy Sweeny from Alberta Environment, Craig Smith from Environment Canada with the data acquisition.

Table of Contents

List of Figures

List of Tables

Chapter 1

Thesis Introduction

1.1 Introduction

Throughout the province of Alberta, there is increasing demand for water due to population growth, and an increasing demand from agriculture and industry. In contrast, the availability of future water resources is uncertain due to climate change, as declining streamflows, earlier spring runoffs, lower snow accumulations, and decreased glacial melt contributions are predicted impacts of climate change in mountain regions (Burn, 1994; Gan, 1998; Demuth and Pietroniro, 2003; Lapp et al., 2005; Sauchyn and Kulshreshtha, 2008). Several studies have shown that declining streamflows are expected to reduce water availability for irrigation, industrial and domestic use, as well as hydroelectric power generation (Gan, 1998; Rood et al., 2005; Byrne and Kienzle, 2008; Sauchyn and Kulshreshtha, 2008). Therefore, the understanding of watershed balances is essential for current and future water resources planning. The upper North Saskatchewan River basin (UNSRB) is important for hydroelectric power generation in Alberta (TransAlta, 2009), as it contains Alberta's two major hydroelectric facilities, - the Brazeau Dam, built in 1965 - and the Bighorn Dam, built in 1971, which created Lake Abraham, the largest reservoir in Alberta with a live storage volume of 420 million m^3. Together these dams produce enough energy to supply the equivalent of 114,500 Alberta households with electricity annually. The Bighorn Dam produces 408,000MWh of electricity annually, while the Brazeau Dam produces 397,000MWh annually (TransAlta, 2009). This study will investigate the impacts of possible future climate change on hydrological processes in the UNSRB, in particular the Cline River Watershed. This watershed not only feeds Lake Abraham for hydropower generation, but also produces approximately 40% of the streamflow at Edmonton, based on analysis of streamflow data downstream of Bighorn Dam.

The UNSRB makes up the headwaters for the North Saskatchewan River (NSR), which is fed from the alpine runoff and snowmelt, as well as from glacial melt from several glaciers on the eastern slopes of the Rocky Mountains, including Peyto Glacier and the Columbia Ice Fields. The NSR joins the South Saskatchewan River, where it becomes the Saskatchewan River, eventually flowing into Hudson's Bay in North Eastern Canada (Marsh, 2008). The UNSRB starts on the eastern slopes of the continental divide, with mountains exceeding 3000m in elevation and descending to sub-alpine forests at about 2000m in elevation, through foothills to open grassland at elevations of about 1000m (Bruce et al., 2003). The alpine head watersheds of the UNSRB produce more than 80% of the water that flows through the NSR system (Pentland et al., 2002).

The spatially constrained montane headwaters of the NSR are a particularly good location to examine physical scenarios related to climate change, and the impacts that these changes will have on future water availability. To properly investigate these impacts there is a need to apply a physically-based distributed hydrologic model to investigate climate change impacts (Bruce et al., 2003). Mountain environments are one of the most sensitive environments in the world to climate change, with increases in global temperatures expected to have impacts on sub-alpine vegetation distributions, retreat of glaciers or alteration of hydrological cycles, with the boreal mountain regions projected to be among the most affected (Nogués-Bravo et al., 2007).

Hydrological models coupled with climate change predictions can be used to determine hydrological effects of climate change in a region, as they provide a framework in order to conceptualize and examine the relationships between climate and the elements of the hydrological cycle within a watershed (Leavesley, 1994; Xu, 1999b). Combining Global Climate Model (GCM) output with a deterministic hydrological model containing physically based equations describing hydrological processes is the most practical and widely used approach to simulating impacts of climate change (Loukas et al., 2002). This approach is applied here to examine the

impacts of future climate change scenarios on streamflows, and subsequent water availability for hydropower generation in the UNSRB.

Models are simplifications of reality, but are an important tool in assessing future scenarios for water management strategies, if accurately parameterized and verified (Beven, 1989). Rigorous parameterization of a model is a crucial step to avoid problems during the model verification process (Refsgaard, 1997). Parameters should be assessed from field data, or should be estimated within a physically acceptable range for available data and literature sources (Kienzle and Schmidt, 2008). Hydrological models use observed meteorological data to model streamflow, and are often verified using observed streamflow or other measurable hydrological variables (Rosso, 1994; Brooks et al., 2006, Liu et al., 2009). A model should be able to reasonably reproduce historical streamflow records, in order to be used in climate change studies, and can only be applied with confidence once the model output has been verified against observed data (Loukas et al., 2002; Jewitt et al., 2004).

1.2 Research Objectives

The primary objective of this research is to estimate the impacts of climate change on water yield, streamflow extremes, and the streamflow regimes in the UNSRB, and consequently, water availability for hydropower generation in this area. The focus of this research in the UNSRB was on the potential impacts on streamflows into two major hydropower reservoirs: Lake Abraham, and Brazeau Reservoir. Due to time constraints, this thesis will focus on impacts on streamflows into Lake Abraham, which is situated at the outlet of the Cline River Watershed. To accomplish this primary objective, four main tasks were established:

1) the parameterization of the ACRU (Agricultural Catchments Research Unit) agro-hydrological modelling system (Schulze et al., 2004),

2) the verification of ACRU output against as many observed hydrological data sets as are available to establish a reliable simulated streamflow record for the baseline period 1961-1990,

3) select appropriate climate change scenarios to be used for impacts simulations, and

4) to perturb the baseline climatic record with projected changes in temperature and percent changes in precipitation from several GCMs, and consequently, simulate streamflow time series under future climate scenarios.

1.3 Thesis Structure

This thesis is divided into five chapters, beginning with this chapter which describes the thesis topic and main objectives. The second chapter comprises a detailed literature review with the most up to date literature available on the major concepts and important background information on various topics of this research. The third chapter, the first of two journal papers, explains the concepts of the ACRU model, the detailed parameterization of ACRU for the UNSRB, and the verification of ACRU output for several hydrological variables based on observed data from in and around the UNSRB. The fourth chapter, the second journal paper, presents the selected climate scenarios, the perturbation methods of the historical climate record, and results of climate change scenarios on the impacts on future inflows into Lake Abraham. The fifth and final chapter includes the summary and conclusions of this research, as well as recommendations for future research in this area. It should be noted that, due to the fact that Chapters 3 and 4 are written as stand-alone journal papers, there is some repetition in each of these chapters.

Chapter 2

Literature Review

2.1 Introduction

This chapter will review the current literature regarding global climate change and how it is expected to impact the global hydrological cycle, with a more detailed review of expected climate change impacts in central Alberta, especially in higher elevation areas. This will be done to establish a base of knowledge of how best to estimate climate change impacts on streamflows in the upper North Saskatchewan River basin (UNSRB), as well as some of the expected climate change impacts in this region. A review of the different types of hydrological models, as well as how hydrological modelling is used to model climate change impacts on streamflows, and why it is beneficial, will be discussed. Climate scenarios, General Circulation Models (GCMs), and methods of regionalizing or downscaling GCMs will also be reviewed, to provide a sound base for their use in determining future climate change impacts in this research.

2.2 Climate Change

2.2.1 Water Balance Equation

The global hydrological cycle, like most systems, is comprised of a series of inputs and outputs of a conservative quantity (water) that cannot be created or destroyed (Dingman, 2002). Hydrological models attempt to accurately predict the partitioning of water in the various pathways of the hydrological cycle. A simplification of the hydrological cycle is often expressed by the water balance equation, common to all hydrological models (Leavesley, 1994). The water balance is the most fundamental component of the hydrological cycle, and the water balance equation quantifies the balance of the hydrological input and outputs in the hydrological cycle. A simplistic version of the equation is shown below.

$$P + G_{in} - (Q + ET + G_{out}) = \Delta S \qquad \text{[Eq. 2.1]}$$

where P is precipitation (liquid and solid), G_{in} is groundwater inflow, Q is stream discharge, ET is evapotranspiration, G_{out} is groundwater outflow, and ΔS is the change in water storage (liquid and solid) in the system over time (Dingman, 2002). This simplified equation for a complex system is used as a logical framework for the assessment of climate change impacts on streamflow within a study area (Forbes, 2007).

2.2.2 Global Climate Change and the Hydrological Cycle

Global greenhouse gas (GHG) emissions such as carbon dioxide, methane, nitrous oxide, water vapor, and sulfate particles in the atmosphere due to anthropogenic activities have seen an increase of 70% between 1970 and 2004 (IPCC, 2007). These increases in GHGs contribute to the warming of the earth by increasing the amount of long wave solar radiation that the atmosphere can trap, causing a rise in the global average temperature. Recent evidence shows that most of the observed increase in global average temperatures over the last 50 years is attributable to observed increases in anthropogenic GHG concentrations (Barrow et al., 2005; IPCC, 2007). The most recent Intergovernmental Panel on Climate Change (IPCC) report gave several conclusions based on research on climate change observations. They predict that over the next two decades a warming of about 0.2°C per decade based on current SRES (Special Report on Emissions Scenarios) emission scenarios. Even if the concentrations of all GHGs are kept constant at 2000 levels, a warming of about 0.1°C per decade would be expected (IPCC, 2007).

It is widely acknowledged that global warming has, and will, greatly impact regions where winter snowpack and summer melt are the major sources of the total annual streamflow (Burn, 1994; Jasper et al., 2004, Byrne and Kienzle, 2008). These regions are expected to, and in some cases have already seen a distinct shift in the amounts of snow versus rain, as well as an earlier snowmelt resulting in changes in runoff patterns that could alter water availability during peak-demand periods (Burn, 1994; Frederick and Major, 1997; Lapp et al., 2005). It is suggested

that observed changes in streamflow (e.g. earlier spring streamflow peak) are strongly related to climatic changes, especially changes in temperature, as even moderate increases in temperature can affect snowmelt dominated watersheds (Stewart et al., 2005).

Changes in runoff can be attributed to changes in precipitation and evaporation, both of which are strongly influenced by changes in temperature. A study of climate change impacts in alpine watersheds by Jasper et al. (2004) showed results suggesting there has been an increase in evapotranspiration (ET), a strong trend of summertime soil moisture depletion, a reduction in the coverage and duration of snowpack, and a shift in the seasonal pattern of runoff, with earlier and reduced peaks due to snowmelt. As temperatures increase the vapor pressure deficit increases, which results in a decrease to relative humidity, and a rise in potential evapotranspiration (PET). A rise in PET will increase ET rates as available moisture levels permit. Mountain glaciers and snow cover on average have declined in both hemispheres. Increased winter runoff and earlier spring peak discharge in many glacier and snowmelt fed rivers are evidence that climate change is already affecting the hydrological system (IPCC, 2007; Rood et al., 2008).

2.2.3 Climate Change and the Regional Hydrological Balance

Climate change is expected to cause changes to hydrological processes around the world, including temperature, precipitation types and volumes, evapotranspiration, which ultimately impact streamflow. Decreased mountain snowpacks, increased winter runoff, reduced summer stream and river flows, and reduced snowmelt-derived streamflows are likely changes expected in the western Rocky Mountains (Stewart et al., 2005; IPCC, 2007; Byrne and Kienzle, 2008; Sauchyn and Kulshreshtha, 2008). Canada's location in the high latitudes means that it is likely to experience some of the largest changes in climate, in particular changes in temperature (Barrow et al., 2005).

2.3 Observations of Climate and Hydrology in Western Canada

2.3.1 Temperature

Temperatures in western North America have increased during the twentieth century, and are consistent with rising greenhouse gases. These increases in temperature are most likely to continue with the most evident increases in winter and spring temperatures (Mote et al., 2005). Since the mid 1960s, an increasing trend in mean annual temperatures in southwestern Canada has been detected, with the more pronounced changes exhibited in the winter and spring (Zhang et al., 2001). The mean annual temperature is thought to have increased primarily as a result of increased winter and spring temperatures. Regional studies have revealed that summer temperatures have been relatively unchanged over the past century, whereas winter and spring temperatures, especially minimum temperatures, have increased (Akinremi et al., 1999; Cayan et al., 2001).

2.3.2 Precipitation

Frontal cyclones account for the majority of precipitation in the colder seasons in the Canadian Rockies, while convective storms dominate the summer precipitation regime (Reinelt, 1970). The Rocky Mountain region in Alberta receives considerable volumes of snow in the winter, with nearly 85% of the area's total annual streamflow derived from this snowpack (Grant and Kahan, 1974). This snowpack supports the peak spring flow and provides a natural store of water that is released through the summer period, when warm and dry conditions increase human and ecological demands (Rood et al., 2008). Changes in the snowpack could greatly change the hydrological regime in basins where streamflow is snowmelt dominated. Mote et al (2005) found decreases of 15-30% in snow water equivalent (SWE) in the Canadian Rockies from observed SWE data collected between 1950 and 1997, and expect losses in the snowpack to continue with increases in temperatures. Increasing winter and spring temperatures would increase the ratio of rain to snow and, thereby, increase winter streamflows and diminish snowpacks (Leung et al.,

2004; Lapp et al., 2005; Mote et al., 2005; Byrne and Kienzle, 2008; Sauchyn and Kulshreshtha, 2008). Zhang et al (2000) found that, in the last half of the twentieth century, there was no significant change in spring precipitation amounts, but the ratio of snow to total precipitation significantly decreased. This is confirmed by Akinremi et al (2001) who found that, there was a 60% increase in the number of rainfall events in central Alberta during the first four months of the year.

2.3.3 Evapotranspiration and Soil Moisture

Increased temperatures and changes in precipitation regimes could result in changes to soil moisture and evapotranspiration rates, as with increasing temperatures there is a subsequent increase in the potential evapotranspiration (Zhang et al., 2001). With lower precipitation and a warmer surface the soil surface becomes drier. Many GCM models have shown a decline in mid-continental soil moisture due to an overall decrease in the precipitation with increased evapotranspiration (Levis et al., 2000). However, observations from various countries in the Northern Hemisphere show that pan evaporation has been gradually decreasing over the last fifty years, contrary to the belief that warming would cause increased evaporation (Barnett et al., 2005). Two expected trend arguments can help to explain this inconsistency. First, decreasing pan evaporation trends may be due to increasing of actual evapotranspiration in some areas while the potential evapotranspiration remains the same due to increases in available moisture. Second, it has been suggested that increased cloudiness and concentrations of atmospheric aerosols reduce surface energy available for evaporation, causing a decrease in pan evaporation (Barnett et al., 2005). Decreases in evapotranspiration can occur as the soil moisture decreases resulting in reduction in cloud formation and enhancement of surface warming from increases to solar radiation reaching the surface (Loaiciga et al., 1996).

2.3.4 Streamflow

Streamflow provides the water to many regions in the world for human and ecological use, and changes to streamflow, both in timing and magnitude, can greatly affect water users in those regions. The consistency of streamflows from the glaciated headwater areas of the UNSRB has declined since the mid-1900s (Demuth and Pietroniro, 2003). Changes in the hydrological regime of pristine or stable, unregulated basins, such as earlier spring melt, generally point to changes in climatic conditions and can be used as indicators of climate change detection (Zhang et al., 2001). Detecting and dealing with changes to streamflow brought on by climate or land use changes are important for water managers to plan and prepare for extreme periods of drought or flooding.

Of primary concern with climate warming is earlier spring melt, and decreases in late summer flows. Continued warming in late winter and spring would advance melting of the snowpack, resulting in earlier spring flows, which would result in reduced summer streamflows, especially in the late summer (Rood et al., 2008; Sauchyn and Kulshreshtha, 2008). Earlier warming of spring temperatures could contribute to an earlier spring runoff in two ways: earlier melt of snow pack, and an increase in the proportion of precipitation that falls as rain instead of snow. Shifts in earlier streamflow timing by one to four weeks in recent decades relative to conditions in the 1950s through the mid-1970s have already been observed (Stewart et al ., 2005). Observed impacts of earlier spring runoff are more established in the recent portion of the data record, which would be expected if the impacts are related to accelerated climatic change from greenhouse gases (Burn, 1994). Several studies in the Rocky Mountains (Barnett et al., 2005; Rood et al., 2005; Rood et al., 2008) have shown that annual flows have declined, winter flows (especially March) were often slightly increased (most likely the result of more rain on snow events), spring runoff and peak flows occurred earlier, and that early summer and autumn flows (July–October) declined at a rate of about 0.2% per year. These observed changes were greatest for the rivers that drain the east-slope of the Rocky Mountains toward the northern prairies

(Barnett et al., 2005). It is possible that the overall decreasing trends in streamflow may have been masked to some extent by increases in glacier melt over the last 25 years (Bruce et al., 2003).

2.4 Future Trends in Climate and Potential Regional Effects

Spatial patterns of climate change are less certain, but climate change, in particular changes in temperature, is expected to cause changes to hydrological processes around the world, with greater impacts expected in high-latitude regions of Canada, and in alpine areas that provide runoff to surrounding lower elevation areas (Zhang et al., 2001; Bonsal et al., 2003; Rood et al., 2005; Sauchyn and Kulshreshtha, 2008). Most studies based on GCM output agree that earlier spring runoffs and increased winter flows, lower summer and late fall streamflows, decreased glacial melt contributions, and lower snow accumulations can be expected under projected climate changes (Burn, 1994; Gan, 1998; Demuth and Pietroniro, 2003; Lapp et al., 2005; Sauchyn and Kulshreshtha, 2008).

A recent report on the impacts of climate change on Prairie Provinces (Byrne and Kienzle, 2008) illustrated various scenarios of projected climate change from 1961–1990 to the 2020s (2010–2039), 2050s (2040–2069) and 2080s (2070–2099). With the exception of a few scenarios for the 2020s, all seven models looked at forecasted climates that lie outside the range of natural variability with most of the projected increases in temperature and precipitation to occur in winter and spring for both forest and grassland regions.

2.4.1 Physiological Response of Vegetation

Climate warming due to increased levels of CO_2 could have an impact on climate systems in response to changing plant physiology. Higher potential vegetation productivity from increased heat and atmospheric CO_2 will be limited by available soil moisture which is expected to decrease (Sauchyn and Kulshreshtha, 2008). Observation in laboratories and field studies have shown that increases in concentrations of CO_2 can stimulate net photosynthesis and increase the

water use efficiency of most plants (Rosenberg et al., 1990; Levis et al., 2000), thereby decreasing evapotranspiration rates. This is often referred to as the ''CO_2 fertilization effect'' and is thought to generally reduce the transpiration through stomatal resistance of plants and their overall water use (Field et al., 1995; Levis et al., 2000). Effects of stomatal resistance are an important part of the evaporative processes in a heavily vegetated watershed. Stomatal resistance is one of the factors in the Penman-Monteith equation, which causes a reduction in evapotranspiration when increased, and an increase in evapotranspiration when decreased. Decreased water use from vegetation in response to CO_2 increases under climate warming is an important factor when assessing the water balance of a watershed, and when applying climate change scenarios in a region. Increased plant growth may increase factors such as leaf area index (LAI) and transpiring plant tissue, thereby offsetting decreases in plant water use (Frederick, 1997).

2.4.2 Affects of Forest Harvesting in UNSRB

Based on the generalized land cover from the National Land and Water Information Service (NLWI, 2008), approximately 62% of the UNSRB is forested. Calculations by Alberta Sustainable Resource Development indicate approximately 110km^2 of the forested area in the UNSRB is harvested each year. This number varies annually, but gives a good estimate to the average annual harvesting rate in the basin (Kevin Gange, Forest Health Officer, Alberta SRD, Personal Communication 2009). Based on these numbers, on average 1% of the forested areas of the UNSRB are harvested each year, with the same area of land in post-harvest recovery, which could take many decades to recover to pre-harvest conditions in mountainous, snow dominated catchments (Moore and Wondzell, 2005).

In general, forest harvesting increases the portion of precipitation available to become streamflow, decreases interception losses, reduces transpiration, decreases soil infiltration capacity (soil compaction), increases rates of snowmelt, and modifies the runoff pathways to

stream channels (Moore and Wondzell, 2005). Snow accumulation also tends to be higher in harvested area than under forest canopies, with cut blocks typically accumulating about 30-50% more snow, most likely due to decreases in interception loss (Storck et al., 2002; Moore and Wondzell, 2005; Winkler et al., 2005). Winkler et al. (2005) found that in montane and boreal forested areas, on average there was 23% less 1 April SWE was found in the mature spruce-fir stand than in the clearcut, and that average snowmelt rates in the mature spruce-fir were 40% of those in the clearcut. In harvested clearings the snow surface is exposed to greater solar radiation as well as to higher wind speeds, resulting in increased melt rates (Adams et al., 1998).

2.4.3 Affects on Hydroelectric Power

The UNSRB has two major hydroelectric reservoirs whose generating capacities are dependent on the timing and magnitudes of mainly alpine runoff (Bonsal et al., 2003). The Brazeau Dam, built in 1965, and the Bighorn Dam, built in 1971, produce enough energy to supply the equivalent of 114,500 Alberta households with electricity annually (TransAlta, 2009).

With the timing of runoff flowing into reservoirs in snowmelt dominated watersheds expected to change, impacts on actual and potential hydroelectric power generation are also probable (Fredericks and Major, 1997). Glaciers store water in different ways for different periods of time, from day to decades, which are important sources of late season streamflows (Jansson et al., 2003). Future forecasts of hydropower generation need to take into consideration changes in the storage and release of water by glaciers, decreased snowpacks, and decreasing spring and summer flows (Hock et al., 2005; Byrne and Kienzle, 2008). According to Noques-Bravo et al. (2007), who based their research on moderate climate change scenarios, changes in discharge regimes in the future could lead to reductions in hydropower potential of 25% or more for southern and southeastern European countries. A study in the Pyrenees by Lopez-Moreno et al. (2008) revealed that the hydrological changes are already noticeably affecting inflows into the Pyrenean reservoirs, with a notable reduction in the annual inflow volumes. There were also

changes in the seasonal distribution of inflow, with a reduction in spring discharge, and the earlier occurrence of the annual maximum monthly flow (Lopez-Moreno et al., 2008).

2.4.4 Glaciers

Glacier mass balance reflects cumulative precipitation and temperature variations in a region, and is linked strongly to streamflow variations (Shea and Marshall, 2007). It is estimated that over the last 100 years that glaciers in western Canada have lost about 25% of glacier area, and possibly larger losses in terms of volumetric ice loss (Luckman, 1998). With increased warming in alpine areas runoff from glaciers is greatly enhanced, but as glacier area decreases water yields from the glaciers will also decrease, with the eventual loss of glaciers, resulting in large reductions in summer runoff (Hock et al., 2005). The time for increased flows due to glacier melt in the UNSRB has already passed, and in the next 20 years glacial contributions to streamflow will decrease leading to reduced late season flows (Demuth and Pietroniro, 2003).

From mass balance data at Peyto Glacier in the southwest corner of the UNSRB, there has been a negative balance since 1976 due to decreased winter accumulation, not to an increase in summer ablation as might be expected (Luckman, 1998). Although the marked decrease in winter precipitation have been shown to be related to the Pacific Decadal Oscillation (Bitz and Liscomb, 1999), significant changes in mass balance are a function of temperature and precipitation, and cannot be attributed to only one variable (Luckman, 1998). Glacier contribution to streamflow can vary greatly. It is estimated that only about 2.5% of the flow of the Bow River, whose head waters are adjacent to the head waters of the UNSRB, results from glacial melt (Hopkinson and Young, 1998), and up to 15% of annual streamflow from glacial melt reported in the Mistaya River Basin in the head waters of the UNSRB (Loijens, 1974). Loijens (1974) showed from field work in 1971 that from July 14-September 3, up to 70% of the streamflow from the Mistaya River Basin was supplied by glacier runoff.

2.4.5 Potential Impacts for Water Availability

In western North America, spring snowmelts supply 50%–80% of the annual flow volume (Barnett et al., 2005). Progressively earlier snowmelt dominated streamflows will challenge many water resource management systems as the predictability and seasonal deliveries of snowmelt and runoff changes (Stewart et al, 2005). Rood et al. (2005) concluded that streamflow has declined in the North American central Rocky Mountains over the past century, and that this region could see streamflow decline by a further 10% by 2050. Declining streamflows are expected to reduce water availability for irrigation, industrial and domestic use, and hydroelectric power generation (Sauchyn and Kulshreshtha, 2008). Decreased runoffs are expected in part due to reduced flows from glaciers and reductions in snowpack, and are expected to accelerate throughout the 21st century, reducing water availability, hydropower potential, and changing seasonality of flows in regions supplied by meltwater from major mountain ranges (IPCC, 2007).

2.5 Hydrological Modelling

Hydrological models use observed meteorological data to model streamflow, which can be verified using observed streamflow or other measurable hydrological variables. Streamflow is sensitive to changes in climate parameters such as precipitation and temperature, making it important to look for evidence of trends in streamflow that could be caused by climate change (Yue et al., 2001). Hydrological models coupled with climate change predictions, can be used to estimate regional climate change impacts, and provide a framework in order to conceptualize and examine the relationships between climate and the hydrological regimes within a watershed (Leavesley, 1994; Xu, 1999b). Combining CGM output with a deterministic hydrological model containing physically based equations describing hydrological processes is the most practical and widely used approach to simulating impacts of climate change (Loukas et al., 2002).

2.5.1 Classification of Hydrological Models

Numerous models and modelling approaches are currently being used to assess the impacts of climate change on water resources. Models can be classified by different criteria including purpose of model application, model structure, spatial partitioning (lumped or distributed), temporal scale, and spatial scale (Leavesley, 1994). To follow is a short review of different model types based on model structure, which are dependent on either simplified laws or the fundamental laws of physics, or an empirical analysis.

2.5.1.1 Conceptual Models

Conceptual models use simplified relationships of physical processes and attempt to account for the linear and nonlinear relations between parts of the water balance equation (Leavesley, 1994). Parameters for conceptual models are not necessarily directly related to the physical observations of the watershed in which it is applied, and the calibration procedure often requires long observed records (Abbott et al., 1986; Refsgaard and Knudsen, 1996). Both of these factors can limit the use of conceptual models in climate change studies as there is increased uncertainty in terms of model inputs (Forbes, 2007)

2.5.1.2 Empirical Models

Empirical or statistical models do not explicitly consider the physical laws of the processes involved in the hydrological cycle, rather they use approximate relationships developed from observed hydrological input and output data to simulate water flows and storages (Leavesley, 1994). Statistical regression methods are often used to develop these relationships, such as snowmelt rates in relation to air temperature (Dingman, 2002). Empirical models only reflect the relations between input and output for the climate and watershed conditions during the time period in which they were developed, meaning these types of models require large amounts of data, and are often non-transferable between watersheds (Leavesley, 1994). These models are

seen as static, as changes cannot be introduced into the model, in terms of climate or land use changes.

2.5.1.3 Physically Based Models

Physically based or deterministic models use mathematical equations that are based on known physical processes to simulate water flows and storages (Dingman, 2002). The ability of physically based models to assess the effects of climate change has been recognized (Bathurst and O'Connell, 1992; Barnett et al., 2005; Barrow and Yue, 2005; Forbes, 2007); however, major limitations to the use of physically based distributed models are the availability and quality of watershed and climate data at the spatial and temporal resolution. These data are needed to both estimate model parameters and to validate model results at this level of detail (Xu, 1999a).

2.6 Spatial Representation of Hydrological Processes

Hydrological processes, represented by mathematical physically-based equations, are nonlinear. Nonlinearity presents many problems when applying distributed modelling concepts in hydrology (Beven, 2001). Besides nonlinearity, there are limits to the amount of detail that can be represented over large watersheds, as well as representing or parameterizing sub-grid scale processes over a large heterogeneous watershed such as the UNSRB (Beven, 2001). In hydrological modelling representing hydrological processes from measured data from points that are primarily not representative of the entire watershed, are problematic for all modellers. One method of dealing with this is dividing up a large watershed into smaller subunits, such as hydrological response units (HRUs). HRUs are distributed, relatively heterogeneously structured units based on meaningful physical and spatial parameters that have common hydrological characteristics and response (Flügel, 1995). This is done to create a more "realistic" representation of the hydrological response of a watershed, and makes it useful for investigating impacts of hydrology based on climate change projections (Beven, 2001).

2.7 Spatial Climatic Data

Spatial climate data are key inputs used to drive hydrological models. In most watersheds climate data only exist for point locations where meteorological stations are located, which is often unrepresentative of the watershed. As a result, values at any other point in the terrain must be interpolated from neighbouring stations or from relationships with other variables, such as lapse rates over different elevations (Marquinez et al., 2003). There are many interpolation techniques such as inverse distance weighting (IDW), various forms of kriging, ANUSPLIN tri-variate spines, and PRISM (Daly, 2006). Comparisons of interpolated data have found ANUSPLIN and PRISM data to produce comparable results and to be superior to several other interpolation methods (Milewska et al., 2005; Daly, 2006; Mbogga et al., 2009).

2.7.1 ANUSPLIN

The software package ANUSPLIN (Hutchinson, 1995) fits smoothing splines (usually second or third order polynomials) through station data in three dimensions: latitude, longitude, and elevation. ANUSPLIN is readily available, easy to apply, and accounts for spatial changes in elevation. However, a spline is by definition smoothly varying. As a result, ANUSPLIN has difficulty simulating sharply varying climate transitions such as temperature inversions and rain shadows, which are characteristic in alpine areas (Daly, 2006).

2.7.2 PRISM

PRISM (Parameter-elevation Regressions on Independent Slopes Model) is used to interpolate climate elements in complex landscapes such as the UNSRB, as it assumes for a localized region that elevation is the most important factor in temperature and precipitation distribution (Daly et al., 2007). PRISM uses point data, a DEM, and an encoded spatial climate knowledge base that generates estimates of annual, monthly, daily, and event-based climatic elements, which are interpolated to a regular grid making them GIS-compatible (Daly *et al*., 2002, 2004, 2008; Daly, 2006). While PRISM accounts for more spatial climate factors than

other interpolation methods, the PRISM data sets are a peer review procedure that brought significant knowledge of regional climate patterns and new station data sets into the development process (Daly et al., 2008). PRISM surfaces are available for purchase for portions of the world.

2.8 The ACRU Agro-hydrological Modelling System

The ACRU (Agricultural Catchments Research Unit) agro-hydrological modelling system was developed in the late 1970s by the Department of Agricultural Engineering (now called the School of Bioresources Engineering and Environmental Hydrology) at the University of KwaZulu-Natal, South Africa (Schulze, 1995). Since then, ACRU has been updated and improved so the hydrological response of watersheds can be modelled with more physically based applications associated with cold climates, as well as terrain dependent hydro-meteorological variables. These updates include the addition of snowpack and snow/glacial melt routines, correcting daily minimum and maximum temperature based on differences of incoming radiation on slopes, or allowing the division of a watershed into up to 9999 HRUs.

ACRU is a multi-purpose, multi-level, integrated physical conceptual model that can simulate total evapotranspiration, soil moisture storage, land cover and climate change impacts on water resources, and streamflow at a daily time step (Schulze, 1995). ACRU was chosen for use in this thesis as it fit the purpose of the study, as it was readily available for use, and as a physically based distributed model is most desirable for simulating spatial patterns of hydrological response within a basin (Bathhurst and O'Connell, 1992). When accurately parameterized and verified, ACRU is capable of simulating many elements of the hydrological cycle, which establishes the fundamental basis for hydrological impact studies.

2.8.1 Theoretical Principles of ACRU

The structure of ACRU is conceptual in that it theorizes the processes that govern the hydrological cycle and physical in that the physical laws of hydrology are defined by mathematical equations within the conceptual framework of ACRU (Schulze, 1995). ACRU is

considered to be a physical-conceptual rather than an optimizing model as simulations are based on physically observed or derivable watershed characteristics (Jewitt and Schulze, 1999).

ACRU is able to simulate watersheds characterized as a lumped model, where one parameter set represents the entire watershed, or a distributed model, which requires the delineation of the watershed into sub-units, each simulated independently. ACRU is applied in this thesis in the distributed mode, and simulates all major processes of the hydrological cycle, including rain and snow interception, infiltration, snowpack, accumulation and soil water storages, glacier melt, separation of precipitation into rain and snow, groundwater recharge, and total evaporation.

2.8.2 Physical Processes of the ACRU Model

ACRU applies a generalized daily water budget approach and considers the spatial and temporal variability for the response of hydrological processes within a watershed. Daily precipitation events are evaluated for each HRU, including initial abstractions by canopy interception and runoff production, with the resulting volume being conceptualized as net daily precipitation available for runoff or infiltration (Forbes, 2007).

The snowmelt routine in ACRU is based on a water retention concept where the storage capacity of liquid water in the snowpack regulates the quantity and timing of water release from the snow storages. The snow sub-module uses a temperature-based method to quantify snow accumulation and ablation processes. The snow module considers precipitation type (i.e. rain, snow, or mixed precipitation), the volumetric properties of snowpack (i.e. snow water equivalent, density, depth, and liquid water retention), heat and mass balances/exchanges of the snowpack (e.g. changes in albedo as snowpack melts), and the temporal changes in physical snowpack characteristics that affect storage and melt (i.e. metamorphosis and sublimation of snowpack). The release of water from the snow module is added to the net precipitation store of the ACRU structure (Schulze, 1995; Kienzle, 2009).

The net portion of precipitation that is not intercepted is modelled in a two-layer soil profile, i.e. the A- and B-horizons, where the B-horizon's depth reaches to the average rooting depth of the plant community within the particular HRU. Soil depth and texture of both surface and subsurface horizons are used to determine total porosity, field capacity, and wilting point, which determines the soil water retention capacity of the soil. Volumetric soil water in excess of the field capacity is redistributed at the saturated rate (determined by texture), while soil water less than field capacity but greater than the wilting point is redistributed at the unsaturated rate both in the upward (subsoil) and downwards (surface and subsoil) directions (Schulze, 1995).

Evapotranspiration takes place from several principle water storages, including previously intercepted snow and rain, snowpack, and soil storages. Daily actual evapotranspiration is determined using the internally pre-determined reference evaporation and monthly plant transpiration coefficients (PTCs) for each land cover type. ACRU separates daily soil evaporation and plant transpiration relative to vegetation phenology. The amount of transpiration between soil horizons is controlled by the root mass distribution between the two horizons. Soil water in excess of the permanent wilting point is considered available for transpiration by plants (Schulze, 1995).

ACRU generates total streamflow from simulated runoff, comprised of both same day and delayed quickflow, and baseflow volumes. Runoff generation is based on a modified Soil Conservation Service (SCS) procedure (United States Department of Agriculture, 1985), where runoff potential is conceptualized as a depth, and is a function of the soil's relative wetness (Schulze, 1995). Baseflows are generated from saturated drainage out of the rooting zone, and added to the groundwater store (Schulze, 1995). Recessions curves from hydrographs of observed streamflow data are used to derive response coefficients to characterize the temporal response of surface runoff and baseflows for each HRU.

2.8.3 ACRU and Climate Change

ACRU must be thoroughly parameterized before simulating streamflow of a particular watershed, as rigorous parameterization of a model is a crucial step to avoid problems during the model verification process (Refsgaard, 1997). Parameters should be assessed from field data, or should be estimated within a physically acceptable range for available data and literature sources (Kienzle and Schmidt, 2008). Hydrological models are often verified using observed streamflow or other measurable hydrological variables (Rosso, 1994; Brooks et al., 2006). A model should be able to reasonably reproduce historical streamflow records, in order to be used in climate change studies, and can only be applied with confidence once the model output has been verified against observed data (Loukas et al., 2002; Jewitt et al., 2004). Concerns with the modification of too many parameters during the calibration or verification process (Beven, 1989) have been expressed. However, for the purpose of this research verified parameters were not just modified to calibrate streamflows.

ACRU has been used extensively for water resource assessments (Everson, 2001; Kienzle et al., 1997; Schulze et al., 2004; Martinez et al., 2008), and climate change impacts (New and Schulze, 1996; New, 2003; Schulze et al., 2004). ACRU has been applied in Chile, Germany, the USA, New Zealand, and a recent version of ACRU, including the snow module, was applied for the first time in Canada in a study on the Beaver Creek watershed in southwestern Alberta (Forbes, 2007). The concepts and physical processes described in ACRU make it highly receptive to changes in land use and climate (Schulze and Smithers, 1995). In ACRU, total evaporation is separated into soil water evaporation and transpiration. This makes it sensitive to temperature change as well as accommodating a transpiration suppression function associated with increases in CO_2 (Schulze, 2000).

2.9 Climate Scenario Development

2.9.1 Climate Scenarios

In 2000, the IPCC published a Special Report on Emissions Scenarios (Nakicenovic et al., 2000), describing the four scenario families; A1, A2, B1, and B2. These families are based on alternative development pathways, covering a wide range of demographic, social, economic, and technological driving forces and resulting GHG emissions. These scenarios are widely used in assessing future climate change impacts, and will be used in this study. The A1 Scenario assumes a world with rapid economic growth, a global population that peaks in mid-century, and rapid introduction of new and more efficient technologies. A1 is divided into three groups that describe different levels of technological change: fossil intensive (A1FI), non-fossil energy resources (A1T), and a balance across all sources (A1B). B1 describes a convergent world, with the same global population as A1, but with more rapid changes in economic structures toward a service and information economy. B2 describes a world with intermediate population and economic growth, emphasizing local solutions to economic, social, and environmental sustainability. A2 describes a very heterogeneous world with high population growth, slow economic development and slow technological change (Nakicenovic et al., 2000; IPCC, 2001).

2.9.2 General Circulation Model Scenarios

General Circulation Models (GCMs) are large scale (250-600km) mathematical models which represent the physical processes and known feedbacks between the atmosphere, ocean, cryosphere, and land, and can be used for the simulation of future climates (Barrow et al., 2005). GCM simulations of the climate are classed as transient simulations, which apply a steady increase in CO_2 atmospheric concentrations, while the climate of the Earth is synchronously simulated (Loaiciga et al., 1996). Thirty year averaging periods are typically used in scenario construction as a compromise between trying to capture the climate change signal without losing too much of the variability in the model results over time. IPCC currently recommends three fixed future time periods for impact studies: the 2020s (i.e., 2010-2039), the 2050s (2040-2069),

and the 2080s (2070-2099). This permits the scenarios to better represent the long-term trend compared to the use of a shorter period, such as 10 years (IPCC, 2007).

Output from a climate model provides a description of the response of a climate system to a particular greenhouse gas scenario. To obtain a climate scenario, output from the GCM is combined with some baseline observed data, typically 1961-1990 (Barrow et al., 2005; IPCC, 2007), as the 1961-90 time period has been assumed not to be impacted by climate change yet (Diaz-Nieto and Wilby, 2005).

A major disadvantage of using GCMs is that they are considered to accurately represent global climate, but that they are often inaccurate when simulating regional climate (Evans and Schreider, 2002). GCMs are not well suited for answering the questions concerning regional-scale hydrological variability as they were not designed for this purpose due in part to their coarse spatial resolution, and general disagreement among GCMs with respect to precipitation changes at a regional scale (Loaiciga et al., 1996). With a coarse spatial resolution and the simplifications of the hydrologic cycle in those models, it is not possible to make reliable predictions of regional hydrologic changes directly from GCMs as a result of climate warming (Loaiciga et al., 1996). Downscaling or regionalization of GCM output is a common method of dealing with the regional inaccuracy. It should be noted that scenarios may play a key role in illustrating future climate changes in a region to help in strategic planning and water management decisions, but lack the confidence associated to allow a scenario to be referred to as a prediction or a forecast (Barrow et al., 2005).

2.9.3 Regionalization Techniques

Techniques developed to derive regional climate from coarse resolution GCMs are known as downscaling. Some of the more common methods include statistical downscaling (SDS), dynamic downscaling (DDS), and a procedure often known as the delta method of downscaling (Loukas et al., 2002). It is important to note that different circulation schemes and

downscaling methodologies yield noticeably different regional climate change scenarios, even when common sets of GCM outputs are used (Wilby et al., 1999).

2.9.3.1 Statistical and Dynamic Downscaling

SDS and DDS have been developed to downscale information from GCMs to regional scales. DDS uses regional climate models (RCMs) to simulate finer-scale physical processes consistent with the large-scale climate changes from a GCM (Schmidli et al., 2007). SDS develops statistical relationships between local climate variables and large-scale predictors, which are applied to the output of GCM experiments to simulate local climate characteristics (Muzik, 2002). Unlike DDS, SDS is limited by the assumption of temporal stationarity in the empirical relations, meaning present climate won't necessarily translate to accurate forecasts of future climate (Hay and Clark, 2003). Wilby et al. (1999) found that SDS of GCM output for current climate was found to be superior to the use of raw GCM output in all respects, and that it is far less data intensive and computationally demanding than the DDS methods. Use of SDS techniques has shown models are not able to reproduce decadal and interannual climate variability and, consequently, the observed streamflow (Hamlet and Lettenmaier, 1999).

2.9.3.2 The Delta Change Method

The delta method is the most conventional method to deal with coarse GCM output, using changes in temperature and precipitation from GCM output to perturb historical time series of meteorological variables (Wilby et al., 1999; Arnell, 2004; Merritt et al., 2006). This is done by calculating the differences between current and future GCM simulations, and adding these changes to observed time-series (Barrow et al., 2005; Forbes, 2007; MacDonald, 2008). This is the most common method to transfer the climate change signal to hydrological models (Andréasson et al., 2004), and will be used in this research. Using the delta method has shown to give more conservative estimates of changes in future runoff when compared to downscaled

GCM methods (Hay et al. (2000). In using the delta method, the climate change scenarios applied are not necessarily the most likely future climates in a region. Rather, they are primarily designed to show the sensitivity to change within a reasonable interval (Xu, 1999a).

It is recommended (IPCC 2007) to use more than one GCM in impact assessments in order to show a range of changes to temperature and precipitation for a study region. The easiest way to make this selection is to use scatter plots of estimated changes to temperature and precipitation from GCM output (Barrow et al., 2005). The median temperature and precipitation change amongst available CGM output can then be used in this research to select five scenarios: four representing the predicted changes in each of the four quadrants created by the temperature and precipitation median lines, and one representing the median conditions.

2.10 Summary

Understanding the physical processes and conceptual uncertainties in modelling and climate change impact studies are essential when tasked with simulating potential changes to streamflow in a watershed. Methods for simulating hydrological responses of a watershed to global climate change by using hydrologic models include coupling GCMs with hydrologic models through statistical downscaling techniques. Estimates of future changes in climate and impacts on hydrological processes are complicated by many uncertainties related to the unknown future evolution of climate-forcing scenarios (Jasper et al., 2004). Proper parameterization and verification of model output prior to simulating impacts of climate change is crucial. It is important to understand how to best apply a range of climate change scenarios with a suitable model in order to properly interpret meaningful results to assess the impacts of climate change in central Alberta.

CHAPTER 3

Parameterization of the ACRU agro-hydrological modelling system and verification of hydrological processes for simulating potential climate change impacts in the upper North Saskatchewan River basin, Alberta, Canada.

3.1 Introduction

Throughout the province of Alberta there is increasing demand for water due to population growth, and an increasing demand from agriculture and industry. In contrast, availability of future water resources is uncertain due to climate change, as some studies have shown that declining streamflows are expected to reduce water availability for irrigation, industrial and domestic use, as well as hydroelectric power generation (Gan, 1998; Rood et al., 2005; Byrne and Kienzle, 2008; Sauchyn and Kulshreshtha, 2008). General impacts forecasted include earlier spring runoffs and increased winter flows, lower summer and late fall streamflows, decreased glacial melt contributions, and lower snow accumulations (Burn, 1994; Gan, 1998; Demuth and Pietroniro, 2003; Lapp et al., 2005; Sauchyn and Kulshreshtha, 2008). Therefore, the understanding of watershed balances is essential for current and future water resources planning. This research focuses on the estimation of the impacts of climate change on streamflows in the upper North Saskatchewan River basin (UNSRB).

Hydrological models coupled with climate change predictions can be used to determine hydrological effects of climate change in a region, as they provide a framework in order to conceptualize and examine the relationships between climate and the elements of the hydrological cycle within a watershed (Leavesley, 1994; Xu, 1999b). Rigorous parameterization of a model is a crucial step to avoid problems during the model verification process (Refsgaard, 1997). Parameters should be assessed from field data, or should be estimated within a physically acceptable range for available data and literature sources (Kienzle and Schmidt, 2008). Hydrological models use observed meteorological data to model streamflow, and are often verified using observed streamflow or other measurable hydrological variables (Rosso, 1994;

Brooks et al., 2006, Liu et al., 2009). A model should be able to reasonably reproduce historical streamflow records, in order to be used in climate change studies, and can only be applied with confidence once the model output has been verified against observed data (Loukas et al., 2002; Jewitt et al., 2004). Models are simplifications of reality, but are an important tool in assessing future scenarios for water management strategies, if accurately parameterized and verified (Beven, 1989). The ACRU (Agricultural Catchments Research Unit) agro-hydrological modeling system (Schulze, 1995) is capable of simulating many the elements of the hydrological cycle, which establishes the fundamental basis for hydrological impact. In the UNSRB, a detailed parameterization was completed, with a rigorous verification process, all of which will be discussed in this chapter.

3.2 Study Area

The upper North Saskatchewan River basin (UNSRB) is situated southwest of Edmonton, Alberta, Canada (see Figure 3.1). The UNSRB has an area of a 20,527km^2 and consists of alpine, subalpine, and foothills landscapes located on the eastern slopes of Alberta's Rocky Mountains. The basin ranges in elevation from approximately790m at the outlet gauging station to just under 3,500m at the Rocky Mountain peaks at the continental divide. Streamflows are dominated by snowmelt, and supplemented by glacial melt from the Columbia Ice Fields, Peyto, Athabasca, and Saskatchewan glaciers (NSWA, 2005). In order to allow for streamflow verification and the estimation of water yield that feed the hydro power reservoirs, the UNSRB was divided into 12 watersheds, based on either a gauging station or hydroelectric dam location to define the outlet (Figure 3.1).

Based on the subdivision, there are five watersheds in the UNSRB that are important for hydroelectric power generation. Watersheds 8, 9, and 11 are upstream of Alberta's largest hydroelectric facility, the Brazeau Dam, which was built in 1965. Watersheds 1 and 2 are upstream of the Bighorn Dam, which was built in 1971 and created Lake Abraham, one of the

largest reservoirs in Alberta. Watersheds 1 and 2 will be the focus of the streamflow portion of the verification process for the UNSRB watershed (Figure 3.1).

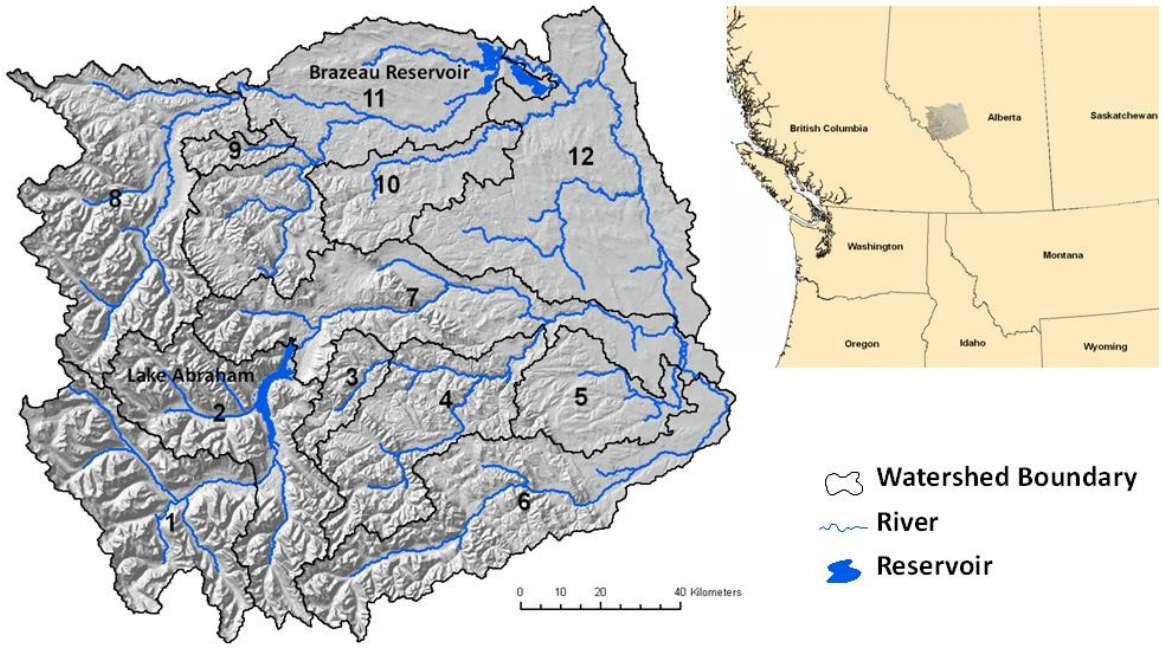

Figure 3.1: UNSRB location in west central Alberta, showing watershed boundaries, river systems, and locations of hydroelectric reservoirs.

3.3 Objectives

The primary objective of this research is to estimate the impacts of climate change on water yield, streamflow extremes, and the streamflow regimes in the UNSRB, and consequently, water availability for hydropower generation in this area. In order to ensure that the model output properly represents the hydrological behaviour of the key elements of the hydrological cycle, the model has to be set up for the base time period, 1961 – 1990, and simulated model output needs to be compared against observed hydrological variables. This objective will be accomplished by setting up the ACRU agro-hydrological modelling system (Schulze, 1995; Smithers and Schulze, 1995; Schulze et al., 2004), from here on referred to simply as ACRU. Parameterization of ACRU is a critical step in the process to properly simulate both historical and future streamflow under potential future climate change scenarios. Once parameterization is complete, output from

ACRU must be verified against observed data to provide confidence in model outputs. The objective of this chapter is twofold: 1) to describe ACRU, and the parameterization of ACRU, and 2) to compare and calibrate ACRU output against available observations, which include temperature time series at climate stations, snow course and snow pillow data, glacier melt from Peyto Glacier, potential evapotranspiration using A-pan data, and streamflow time series.

3.4 Methods

3.4.1 The ACRU Agro-Hydrological Modelling System

The ACRU agro-hydrological modelling system has been developed at the Agricultural Catchments Research Unit (ACRU), a research group within the School of Bioresources Engineering and Environmental Hydrology (formerly the Department of Agricultural Engineering at the University of KwaZulu-Natal, Republic of South Africa) since the late 1970s (ACRU, 2007). ACRU is a multi-purpose, multi-level, integrated physical-conceptual model that can simulate total evaporation, soil water and reservoir storages, land cover and abstraction impacts on water resources and streamflow at a daily time step. The ACRU model revolves around multi-layer soil water budgeting with specific variables governing the atmosphere-plant-soil water interfaces. Surface runoff and infiltration are simulated using a modified SCS equation (Schmidt and Schulze, 1987), where the daily runoff depth is proportional to the antecedent soil moisture content.

A number of ACRU input variables are estimated from the physical characteristics of the watershed. When not all required variables are available, they are estimated within physically meaningful ranges based either on the literature or local expert knowledge. Spatial variation of rainfall, soils and land cover is facilitated by operating the model in distributed mode, in which case the catchment is subdivided into either sub-watersheds or hydrological response units (HRUs), each representing a relatively homogenous area of hydrological response.

Precipitation is separated into rain or snow using either a threshold temperature, or a more dynamic temperature based method developed by Kienzle (2008). Subsequent snow processes, such as canopy interception, sublimation, metamorphosis, or change in albedo and density, are simulated in a physically explicit manner. The snow melt simulation is based on either pre-determined monthly snowmelt factors, or a dynamic degree-day factor, which is determined by the model on a daily basis from incoming radiation and albedo estimates.

ACRU has been used extensively for water resource assessments (Everson, 2001; Kienzle et al., 1997; Schulze et al., 2004; Martinez et al., 2008), and climate change impacts (New and Schulze, 1996; New, 2003; Schulze et al., 2004), and often requires extensive GIS pre-processing (Kienzle, 1993; 1996; Schulze et al., 1995). Comprehensive model manuals are available through the internet at the ACRU web page (Schulze, 1995; Smithers and Schulze, 1995; ACRU, 2007). ACRU is well described by Kiker et al. (2006). However, the snow modelling manual is not yet available. The conceptual structure of ACRU is shown in Figure 3.2.

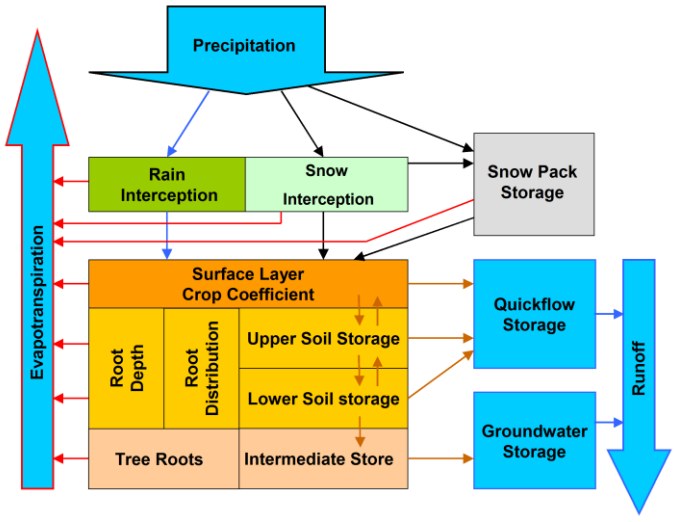

Figure 3.2: Major components of the ACRU agro-hydrological modelling system illustrating the conceptual representation of the water balance (Kienzle and Schmidt, 2008).

3.4.2 Model structure for UNSRB

3.4.2.1 Creation of a Digital Elevation Model (DEM)

At the time of the study, the only DEM available was the Shuttle Radar Topography Mission (SRTM), with a grid cell size of 75m. This DEM had two severe linear elevation discontinuities running through the alpine region of the study area, making it unusable for further GIS analyses. Therefore, a new DEM was created, using 1:50,000 topographic maps sheets from the National Topographic System of Canada downloaded from the GeoGratis web page. GeoGratis is a portal provided by the Earth Sciences Sector (ESS) of Natural Resources Canada (NRCan), which provides no cost geospatial data. The 'Topo to Raster' tool (ESRI, 2008) was used to create a 100m resolution DEM of the study area from contour lines and elevation point data from each of the 36 map sheets. The topographic map sheets also contained river layers. These were used to further enhance the DEM along the rivers in order to ensure that the DEM based watershed delineation would be consistent with the actual stream network.

3.4.2.2 Watershed Delineation

The UNSRB was divided into 12 watersheds by GIS analysis of the DEM such that the watershed outlet coincided with the location with one of the ten respective Water Survey of Canada (WSC) gauging stations or the location of either of the two hydroelectric dams. Delineating these watersheds allowed the model to be run on each of the watersheds individually. Information on each the watershed is shown in Table 3.1.

Table 3.1: Overview of delineated watersheds in the upper North Saskatchewan River Basin

Watershed Number	WSC Station ID or Dam Name	Area (km^2)	Maximum Elevation (m)	Mean Elevation (m)	Minimum Eleveation (m)	Dominant Land Covers	Number of HRUs
1	05DA009	1921.1	3484.4	2193.6	1317.4	Exposed/Built-up Land, Glaciers, Coniferous Forest	169
2	Bighorn Dam	1935.0	3193.8	2140.1	1246.3	Exposed/Built-up Land, Coniferous Forest, Grassland	139
3	05DC011	354.8	2710.2	1870.6	1437.7	Coniferous Forest, Exposed/Built-up Land	45
4	05DC006	1494.1	3136.5	1805.3	1051.0	Coniferous Forest, Exposed/Built-up Land, Shrubland	128
5	05DB002	856.9	1977.6	1259.4	987.5	Coniferous Forest, Grassland, Shrubland	80
6	05DB006	2257.8	3266.2	1746.9	983.9	Coniferous Forest, Exposed/Built-up Land, Grassland	195
7	05DC001	2204.8	3104.0	1442.1	955.3	Coniferous Forest, Exposed/Built-up Land, Shrubland	189
8	05DD007	2618.3	3260.6	2081.9	1256.6	Exposed/Built-up Land, Coniferous Forest, Deciduous Forest	185
9	05DD004	196.7	2230.7	1586.3	1288.9	Coniferous Forest	24
10	05DD009	865.5	2052.0	1255.7	923.2	Coniferous Forest, Shrubland, Water/Wetlands	71
11	Brazeau Dam	2791.5	2934.3	1362.9	933.7	Coniferous Forest, Exposed/Built-up Land, Water/Wetlands	176
12	05DE006	3030.4	1539.2	1027.5	752.7	Coniferous Forest, Water/Wetlands, Shrubland	127

3.4.2.3 Hydrological Response Units

Each watershed was further divided into hydrological response units (HRUs), which are distributed, relatively homogeneous bio-physical units that are assumed to have similar hydrological characteristics and response (Flügel, 1995). Each HRU is later parameterized individually for input into ACRU. The HRUs were delineated based on elevation, land cover, mean annual radiation, and watershed boundary. The DEM was classified into 29 elevation bands, ranging in 100m increments from 700m to 3,500m. A generalized land cover (NLWI, 2008) was resampled to match the 100m DEM and classified into eleven land cover classes (Section 3.4.3.5). Mean annual radiation was calculated in ArcGIS using the Area Solar Radiation tool (ESRI, 2008) at a 3 hour interval, and classified into four 25% quantile classes. The watershed boundaries were used so that HRUs were confined to a single watershed, allowing each watershed to be modelled independently from each other. An overlay analysis in ArcGIS was performed using these four data layers, which resulted in 1528 HRUs.

Each HRU was parameterized to have a unique combination of hydrological variables, most of which were derived by GIS overlay analysis. The area of each HRU was calculated based in its true, sloped area. ACRU can correct for most climate parameters, usually on a monthly basis, to account for spatial differences between a climate station used to "drive" the model and each HRU. These correction values help to ensure that estimated or observed data for each HRU is corrected for the physical characteristics that are present in the HRU.

3.4.3 Parameterization of ACRU

3.4.3.1 Climate Data

In order to model impacts of climate change, a base period of climate data from 1961-1990 is used instead of the 1971-2000 time period, as it is assumed that it has not been significantly impacted by climate change (Diaz-Nieto and Wilby, 2005). Climate stations used in this study were set up and maintained by Environment Canada Meteorological Service. Only three stations had 30 or more years of mostly complete data, which are required to create complete daily time series of climate inputs to drive the model for all HRUs that make up the UNSRB (Figure 3.1); Clearwater (Station ID 3011663), Bighorn Dam (Station ID 30506GN), and Nordegg RS (Station ID 3054845). As none of the stations had complete daily records for the 1961-1990 time period, infilling the missing station data was required for each of the three stations. As precipitation inputs from Bighorn Dam appeared to be too low to adequately model precipitation in the watershed along the continental divide in the western part of the watershed, precipitation data from the climate station in Jasper were averaged to the daily precipitation data at Bighorn Dam for the 1961-1990 time period.

To infill each of the three base stations, surrounding stations were selected that were geographically close to each of the base stations. The number of surrounding stations required depended on the amount of missing data from the base station. To account for potential seasonality differences between the climate stations, a regression analysis was performed on a monthly basis between each neighboring station and the climate station to be infilled. This was done for maximum and minimum temperature, as well as precipitation. In order to infill missing temperature data, stations are ordered, on a monthly basis, from highest to lowest correlation for maximum daily temperature, as it is less variable than daily minimum temperature values due to processes such as cold air drainage. For precipitation, stations were simply ordered from highest to lowest correlation on a monthly basis. The regression equation of each month for each climate

station is then applied to the daily station data before it was used to infill the missing data at the base station.

An interpolated climate surface is needed to calculate precipitation correction factors for each of the HRUs in the study area. As the climate data in the study area were too sparse and incomplete to be able to interpolate any type of meaningful climate surface, PRISM, an existing interpolated climate data set was used. PRISM, or Parameter-elevation Regressions on Independent Slopes Model (Daly, 2006), is uniquely designed to map climate in the most difficult situations, such as areas with high mountains and rain shadow effects. Mean monthly PRISM surfaces at a 2km resolution for maximum and minimum temperature, and precipitation for Alberta were purchased. These surfaces were clipped to fit the study area, and then downscaled to a 100m grid cell size using a spline interpolation method. Temperature and precipitation values from the PRISM surfaces were checked against station values from various stations in the UNSRB. All stations correlated well with a coefficient of determination ranging from R^2= 0.996 to R^2= 0.904, with an average R^2=0.989. As most stations in the basin were probably used to create the PRISM surfaces, these high coefficients of determination were expected. PRISM values were used as a first approximation, but may have to be altered once all other hydrological variables are confirmed in the verification analysis.

3.4.3.2 Temperature

Regional mean monthly lapse rates for maximum and minimum temperatures were initially calculated from the monthly maximum and minimum temperature PRISM surfaces and elevations from the DEM. Maximum temperature lapse rates were later calibrated based on glacial melt output from Peyto Glacier after initial runs in a heavy glaciated watershed showed that magnitude of the lapse rates were too high. A lower static lapse rate used in a study by Shea et al. (2009) was the basis for calibrating the lapse rates. To account for the differences in temperature between different slopes due to radiation inputs, a mean monthly radiation

adjustment factor is calculated using monthly radiation surfaces simulated in ArcGIS. This resulted in higher temperatures on south-facing HRUs, when compared to north-facing HRUs with the same elevation.

3.4.3.3 Precipitation

Precipitation is adjusted on a daily basis for each HRU relative to the base station. To account for the spatial and elevation differences in precipitation between an HRU and the base station, monthly precipitation adjustment factors for each HRU were calculated as a ratio of the PRISM precipitation value for each HRU and the monthly precipitation values from the base station. Precipitation inputs are also corrected based on size of the watershed. As precipitation is measured at a point and record local events, high recorded precipitation events should not be transferred to an entire watershed without adjustment. This is especially true during the summer months, when convective precipitation events result in localized, high intensity rainfall. The implementation of an areal precipitation reduction factor (ARF) reduces large, daily extreme events as a function of the precipitation event and the size of the watershed. All other daily precipitation values are then increased to balance the initial total precipitation depths. Finally, interception of precipitation by the vegetation canopy is estimated using the leaf area index (LAI) (Schulze, 1995; Forbes, 2007).

3.4.3.4 Evapotranspiration

Evapotranspiration takes place from several principle water storages, including previously intercepted snow and rain, snowpack, and soil storages. Daily actual evapotranspiration is determined using the internally pre-determined reference evaporation and monthly plant transpiration coefficients for each land cover type. These were internally converted to daily values using Fourier transformation, which is a smoothing algorithm that breaks down monthly input values into a smoothed daily times series. ACRU separates daily soil

evaporation and plant transpiration. The amount of transpiration between soil horizons is controlled by the root mass distribution between the two horizons. Soil water in excess of the permanent wilting point is considered available for transpiration by plants (Schulze, 1995).

In order to apply the Penman (1948) evaporation method available in ACRU, daily climate data are required, including daily minimum and maximum temperature, relative humidity, wind, incoming solar radiation, sunshine hours, and precipitation. The physically based Penman method for reference evaporation was used at a daily time step since it can simulate daily A-pan equivalent evaporation (mm/day), and it is the preferred technique by the model developers (Schulze, 1995). The mass transfer component of the Penman equation describes the change of vapor from a vegetated surface (Schulze, 1995). Saturated vapor pressure is empirically related to observed mean air temperature using Tetens' (1930) equation which is internally calculated in ACRU (Schulze, 1995).

Daily shortwave radiation values for each HRU were estimated by first calculating daily shortwave radiation for each base station using the Area Solar Radiation tool in ArcGIS (ESRI, 2008), and then adjusting those values to each HRU using monthly radiation correction factors, which were calculated for the entire UNSRB using the DEM. Shortwave radiation surfaces for each month were simulated with transmittivity and diffuse radiation values derived from the Environment Canada climate station at Edmonton City Centre Airport (Station ID 3012208), approximately 215km northeast of the center of the UNSRB.

Monthly mean potential sunshine hours were calculated for the UNSRB using the Area Solar Radiation tool in ArcGIS (ESRI, 2008). These simulated values were then corrected using observed actual sunshine hours from three climate stations, located northeast of the UNSRB: Ellerslie (Station ID 3012295), Edmonton City Centre Airport (Station ID 3012208), and Edmonton International Airport (Station ID 3012205). The correction factor for actual sunshine

hours is used to correct the differences between the average HRU sunshine hour values calculated from the simulated monthly surfaces, and the observed data.

A thirty year time series of observed daily wind and relative humidity was compiled by infilling data from the Rocky Mountain House (AUT) (Station ID 3015523) climate station. This station was used as the base station for both variables as it was the only station located in the study area that had relatively complete long term wind and relative humidity data. The infilling procedure for wind and relative humidity were the same as for temperature and precipitation described earlier. Daily relative humidity data from six stations in the study area with short term data were used to interpolate monthly surfaces for relative humidity. The surfaces were calculated in a GIS using a natural neighbor interpolation (ESRI, 2008) for each month. The ratio of the monthly mean values of relative humidity from Rocky Mountain House station and the interpolated surfaces was calculated to adjust monthly relative humidity values for each HRU. Four seasonal wind maps (i.e. Dec, Jan, Feb, (DJF) Mar, Apr, May, (MAM), Jun, Jul, Aug, (JJA), and Sep, Oct, Nov (SON)) of interpolated wind data from Environment Canada's Canadian Wind Energy Atlas (Government of Canada, 2003) were downloaded and georeferenced to the study area using ArcGIS. Mean monthly values for each HRU were calculated based on the wind maps, and then divided by the monthly mean station value from the base station to correct the daily wind data. The spatial relative humidity and wind adjustment factors were used to correct daily relative humidity and wind data from the base station relative to each HRU.

3.4.3.5 Land Cover Data

The *Circa 2000 Land Cover* data set, a generalized land cover map developed by the National Land and Water Information Service from multi-spectral Landsat satellite imagery for the agricultural extent of Canada (NLWI, 2008), was downloaded for this research. The original land cover data included eleven classes, which were later classified into nine classes: water/wetlands, exposed/developed land, shrubland, grassland, annual cropland, perennial crops

and pasture, coniferous forest, deciduous forest, and mixed forest. Some of the larger lakes, including both reservoirs at the hydroelectric dams, were not part of the original *Circa 2000 Land Cover* data set. A detailed shapefile of lake polygons was used in an overlay analysis in a GIS to create a separate land class for lakes. Glaciers were also not part of the original *Circa 2000 Land Cover* data set. Including glaciers as a land cover is critical as they have been shown to contribute up to 25% of the annual basin yield in extreme low flow years in glaciated watersheds (Young, 1991; Hopkinson et al., 1998). A shapefile of glaciers was compiled from information from the NTS map sheet data that was used to create the DEM. The shapefile was integrated into the land cover data set using GIS overlay analysis, creating a glacier land cover class. After adding the lakes and glaciers separately, there were a total of eleven land cover classes in the land cover data set.

3.4.3.6 Soil Data

ACRU requires soil texture and depth information for both the A-horizon and the B-horizon. If not otherwise available, the porosity, wilting point, field capacity, the portion of water redistributed from surface to subsurface horizons, and from subsurface to groundwater store can be estimated from the texture information, using internal look-up tables in ACRU (Schulze, 1995; Smithers and Schulze, 1995). One of the major challenges in this study was that soils are a key part in hydrological modelling; however, soils data in the study area were very inadequate.

A 1:50,000 soils map of the mountain parks area was obtained from Parks Canada, which included the dominant soil type (i.e. brunisol), for each land cover polygon. Soil data for the agriculture regions in Alberta have been documented in the AGRASID database (Government of Canada, 2001). The AGRASID database only covered 4% of the study area in the SE corner, but provided soil depth and texture information. Several published soil surveys and journal articles were also used as guides to facilitate the realistic estimation of soil types and soil depth as it is associated with land cover (Peters and Bowser, 1960; Pettapiece, 1971; Peters, 1981). The

acquired soils data and information were compiled in a GIS, where a regression analysis was performed between the soil parameters and land cover. This resulted in a number of GIS soil layers: a texture layer with percent sand, silt, and clay, and a soil depth layer for both A- and B-horizons. Using the percent sand and clay values and a soils triangle (Dingman, 2002), soil textures were assigned to each land cover type. Finally, soil texture and depth for the A- and B-horizons were calculated for each HRU. Based on the scarcity of soils information, the quality of these estimates remained uncertain.

3.4.3.7 Albedo and Rooting Depths

Literature values for monthly albedo values for each land cover were used as model inputs as no observed albedo values were available (Brutsaert, 1981; Gerrard, 1990; Pomeroy and Dion, 1996; Ahrens, 2006). Monthly average albedo values in summer are 0.26 for grass, and 0.15-0.16 for all forest types. In winter months, albedo values are modified daily as a function of snow cover. After fresh snowfall, the albedo is increased to 0.80, after which it decreases by 1.5% per day until it reaches 0.6. After the snow depth declines to 75mm, the albedo decreases rapidly, as an increasing proportion of the land surface is assumed to be snow free.

Model inputs for rooting depths for each land cover were taken from the literature as no observed values for these parameters were available (Strong and La Roi, 1983; Canadell et al., 1996; Jackson et al., 1996). In ACRU, the depth of the B-horizon is equivalent to the rooting depth. Proportions of root distribution between the A- and B-horizons were also estimated from the literature (Schulze, 1995; Smithers and Schulze, 1995).

3.4.3.8 Plant Transpiration Coefficients

As evapotranspiration is a critical part of the water balance, and with no estimates of plant water use for vegetation found in the study area available in the literature, plant transpiration coefficients (PTCs) were calculated for most of the vegetated land covers to provide

the basis for the simulation of actual evapotranspiration. Values for PTCs were calculated from observed metrological and flux data from grassland, aspen forest, and coniferous forest sites from Fluxnet Canada, and AmeriFlux flux towers in Alberta, Saskatchewan, and Colorado respectively. These stations were used as they were the most representative of the vegetation in the UNSRB from available flux stations. Data were obtained for 2005 for aspen and coniferous forests, and for 2007 for a grassland site. Measured latent heat flux data from each station were used to calculate the actual evapotranspiration (AET) for each site, using Equation 3.1 (Hornberger et al. 1998):

$$ET = E_l/\rho_w * \lambda_v \qquad \text{[Eq. 3.1]}$$

With

ET = evapotranspiration rate [m s^{-1}],

E_l = latent heat flux [J m^{-2} s^{-1}],

ρ_w = density of water [kg m^{-3}], and

λ_v = latent heat of vaporization [2.45×10^6 J kg^{-1}].

Meteorological data at each site were used in the Penman-Monteith equation to calculate potential evapotranspiration (PET) at each site. Canopy height and latitude of the sites were included as part of each calculation. The stomatal resistance value was set to "1" for each of the three sites to essentially eliminate stomatal resistance and control on calculated PET values. The AET was then divided by the PET value for each month to give a monthly PTC for grasslands, deciduous forest, and coniferous forest. Monthly PTC values are only needed from April to November, as the winter months (December to March) have little to no transpiration from plants as they are dormant in the winter. Any evaporation in the winter months is accounted for internally in ACRU with the Penman (1948) evaporation routine. PTCs were calculated for grassland areas in the UNSRB, but the data used were collected at a grassland site in the southern,

more arid part of Alberta. To account for a likelihood of increases in moisture in the study area compared to the values measured in a dryer climate, a value of 0.15 was added to each monthly PTC from March to November. PTCs for the coniferous forest were calculated from the Niwot Ridge Ameriflux tower in Colorado, which is about twelve degrees latitude south of the study area, but the coniferous forest stands and climate are fairly representative to what is found in the UNSRB. The July and December PTCs that were calculated from this site were adjusted to more represent the shape of the aspen site curve for those two months. The July value was increased from 0.50 to 0.69, and the December value was lowered from 0.25 to 0.18. This was done to adjust for differences in site location and climate differences between the Niwot Ridge site and the study area, as the seasonality from the aspen site, which is one degree north in latitude to the UNSRB, is more representative than seasonality from the coniferous site.

The PTCs for the mixed forest were calculated as the average between the aspen and coniferous stands as a 50/50 mix of both tree types is assumed. Shrubland PTCs were calculated by taking 60% of the grassland and 40% of the deciduous forest values. This was done based on field observations in the UNSRB, as most of what could have been classed as shrubland was comprised of deciduous shrubs with grasses as understory. The calculated PTC values are presented in Figure 3.3.

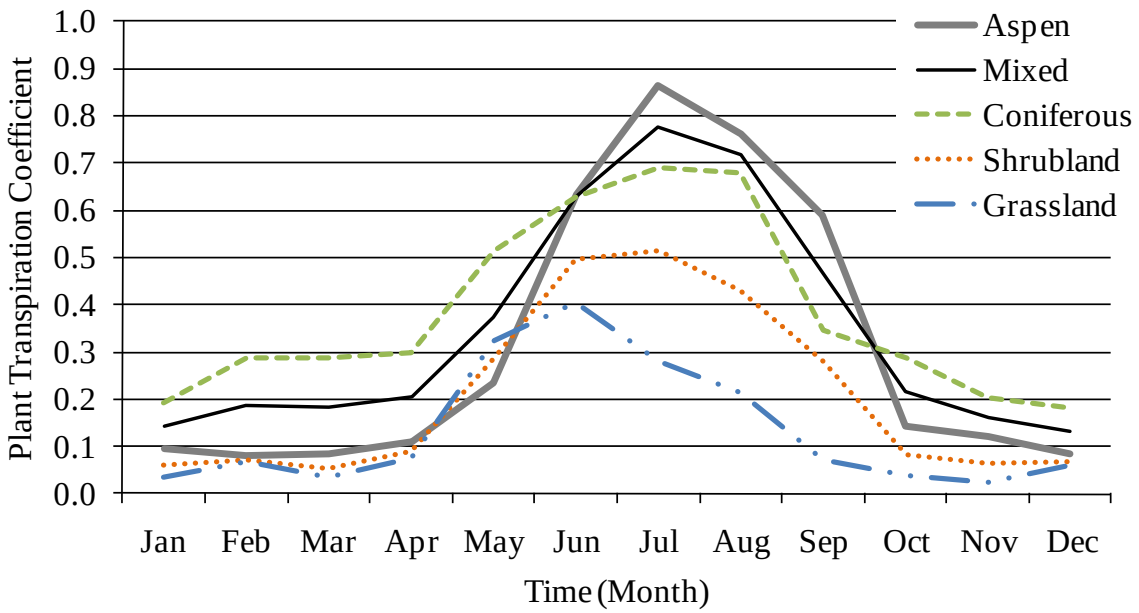

Figure 3.3: Calculated monthly PTC values from Fluxnet Canada and AmeriFlux data sets.

PTCs for cropland (annual and perennial crops) were calculated using the method after Krogman and Hobbs (1983). The PTCs for annual cropland are based on the three most common crops in central Alberta; wheat, barley, and alfalfa. Monthly PTCs from those crops were averaged to give a monthly PTC for the annual cropland land cover. PTCs for perennial crops/pasture were calculated by taking the average between alfalfa and grassland for each month. Most pasture land is a good mix of grasses, with some alfalfa. Wetlands were the only vegetated land cover type that was not calculated. Literature values in a study by Read et al. (2008) were averaged with the calculated PTC grassland values. An average was taken to better represent the more sedge-based wetlands observed in the UNSRB, as the wetlands from the literature were from reed bed wetlands. PTC values used in ACRU are listed in Table 3.2, with PTCs for crop being set to zero during the winter months. Figure 3.4 shows how the PTC values impact on the calculation of evapotranspiration in ACRU as a function of soil moisture, PET, and AET for the year 1973.

Table 3.2: Plant transpiration coefficients used in ACRU for land covers in the UNSRB.

Land Cover	Jan	Feb	Mar	Apr	May	Jun	Jul	Aug	Sep	Oct	Nov	Dec
Water/Wetlands	0.16	0.12	0.14	0.23	0.39	0.55	0.47	0.46	0.31	0.20	0.17	0.21
Shrubland	0.06	0.07	0.05	0.09	0.29	0.50	0.51	0.43	0.28	0.08	0.06	0.07
Grassland, Native Grass	0.04	0.07	0.04	0.08	0.32	0.40	0.28	0.21	0.07	0.04	0.02	0.06
Annual Cropland	0.00	0.00	0.00	0.34	0.44	0.97	1.14	0.53	0.31	0.07	0.04	0.00
Perenial Crops and Pasture	0.00	0.00	0.00	0.10	0.59	0.81	0.76	0.64	0.58	0.06	0.01	0.00
Coniferous Forest	0.19	0.29	0.29	0.30	0.51	0.63	0.69	0.68	0.35	0.29	0.20	0.18
Deciduous Forest	0.09	0.08	0.08	0.11	0.23	0.64	0.86	0.76	0.59	0.14	0.12	0.08
Mixed Forest	0.14	0.19	0.18	0.20	0.37	0.63	0.78	0.72	0.47	0.21	0.16	0.13

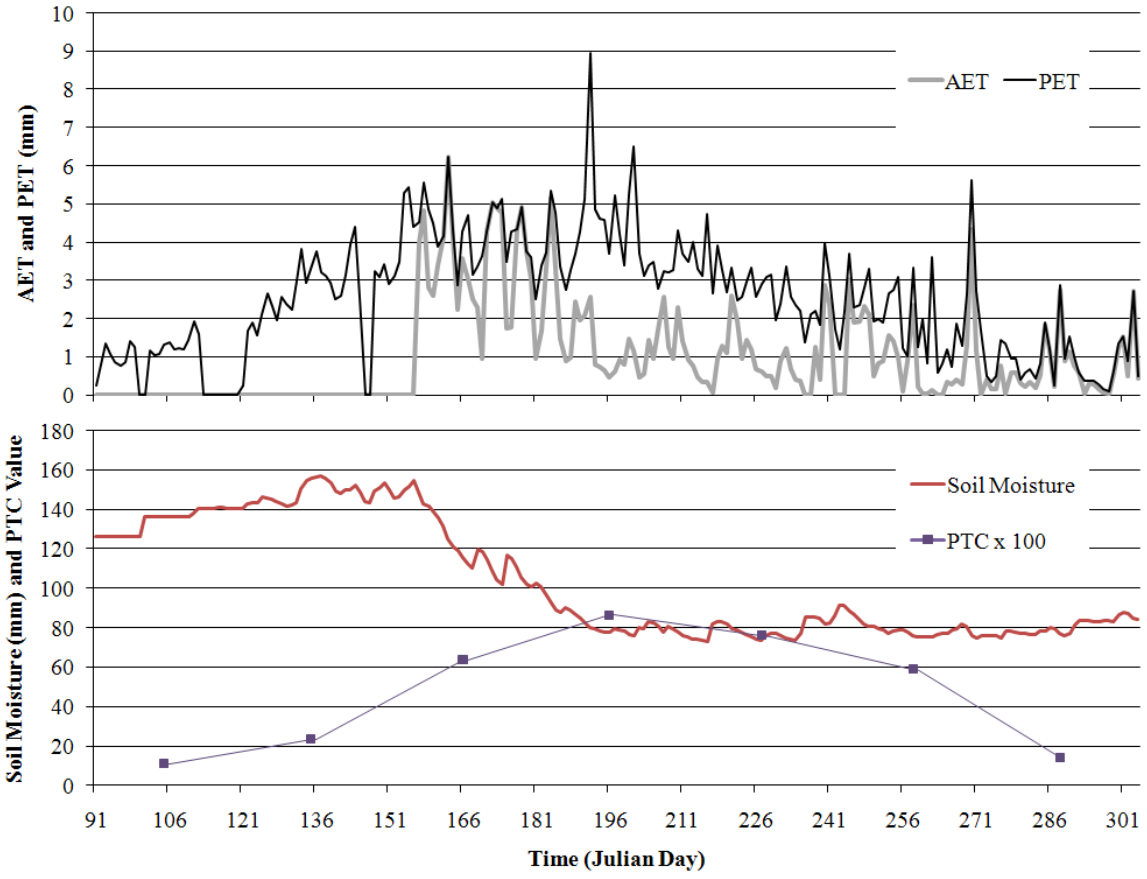

Figure 3.4: Monthly PTC value and daily simulated soil moisture (top) and daily simulated PET and AET (bottom) for one year from aspen forest HRU.

McWhorter and Sunada (1977) provide estimated monthly PTCs for several types of vegetation in the western United States, which were used as comparison against the calculated PTC values for the UNSRB. These values include a number of species from a number of western states, but were used to provide confidence in the calculated PTCs in terms of maximum

evapotranspiration rates and seasonality. For all three forest types, the peak calculated PTC was close to the peak value in the literature. For grassland and shrubland, the calculated curve matched the same of the values in the literature, but differed in magnitude. The difference in magnitudes and seasonality's from the literature is likely due to differences in number and location of species used to derive the values, but overall trends and magnitudes of PTCs calculated for the UNSRB agree with the literature.

3.4.3.9 Forest Canopy Coverage and Leaf Area Index

Values for forest canopy coverage were derived from field measurements in the southern part of the watershed from a study by Visscher et al. (2004), and calculated values from Alberta Vegetation Inventory (AVI) data, which is a photo-based inventory supported with air and ground observations (Government of Alberta, 2009). Values from Visscher et al. (2004) were observed in July, with AVI data based on observations in August, both months considered to be at peak biomass. A few non-peak biomass measurements for deciduous stands were used as a baseline for winter canopy cover values for deciduous forests (D. Visscher, personal communication, October 19, 2009). Canopy cover values for July and August were the average of measurements by Visscher, and the AVI values for deciduous and coniferous stands. Non-peak measurements in deciduous stands were used as winter canopy cover values. Monthly values for coniferous stands did not change, as overall seasonality of canopy coverage for pine/spruce stands varies little. Monthly values for deciduous forests were changed based on the phenological changes typically observed in central Alberta. For deciduous forests, the magnitude of these changes was calibrated to the curve of observed LAI values. There is no direct way to correlate canopy cover with LAI values; however it was the only data available to create a seasonal curve for a deciduous forest canopy for the UNSRB. Seasonality curve for LAI values can be seen in Figure 3.5. Monthly values for mixed forest stands were a monthly average of coniferous and deciduous stands.

Seasonal changes of LAI are used in ACRU to simulate changes in plant evaporation, soil water evaporation, and canopy interception. The latter is estimated using the Von Hoyningen-Huene method (Schulze, 1995). LAI data were obtained from MODIS (Moderate Resolution Imaging Spectroradiometer) satellite images that were downloaded from the National Snow and Ice Data Center (NSIDC) for the 2004 calendar year. Leaf Area Index (LAI) is a dimensionless value, being a ratio of the total one-sided leaf area per unit of ground surface area (Chen and Black, 1992). 2004 was used as it was most representative of a 'typical' year for moisture in the study area of the years available from the NSIDC website. An overlay analysis was carried out using the monthly MODIS images and the generalized land cover file to calculate mean monthly LAI values for each land cover class. For several land cover classes, December and January values were adjusted to smooth out the distribution to better reflect phenology of the various land cover types during the winter months. As the generalized land cover file was used to derive the LAI values for each land cover, the LAI values are assumed to be locally over- or under-estimated, but are overall representative for all land cover types. The seasonal changes of LAI values are presented in Figure 3.5.

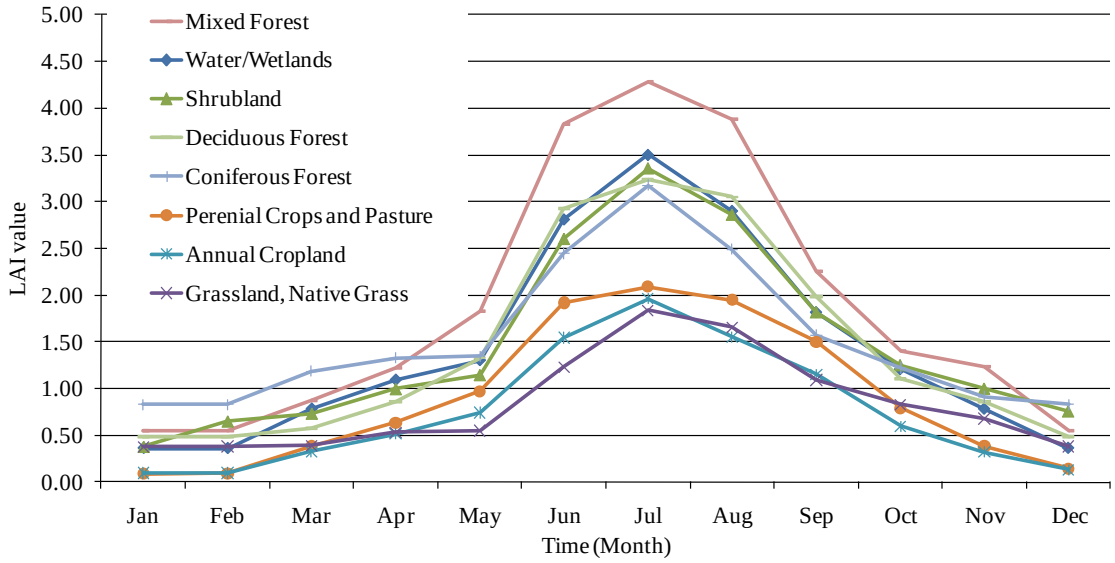

Figure 3.5: Adjusted LAI values for each land cover in the UNSRB derived from monthly MODIS images.

3.4.3.10 Snow and glaciers

In order to properly model magnitudes and timing of streamflow in the UNSRB, snow melt and glacial melt needed to be properly modelled and accounted for. In ACRU, snow water equivalent (SWE) is simulated differently in forested HRUs than in non-forested HRUs. When an HRU is predominantly forested, canopy interception and losses, changes in albedo values, net radiation, and temperature are calculated in a forest specific way, such as differences in albedo and radiation inputs in a forested versus an open area.

The threshold temperature that determines if precipitation falls as rain or snow, as well as the temperature range within which a proportion of precipitation falls as rain, were calculated for each HRU based on its average elevation and an empirical equation developed for the UNSRB. The critical temperature is based on the Kienzle Method (Kienzle, 2008), a curvi-linear threshold temperature based on temperature and elevation that determines, for a given air temperature, whether precipitation falls as rain or snow. The snow melt simulation is based on a dynamic degree-day factor, which is determined in ACRU on a daily basis from incoming radiation and albedo estimates.

The glacier melt routine in ACRU is simple in structure, and is based on a single variable, the glacier melt coefficient, which is based on the dynamically derived snow melt factor increased by a multiplier factor. All other variables that affect glacier melt like radiation, temperature, and albedo, have already been discussed and are used as part of the snowmelt routine in ACRU. Glacier melt begins after the snowpack is less than 10mm SWE, as redistribution of snow on the glacier would expose significant parts of the glacier. Reported glacier melt factors range between one and two times the snowmelt factor (Comeau et al., 2009; Shea et al., 2009).

3.4.3.11 Streamflow

ACRU generates total streamflow from simulated runoff, comprised of both same day and delayed quickflow, and baseflow volumes. Runoff generation is based on a modified Soil Conservation Service (SCS) procedure (United States Department of Agriculture, 1985), where runoff potential is conceptualized as a depth, and is a function of the soil's relative wetness (Schulze, 1995), conceptually representing the antecedent watershed conditions. The coefficients of initial abstractions are used in the SCS stormflow calculations and refer to initial amounts of precipitation that do not contribute to the generation of stormflow because of the processes of initial infiltration, interception, or temporary surface storage in hollows, before stormflow begins.

Baseflows are generated by soil water when it exceeds field capacity and percolates as groundwater recharge and is added to the groundwater store (Schulze, 1995). Recessions curves from hydrographs of observed streamflow data are used to derive response coefficients to characterize the temporal response of surface runoff and baseflows for each HRU. These parameters control the stormflow and baseflow responses for each HRU. Stormflow response, or the fraction of the total stormflow that will run off from the HRU on the same day as a rainfall event, is a coefficient that can be changed from a value of 0.01 to 1.00. This coefficient was calibrated to be 0.2 in Watershed 1 and 0.25 in Watershed 2. Baseflow response, or the fraction of water from the intermediate/groundwater store that becomes streamflow on a particular day, is a coefficient that can be changed from a value of 0.001 to 1.000. This baseflow response coefficient was calibrated to be 0.006 for Watershed 1 and 0.001 for Watershed 2.

3.5 Verification of hydrological processes

ACRU was verified against five observed data sources: air temperature, A-pan potential evapotranspiration, snowpack accumulation and melt from snow pillows and snow courses, Peyto Glacier glacial melt contributions and its equilibrium line altitude, and daily observed streamflow time series for two WSC stations. Table 3.3 lists the data source used in this calibration and

verification study, with the respective locations presented in Figure 3.6. In order to reveal if the simulated hydrological variables were representative of the observed ones, seasonal changes, daily and monthly time series are compared statistically, including the coefficient of determination (r^2), the regression coefficient (slope), the regression intercept, and the difference of the variances and means. The Nash-Sutcliff coefficient (E) is typically used to evaluate hydrological model performance (Legates and McCabe, 1999), and were used in this analysis.

Table 3.3: Observed data stations and sources for verification of hydrological processes from ACRU output.

	Station Name	Station ID	Elevation (masl)	Observed Time Period	Observed Data	Observed Variable
1	Chedderville CDA EPF	3011520	1036	1954-1977	Annual	Max and Min Temperature
8	Sask River Crossing 2	3055754	1392	1976-2007	Annual	Max and Min Temperature
7	Ram Falls	3055379	1641	1989-2007	Annual	Max and Min Temperature
6	Parker Ridge	3054998	2023	1978-2007	Annual	Max and Min Temperature
9	Scalp Creek	3055761	2042	1982-2007	Annual	Max and Min Temperature
4	Cline LO	30516F5	2050	1975-2007	Seasonal	Max and Min Temperature
5	Grave Flatts LO	3052940	2074	1960-2007	Seasonal	Max and Min Temperature
3	(AE) Bow Summit	3050PPF	2080	1998-2007	Annual	Max and Min Temperature
2	Baldy LO	3050490	2083	1960-2007	Seasonal	Max and Min Temperature
10	Upper Parker Ridge	3056657	2317	1998-2007	Annual	Max and Min Temperature
11	Ellerslie	3012295	694	1964-1986	Seasonal	A-pan evaporation
12	Edmonton INT'L A	3012205	723	1959-2008	Seasonal	A-pan evaporation
13	Highvale	3013247	747	1977-2006	Seasonal	A-pan evaporation
14	Limestone Snowpillow	40024	1950	1984-2008	Annual	SWE
15	Southesk Snowpillow	40040	2200	2006-2008	Annual	SWE
16	Brazeau Reservoir	40072	970	1977-2008	Seasonal	SWE
17	Crimson Lake	40378	970	1973-2007	Seasonal	SWE
18	Caroline (AB0)	AB0	1070	2002-2006	Seasonal	SWE
19	Clearwater RS (AB1)	AB1	1280	2002-2006	Seasonal	SWE
20	Brown Creek	40379	1340	1977-2008	Seasonal	SWE
21	Nordegg	40305	1465	1974-2008	Seasonal	SWE
22	Watchman Creek	40385	1830	1985-2002	Seasonal	SWE
23	Nigel Creek	40382	1920	1968-2008	Seasonal	SWE
24	Limestone East (AB4)	AB4	1950	2002-2006	Seasonal	SWE
25	Limestone Ridge	40024	1950	1983-2008	Seasonal	SWE
26	Job Creek 2	40021	2005	1993-2008	Seasonal	SWE
27	Golden Eagle	40378	2090	1985-2008	Seasonal	SWE
28	Job Creek 1	40021	2100	1985-2008	Seasonal	SWE
28	Limestone West (AB5)	AB5	2120	2002-2006	Seasonal	SWE
29	Southesk	40040	2200	1986-2008	Seasonal	SWE
30	Peyto Glacier	-	2140-3180	1966-2007	Annual	Glacier Mass Balance/ELA
31	NSR below Bighorn Dam	-	1246	1911-2008	Annual	Streamflow
32	NSR at Whirlpoot Point	05DA009	1373	1970-2007	Seasonal	Streamflow

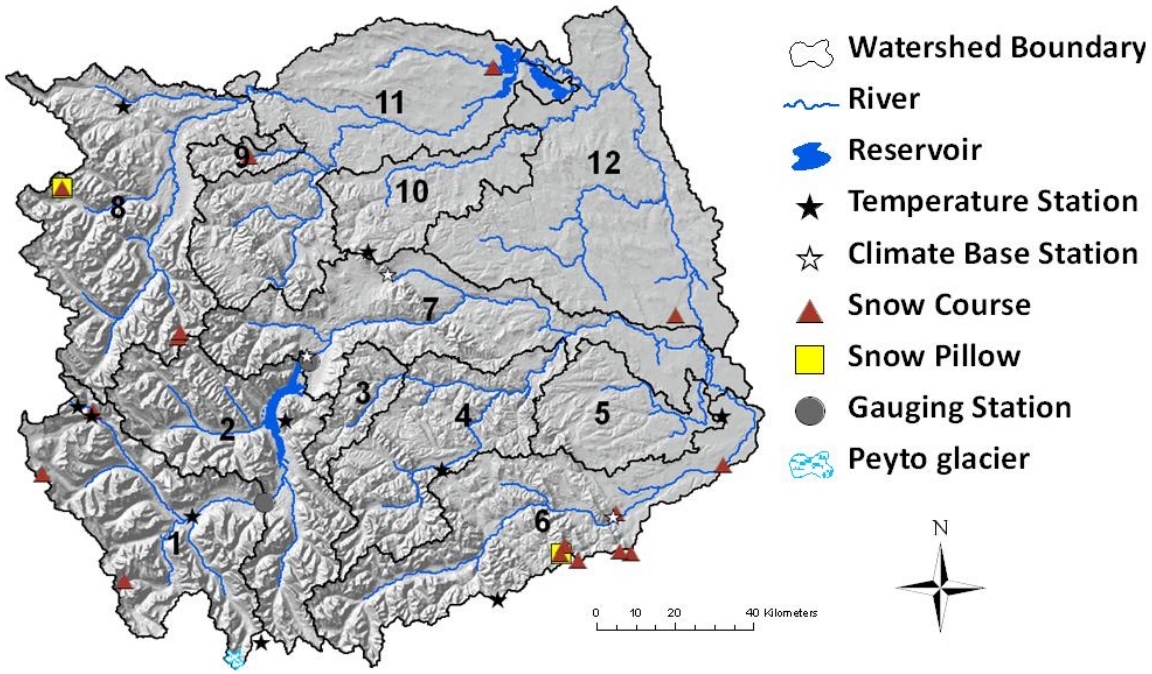

Figure 3.6: Location of all verification sites in the UNSRB, except stations with observed A-pan which are found north east of the UNSRB. Watersheds are numbered, with locations for each of the hydroelectric reservoirs, and river system of the UNSRB.

3.5.1 Verification of Temperature

Observed daily maximum and minimum temperature data from ten climate stations across the study area were used to verify that the derived monthly minimum and maximum temperature lapse rates were properly simulating temperatures across the UNSRB. Observed daily minimum and maximum temperatures were used to calculate mean daily temperatures from each of the ten stations, which were then verified against simulated daily mean temperatures. ACRU used the mean daily air temperature for calculations of hydrological variables such as daily evapotranspiration, the separation of precipitation into rain and snow, and snow or glacier melt.

3.5.2 Verification of Potential Evapotranspiration

The US Class A-pan is one of the most widely used methods to measure potential evapotranspiration (PET) (Stanhill, 2002). The only available observed A-pan evaporation data

were collected at three climate stations outside the study area, all of which are just over 100km northeast of the study area (Table 3.3). The observed data were used to determine if simulated PET was within physically meaningful ranges for the UNSRB. All three stations with observed A-pan data had very similar values for each of the six months of observed data (May-October). Thus, monthly A-pan values were averaged for all three stations. A-pan has been shown to overestimate crop reference evaporation by up to 30% (Van Zyl et al., 1989), so observed values were reduced by 30%. To use these observed data to verify that the model was adequately simulating the seasonality and magnitude of PET in the region, an HRU with a similar land cover, elevation, and closest to the A-pan stations was selected (HRU 1497).

3.5.3 Verification of Snow Water Equivalent

Observed snow water equivalent (SWE) data from 15 snow courses and two snow pillows in the study area were used to verify that snowfall depths and timing of spring melt were properly simulated (Table 3.3, Figure 3.6). Eleven of the snow courses found throughout the watershed and the two snow pillows were provided by Alberta Environment. Another set of more recent snow course from the southern part of the watershed, with detailed description of the area surrounding each snow course, was obtained from the Foothills Orographic Precipitation Experiment (FOPEX) by Environment Canada (Smith, 2009). Snow course measurements are carried out approximately once a month. Snow pillow daily time series were used to determine if the snow pack development, maximum annual SWE, and timing of spring melt were properly simulated.

3.5.3.1 Challenge of modelling SWE

In ACRU, forested and non-forested HRUs are simulated differently. The forest canopy cover has a much higher interception rate, resulting in lower snowfall reaching the ground. Forests have larger leaf area indices, which has also an impact on ground air temperature. And lastly, forests are simulated to have enhanced evapotranspiration due to canopy turbulence.

When an HRU was considered forested, SWE was often severely under-simulated. Conversely, SWE was often well over-simulated in non-forested HRUs. This was an indication that ACRU's forest functions were too restrictive to snow accumulation, and thus not representative of the study area.

Based on field experience, snow courses are often located in forests, where there is a mix of open and forested areas. Clearings and open canopy forests were both observed during a field trip to the study area in August 2009. Photos obtained from Alberta Environment for the two snow pillow locations revealed that both were in small clearings within a larger forested area (see Figure 3.7). Both these areas have characteristics of open areas and forested areas. The generalized land cover is not detailed enough to distinguish between various forest densities, and consequently, HRUs were classified either (fully) forested or (fully) non-forested. This could have been the case with the Southesk snow pillow as just to the north of the snow pillow is a large, mainly non-forested area, partly seen in Figure 3.7.

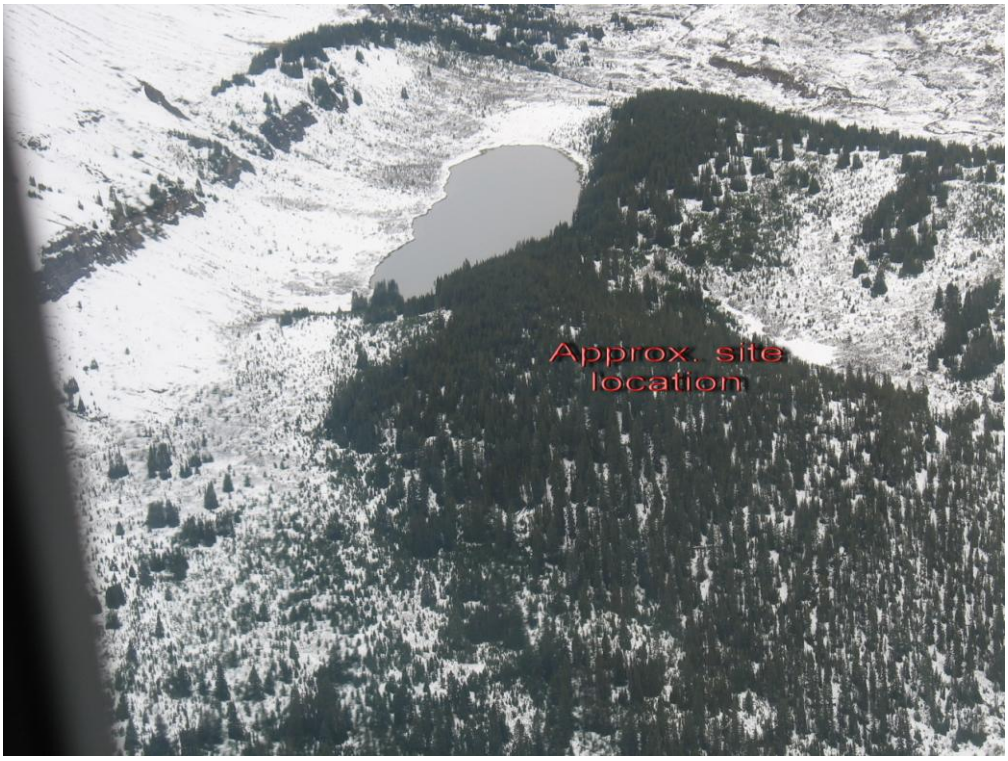

Figure 3.7: Southesk snow pillow (top) and Limestone snow pillow (bottom), both in forested HRUs, but clearly have characteristics of both forested and open areas. (Photos courtesy of Jon Pedlar and Rick Pickering from Alberta Environment).

Based on Figure 3.7 and initial simulations showing that a non-forested HRU more closely simulated the observed SWE measurements in forested HRUs, it was decided to use a ratio of simulated output assuming both forested and non-forested conditions for the same HRU. This accounts for the location of the snow stations being partly open and partly forested. Daily SWE values were simulated twice, once assuming a forest, and once assuming a non-forest. A ratio of 70% non-forested and 30% forested SWE values were found to result in the best comparison with observed data. However, for streamflow simulations and verification, and later the evaluation of the impact of climate change on streamflows, HRUs remained either fully forested or fully non-forested.

3.5.4 Verification of glacial contributions to streamflow

Glacial mass balance data from Peyto Glacier were used to verify that average annual streamflow contributions from glacial melt and the average equilibrium line altitude (ELA) were properly simulated. Peyto Glacier is located in the very southwest corner of the UNSRB (Figure 3.6), and has been extensively monitored and studied for a number of decades (Loijens, 1974; Luckman, 1998; Demuth and Pietroniro, 2003; Comeau et al., 2009; Demuth and Keller, 2009; Shea et al., 2009). ELA, the average highest altitude at which glacier melt occurs for any given year, was used to verify that glaciers in higher altitudes were not being melted out every year, and that, on average, only glaciers at or below the reference ELA were producing significant glacial melt volumes to streamflow. The average cumulative net balance for Peyto Glacier for the last 30 years was also used to calibrate and verify that average annual glacial melt contributions from Peyto Glacier closely associated with observed data.

3.5.5 Verification of Streamflow

Streamflow verification was done for each watershed in the UNSRB. Here, only the results of streamflow verification on Watersheds 1 and 2 were reported, which produce the streamflow feeding into Lake Abraham, the reservoir for the Bighorn Dam (Table 3.3, Figure

3.6). Observed streamflow data from a Water Survey of Canada (WSC) gauging station were used for Watershed 1. The data for Watershed 2 is just downstream of the Bighorn Dam, so calculated naturalized flow data provided by Alberta Environment was used.

3.5.5.1 Method to calibrate and verify simulated streamflow with observed data

The WSC gauging station at the outlet of Watershed 1 provided only observed data for 1970-2007. Consequently, the calibration using the entire 1961-90 time period was not possible. A further complication is the fact that the climate base station used to provide daily climate time series to the model consistently has years where there is an obvious mismatch between the precipitation observed at the climate station and the streamflow observed at the watershed outlet (see Figure 3.12). For these reasons it was decided to calibrate streamflow for a minimum 10 year continuous time period where: 1) the magnitude of precipitations from the climate station matched the observed streamflow, considering a typical range of runoff coefficients observed for the watershed and 2) that the time period selected contained at least one of the lowest and one of the highest observed peak flows in the whole time series. After detailed analyses, the 1981-1992 time period was selected for Watersheds 1 and 2.

Once Watershed 1 was satisfactorily simulated in terms of overall water yields, annual hydrographs, and seasonality for the calibration time period, streamflow for the whole 1961-1990 time period was simulated and compared against observed streamflows for all years with observed data. After the ACRU setup for Watershed 1 was considered complete, Watershed 2 was simulated and calibrated in a similar fashion.

The calibration of simulated streamflow to observed streamflow followed a series of processes, depending if initial parameter settings resulted in over or under-simulations. Watershed 1 was the only watershed to have initial under-simulations of streamflow, and initial glacial melt variables needed to be calibrated using available information for Peyto Glacier. To

deal with over-simulation of streamflow, four variables were considered to be changed: soil depth, wind, relative humidity (RH), and precipitation. These data sets had the highest uncertainty, as only limited data and coarse approximations were available for all four variables. Generally, volumes for each watershed can be calibrated by increasing evapotranspiration (increasing wind and decreasing RH), and potentially increasing soil depths within physically possible ranges. To further correct over-simulation of water yields, and to help correct major difference in seasonal runoff, precipitation correction factors could be further adjusted to account for the disconnection between precipitation input values from a base station and hydrographs from a watershed. After simulated water yields were within an acceptable range from the observed, two parameters were calibrated to fit the observed recession curves: the baseflow generation and the fraction of total stormflow that will run off from an HRU on the same day.

3.6 Verification Results

3.6.1 Temperature

Observed daily maximum and minimum temperature data from ten climate stations across the study area were used to verify that the monthly mean temperatures were properly simulated in model runs. Mean temperatures from simulated output and observed data were calculated and compared at all ten climate stations. Figure 3.8 shows the seasonality of mean temperatures, with good association of simulated and observed temperatures. Objective measures of modelling performance for monthly and daily mean temperatures simulated by ACRU are show in Table 3.4. Monthly and daily temperatures are slightly over-simulated, with monthly mean temperatures being statistically not different ($p=0.46$) and daily temperatures statistically different ($p=0.00$) as indicated from the P-values from the two-tailed t-tests. Both daily and monthly differences between variances are low (-4.64% and -3.79% respectively), thereby decreasing the reliability of the t-statistic. Correlation statistics were also good, as seen in Table 3.4.

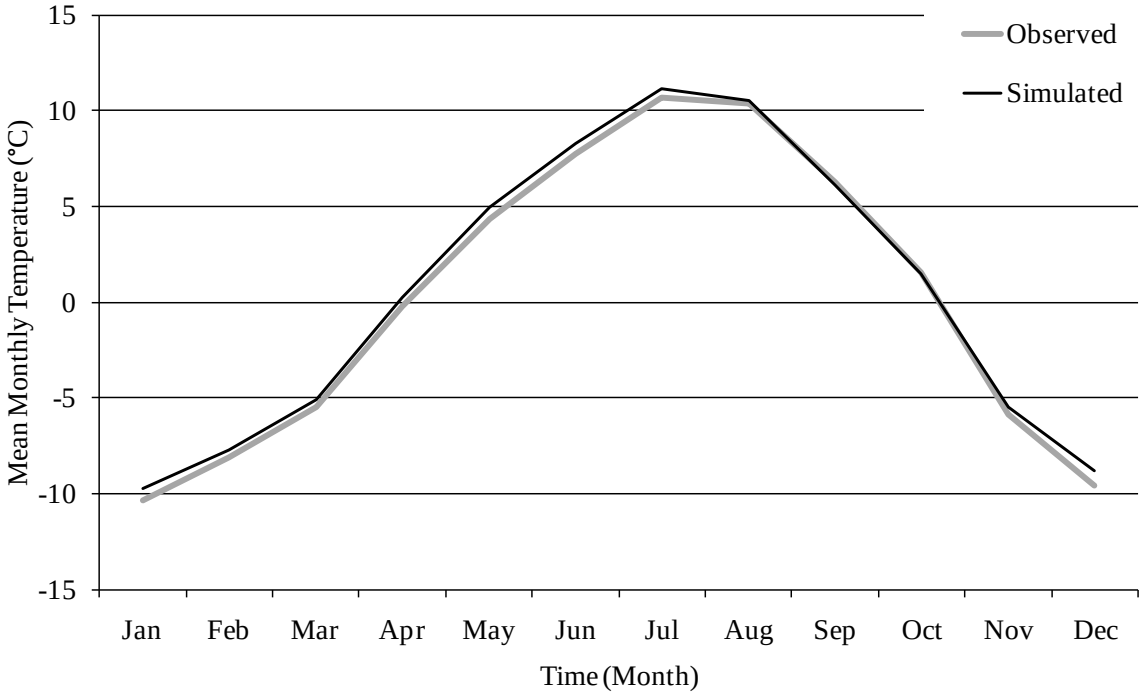

Figure 3.8: Mean monthly temperatures for simulated and observed data from 10 climate stations in the UNSRB.

Table 3.4: Daily and monthly model performance of model output when compared to all ten observed temperature stations.

	Daily	Monthly
Observed Sample Size (Days/Months)	37402	499
Simulated Sample Size (Days/Months)	37402	499
Observed Mean (°C)	3.30	0.40
Simulated Mean (°C)	3.67	0.77
P(T<=t) two-tail	0.00	0.46
Observed Variance	78.98	67.04
Simulated Variance	75.48	64.59
% Difference	-4.64	-3.79
Coefficient of Determination (r^2)	0.88	0.98
Regression Coefficient (Slope)	0.92	0.97
Regression Intercept	0.75	0.39

3.6.2 Potential evapotranspiration (PET)

Simulated PET from HRU 1497 was compared to the observed average of all three stations northeast of the study area. Table 3.5 shows the statistical analysis of simulated A-pan compared to observed. Based on the P-value from a two-tailed t-test, the means are not statistically different (p=0.14). Simulated variance has a -2.5% difference from the observed, and simulated data show an overall correspondence with the observed with an r^2=0.78. The regression coefficient (0.87) is less than unity, and indicates an overall under-simulation of PET, with a y-intercept of -0.58. Seasonality of A-pan was properly simulated, however magnitudes were consistantly under-simulated.

Table 3.5: Monthly model performance of model output when compared to observed A-pan data.

Observed Sample Size (Months)	100
Simulated Sample Size (Months)	1519
Observed Mean (mm)	3.17
Simulated Mean (mm)	2.19
% Difference	-30.91
P(T<=t) two-tail	0.14
Observed Variance	1.20
Simulated Variance	1.17
% Difference	-2.50
Coefficient of Determination (r^2)	0.78
Regression Coefficient (Slope)	0.87
Regression Intercept	-0.58

3.6.3 Snow water equivalent (SWE)

Model output was visually and statistically compared to observed data from 15 snow course and two snow pillow sites. Figure 3.9 presents a typical comparison of simulated and observed, in terms of the magnitude of peak SWE depth, and the timing of snowpack melt from a snow pillow. Figure 3.10 presents a typical comparison of simulated and observed SWE time

series for a snow course. When compared to all observed SWE, overall SWE depths were simulated fairly well, considering the geographical extent of the watershed, and the few climate base stations available to drive the model. Peak SWE is sometimes over- and sometimes under-simulated, while some years are well simulated.

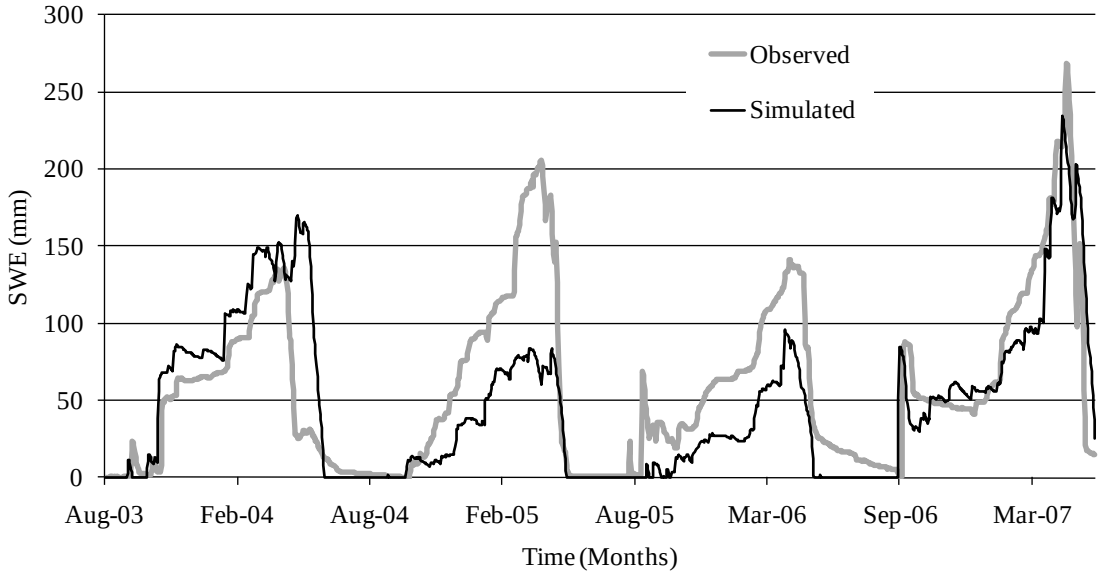

Figure 3.9: Four years of simulated and observed SWE at Limestone Snow Pillow in the southern part of the UNSRB.

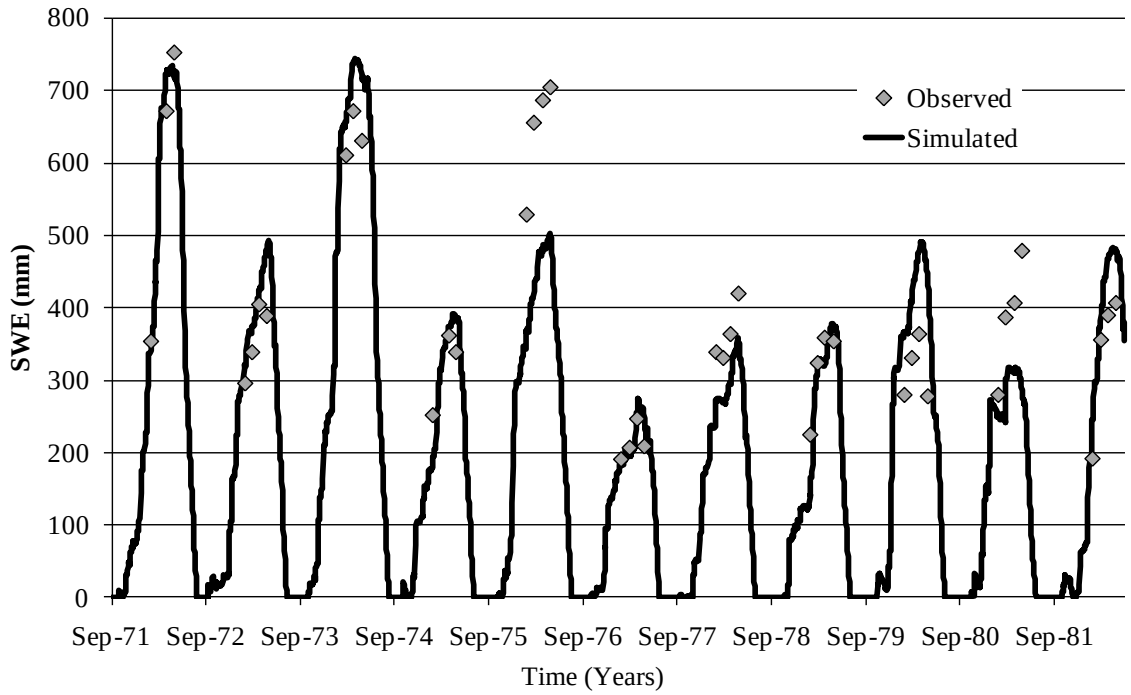

Figure 3.10: Ten years of simulated and observed SWE at Nigel Creek snow course in the western part of the UNSRB.

The 15 snow courses had a total of 882 observations, and the two snow pillows a total of 7625 observations, for a total of 8507 days with observed data. Table 3.6 shows the statistical analysis for all the daily observed and simulated SWE for the snow courses, the snow pillows, and all SWE data. Daily SWE depths are slightly under-simulated, with daily SWE depths not statistically different for the snow courses ($p=0.45$). SWE depths are considered statistically different for the snow pillows and when all the snow data is compared together, as indicated from the P-value of the two-tailed t-test (Table 3.6). The overall simulation of high and low snowfall years is preserved, as the difference between variances is low (4.03%) when compared to all observed SWE data. Overall correlation statistics are good when all SWE data are compared with simulated and relatively good correlation between observed and simulated SWE depths for all three data groups. The regression coefficient is less than unity when simulated is compared to the observed for all SWE data groups, indicating a systematic and overall under-simulation.

Table 3.6: Model performance for all observed snow course, observed snow pillow, and all observed snow data.

	Snow Course	Snow Pillow	All SWE
Observed Sample Size (Days)	882	7625	8507
Simulated Sample Size (Days)	882	7625	8507
Observed Mean (mm)	190.59	74.12	86.20
Simulated Mean (mm)	196.99	67.83	81.21
% Difference	3.25	-9.27	-6.14
P(T<=t) two-tail	0.45	0.00	0.01
Observed Variance	34342.08	5414.08	9670.20
Simulated Variance	28013.48	6274.50	10075.89
% Difference	-22.59	13.71	4.03
Regression			
Coefficient of Determination (r^2)	0.61	0.57	0.63
Regression Coefficient (Slope)	0.70	0.81	0.81
Regression Intercept	62.85	7.65	11.33
Regression Through Origin			
Coefficient of Determination (r^2)	0.54	0.56	0.62
Regression Coefficient (Slope)	0.87	0.86	0.87

3.6.4 Glacial contributions to streamflow

Glacial mass balance data from Peyto Glacier were used to verify that average annual streamflow contributions from glacial melt were properly being simulated, and that the average equilibrium line altitude (ELA) was also being simulated properly. Based on the mass balance information (WGMS, 2009), the annual glacial melt has been very steady between 1977 and 2004 at approximately 730mm, with very few years significantly deviating from this value. ACRU's glacier melt factor was calibrated accordingly, and the degree day melt factor is 0.84-1.5 times the dynamic snow melt factor. The average ELA simulated in the UNSRB is around 2700masl. The ELA for Peyto, and other glaciers in this area fluctuates annually, but on average is reported to be between 2612masl (WGMS, 2009) and 2700masl (Demuth and Keller, 2009), but can be high as 3190masl in warm years. This glacier melt is simulated to result, on average, in a

situation where HRUs below the ELA contribute about 85-90% of the glacial melt, while 10-15% occurs above the ELA.

3.6.5 Streamflow

3.6.5.1 Watershed 1

Simulated streamflow produced in Watershed 1 was compared to the observed data from the gauging station at the outlet. Table 3.7 shows the statistical analysis for daily and monthly simulated and observed streamflow data for the 1981-92 calibration time series, and the 1970-90 verification time series. Watershed 1 has only observed streamflow data starting in 1970, so the historical base period 1961-90 could only be verified for the period 1970-90. Total water yields were slightly under-simulated for both time series by around 4% for the calibration time series and less than 1% for the full 1970-90 time series. Mean flows were simulated well as none of the simulated means were statistically different ($p>0.05$) from the observed, as indicated from the P-values of the two-tailed t-tests in Table 3.7. The difference between variances is fairly low for daily statistics, and very good for monthly statistics, indicating that simulation of peak and low flows were preserved. Overall correlation statistics are good, with relatively good correlation between observed and simulated flows, as indicated by a high r^2 value for all daily and monthly time series. Figure 3.11 shows scatter plots with the regression equations for both daily and monthly streamflow time series. The regression coefficient is less than unity on a daily and monthly basis for all time series, which indicates a slight under-simulation of high flows. The Nash-Sutcliff coefficient is also high for both daily (0.83) and month streamflow simulations (0.99), indicating a strong overall fit with the observed streamflow data. Overall, ACRU simulated the behavior of Watershed 1 reasonably well with peak and low flows simulated well overall, including the recession curve for baseflow.

Table 3.7: Daily and Monthly stats for both the 1981-92 calibration period, and from 1970-90 for Watershed 1.

	Daily		Monthly	
	1981-92	1970-90	1981-92	1970-90
Observed Sample Size (Days/Months)	4383	7510	144	248
Simulated Sample Size (Days/Months)	4383	7510	144	248
Observed Mean (m^3/s)	14.7	14.5	14.6	14.5
Simulated Mean (m^3/s)	14.1	14.4	14.0	14.4
% Difference	-4.3	-0.8	-4.3	-0.5
P(T<=t) two-tail	0.11	0.70	0.76	0.96
Observed Variance	342	336	294	285
Simulated Variance	289	328	258	295
% Difference	-18.7	-2.3	-13.9	3.4
Observed Standard Deviation	18.5	18.3	17.2	16.9
Simulated Standard Deviation	17.0	18.1	16.1	17.2
% Difference	-8.9	-1.2	-6.7	1.7
Coefficient of Determination (r^2)	0.86	0.83	0.95	0.91
Regression Coefficient (Slope)	0.85	0.90	0.91	0.97
Regression Intercept	0.26	0.22	0.11	0.06
Nash-Sutcliff Coefficient		0.83		0.99

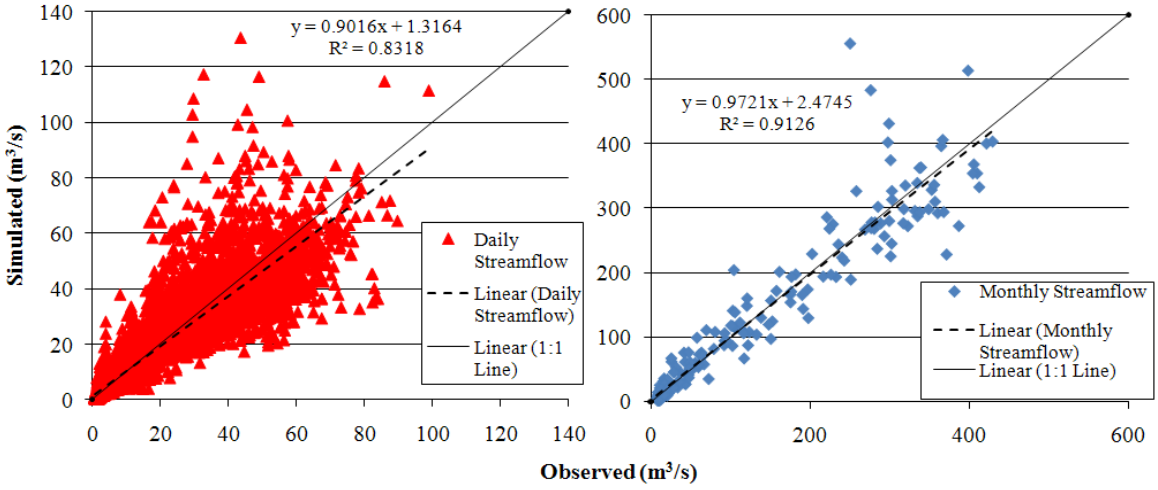

Figure 3.11: Daily and monthly regression scatter plots for observed and simulated streamflow for Watershed 1 for the 1970-1990 time series.

3.6.5.2 Watershed 2

Simulated streamflow from Watershed 2 was compared to the naturalized streamflows from a station just downstream of Bighorn Dam, provided by Alberta Environment. Table 3.8 presents the statistical analysis for daily and monthly observed and simulated streamflow data for the 1981-92 calibration time series, and the 1961-90 simulation time series. Total daily water yields were slightly under-simulated for the calibration time series (0.59%) and slightly over-simulated for the 1961-90 time series (2.18%). Mean flows were simulated well as none of the simulated means were statistically different ($p>0.05$) from the observed, as indicated from the P-values of the two-tailed t-tests (Table 3.8). The difference between variances is very good for daily and monthly statistics, indicating that simulation of peak and low flows were preserved. Overall correlation statistics are good, with a strong correlation between observed and simulated flows as shown by a high r^2 value for all daily and monthly time series. Figure 3.12 shows scatter plots with the regression equations for both daily and monthly streamflow time series. The regression coefficient is less than unity on a daily and monthly basis for all time series, which indicates a slight under-simulation of high flows, more so on a daily than a monthly basis. The Nash-Sutcliff coefficient is also high for both daily (0.82) and month streamflow simulations (0.99), indicating a strong overall fit with the observed streamflow data.

Table 3.8: Daily and Monthly stats for both the 1981-92 calibration period, and from 1961-90 for Watershed 2.

	Daily		Monthly	
	1981-92	**1961-90**	**1981-92**	**1961-90**
Observed Sample Size (Days/Months)	4383	10957	144	360
Simulated Sample Size (Days/Months)	4383	10957	144	360
Observed Mean (m^3/s)	78.4	81.2	78.0	80.8
Simulated Mean (m^3/s)	78.0	83.0	77.6	82.5
% Difference	-0.6	2.1	-0.6	2.1
P(T<=t) two-tail	0.80	0.16	0.96	0.78
Observed Variance	8147	8756	6869	7419
Simulated Variance	6951	8445	6107	7402
% Difference	-17.2	-3.7	-12.5	-0.2
Observed Standard Deviation	90.3	93.6	82.9	86.1
Simulated Standard Deviation	83.4	91.9	78.1	86.0
% Difference	-8.3	-1.8	-6.1	-0.1
Coefficient of Determination (r^2)	0.87	0.83	0.96	0.92
Regression Coefficient (Slope)	0.86	0.89	0.92	0.96
Regression Intercept	0.24	0.23	0.13	0.11
Nash-Sutcliff Coefficient		0.82		0.99

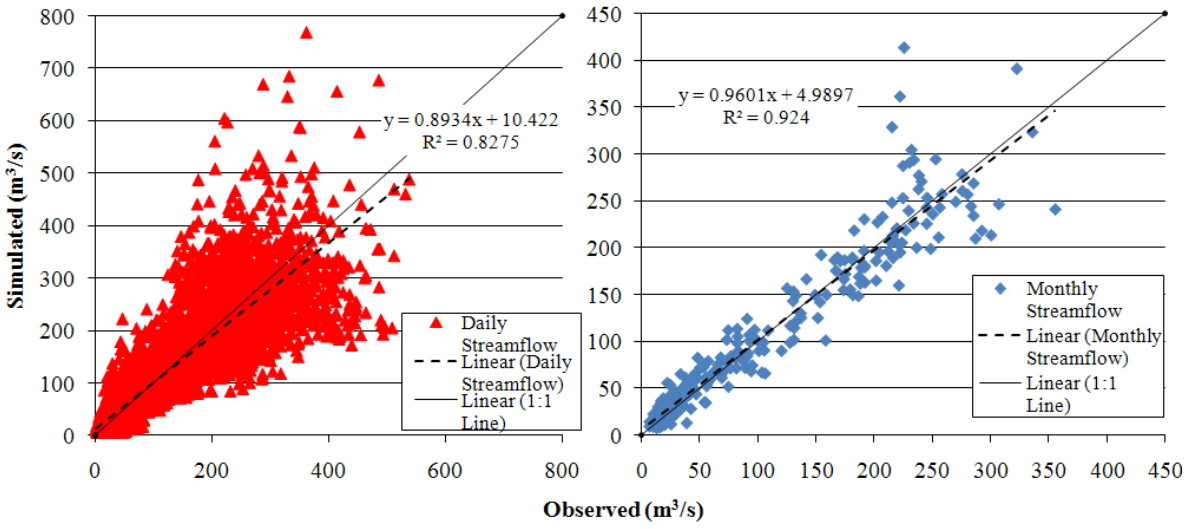

Figure 3.12: Daily and monthly regression scatter plots for observed and simulated streamflow for Watershed 2 for the 1961-1990 time series.

Generally, ACRU simulated the behavior of Watershed 2 well. The timing of peak and baseflows are simulated well (Figures 3.13 and 3.14). When the whole 1961-90 time series is evaluated, peak flows are sometimes over-simulated, sometimes under-simulated, and most often match the observed flows well. This is to be expected when climate data are transferred from a base station, which has a distance of up to 75km to the watershed HRUs. Timing and magnitudes of baseflows show a similar pattern of over and under-simulation as seen in the peak flows, but the overall recession curve is simulated very well. Figure 3.15 shows the seasonality of observed and simulated for the whole 1961-90 time series, which was well simulated overall with slight over-simulations in August, October, and November.

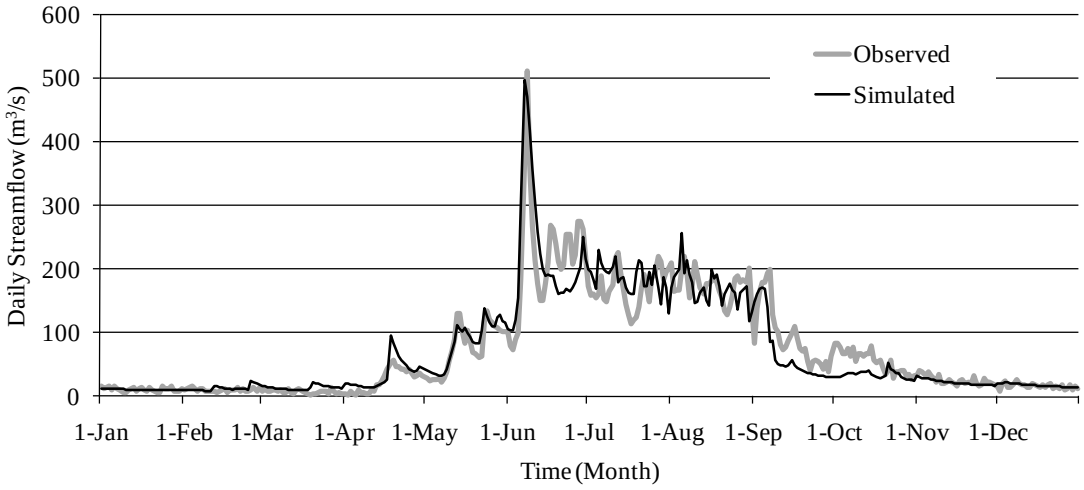

Figure 3.13: Annual hydrograph for Watershed 2, showing timing and magnitudes of simulated peak and low flow compared to the observed.

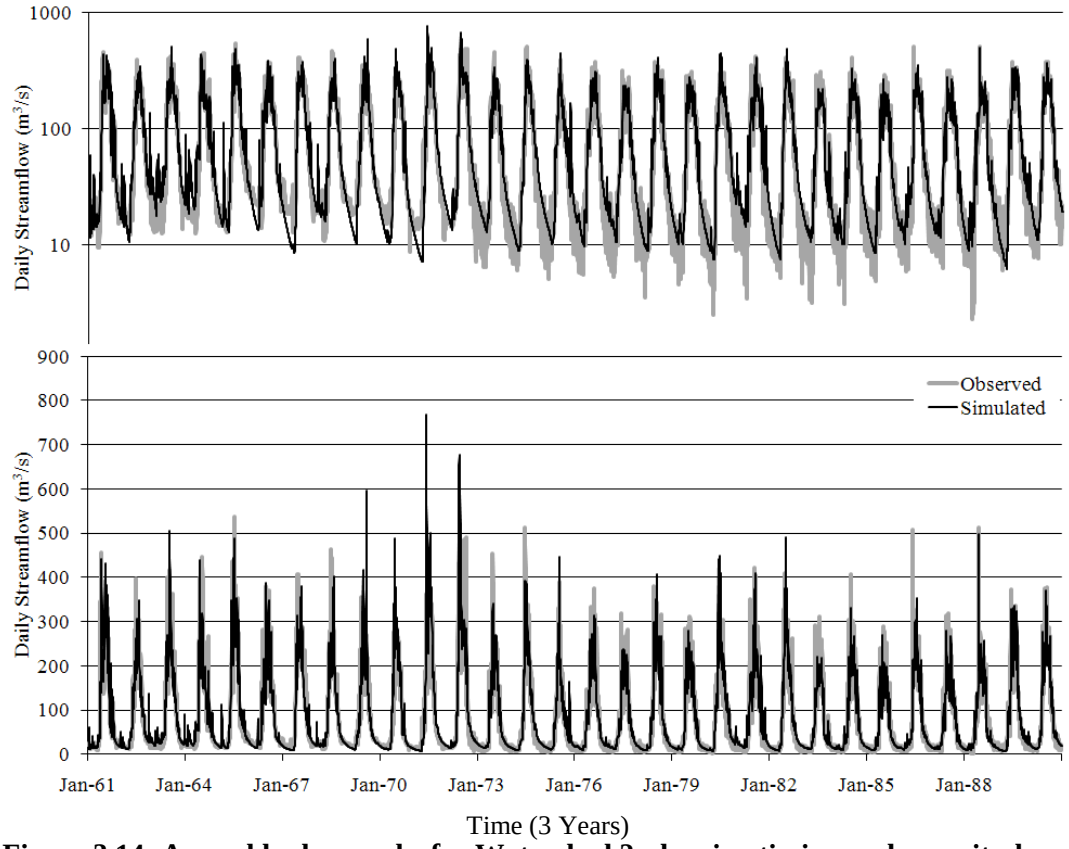

Figure 3.14: Annual hydrographs for Watershed 2, showing timing and magnitudes of simulated peak and low flow compared to available data for the 1961-90 time series. A logarithmic scale (top) shows the low flows better than the normal.

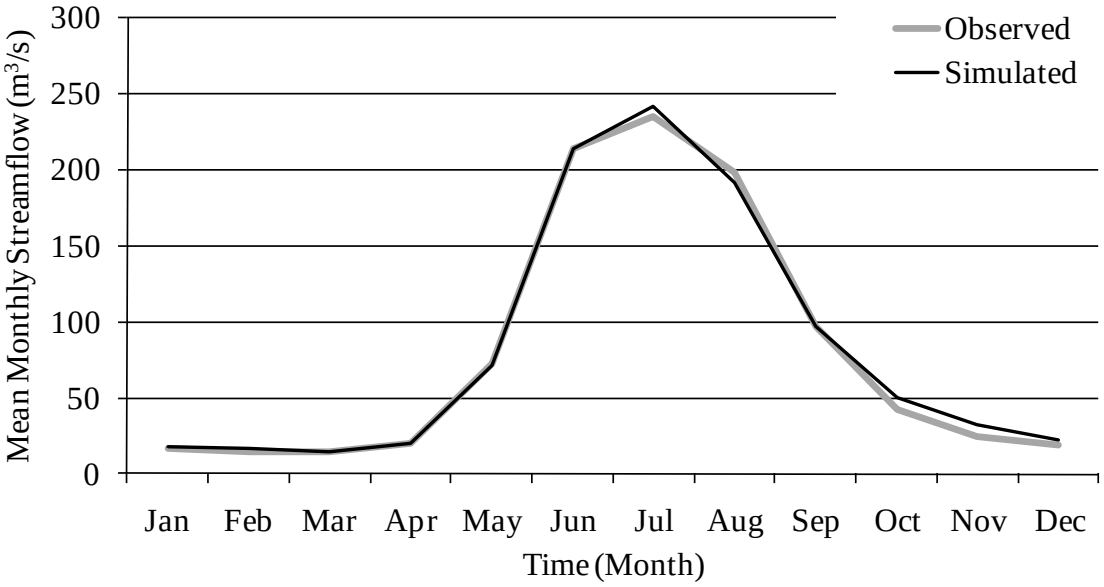

Figure 3.15: Simulated and observed mean monthly flows from Watershed 2, showing overall proper simulation of streamflow on a seasonal basis.

3.7 Discussion and Conclusions

As the seasonality of precipitation at the climate base station is different from the seasonalities in various parts of the watershed, wide ranging precipitation correction factors needed to be applied, which were calculated from monthly PRISM precipitation surfaces. The higher the elevation of the HRUs, the larger the monthly wind and precipitation correction factors were. During the period November to March corrections factors were two to four times larger than during the period April-October. High precipitation correction factors were expected, as the climate base station is approximately 800m lower than the mean watershed elevation. Correction values for slope area under estimation also had the largest correction factors for higher elevation terrain, as those areas typically have steeper slopes than lower elevation areas. There were no spatial trends or patterns of correction factors applied for relative humidity, actual sunshine hours, radiation differences on slopes, and spatial radiation differences relative to the base station.

3.7.1 Justification of UNSRB verification

Many studies that require the simulation of streamflow use only observed streamflow to verify model output or to calibrate a model (Rosso, 1994; Jewitt and Schulze, 1999; Forbes, 2007). With the ability of ACRU to output many key variables in the hydrological cycle, it was attempted to verify as many of those outputs as time and available observed data would permit. The justification behind the verification of multiple ACRU outputs was to: 1) instill confidence that selected key variables, such as air temperature, snowpack, potential evapotranspiration, and glacier melt were properly simulated, 2) to reduce some of the uncertainty associated with limited input data, especially climate and soils data, and 3) to gain confidence that the observed streamflow is simulated based on realistic selection of those bio-physical variables that represent and govern the hydrological processes in the watershed. Verifying temperature first was required to establish whether the derived lapse rates for the region were realistic, and to ensure that all other ACRU correction factors used to correct for spatial and temporal differences that impact

temperature such as elevation, aspect, and land cover, were resulting in proper temperature simulations. Once temperature was adequately verified, available A-pan data from outside the study area was used to verify that the seasonality and magnitudes of simulated PET were within realistic bounds. Verification of SWE was carried out to determine that overall snow depths and spring melt times were adequately simulated. At this point, some major hydrological inputs and outputs had been verified, and found to be adequately simulated in terms of timing and magnitudes. To verify that annual glacial melt contributions to streamflow and the average ELA of glaciers in the region were properly simulated, a glacial melt factor was calibrated to match simulated output of these variables to observed data in the area. This formed the basis for the final streamflow verification, as now only a limited number of hydrological variables needed to be calibrated within expected physical ranges, which included soil depth, precipitation, and recession constants for each of the two watersheds.

3.7.2 Verification of ACRU output

Monthly statistics were used to verify that ACRU output was consistent with that of the physical system it represents. However, daily and monthly temperature time series rather than just monthly time series were used as statistical results. Although daily simulated mean temperatures are considered statistically different, extreme warm and cold periods are captured in the simulations, indicated by a small difference in variance (4.76%) and the seasonality was preserved. Overall correlation statistics resulted in a good correlation between observed and simulated temperatures for monthly (r^2=0.98, n=499), and daily (r^2=0.88, n=37,402) time series (Table 3.4). The regression coefficients for monthly (0.99) and daily (0.92) time series are close to unity.

Simulated PET from a grassland HRU situated at the eastern boundary of the UNSRB was compared to the average of three A-pan observation sites situated outside and to the northeast of the study area. The simulated seasonality compares well with the observed PET, peaking in

June, followed by a gradual decline from July to October. Means are not statistically different ($p=0.14$), however, a consistant under-simulation of PET is evident. Research by Bosman (1987) highlighted the need for proper pan installation and consideration of micro site conditions, both of which can cause readings from adjacent A-pans to vary significantly by over 20% in the long term. Sites with observed A-pan used to verify PET for the UNSRB were located in more urban areas, with one of the observed stations at an airport. These changes in landscape result in changes to albedo, creating a heat island effect, likely contributing to modelled PET under-simulations. A-pan data was used to verify that ACRU was reasonably simulating seasonality and magnitudes of PET, but it should be noted that decreased simulated PET will result in more simulated runoff. Chiew and McMahon (1992) found that the correlations between potential evapotranspiration and A-pan data were poor, and that A-pan data should be treated with caution if used to approximate daily potential evapotranspiration.

Daily SWE depths are under-simulated and are not considered statistically different for the snow course sites ($p=0.45$), but are considered statistically different for snow pillow comparisons ($p=0.00$) and when all SWE measurements ($p=0.01$). Overall the means and variance were preserved (Table 3.6). Preserving mean SWE and its variance is important because a large portion of the annual runoff comes from snowmelt and glaciers. Generally, SWE was simulated well when compared to the snow courses, however, simulated SWE did not match well with observations from three snow courses: Limestone and both Job Creek snow courses (Table 3.3, Figure 3.6). SWE at the Limestone snow course was mostly under-simulated, while SWE at both Job Creek snow courses were mostly over-simulated. It is evident that local conditions, potentially influenced by mountain winds, snow redistribution, sun shading effects, and specific land cover composition and density, cannot be simulated well when only very sparse and generalized data are available for model parameterization. However, the observation made at the three snow courses also indicate that, on a watershed basis, simulation errors tend to balance each

other out. Snow pillows show the same pattern of under and over-simulations, as some years were simulated well. With the monitoring of continuous SWE observation, snow pillow derived SWE time series allow the analysis of the speed and timing of spring snow melt. Snow melt is simulated to melt out too early in some years, too late in some years, and well in other years. Again, as snow accumulation and melt depend on many local conditions, such as localized redistribution, incoming radiation, and surrounding land cover composition and density, only average conditions can be expected to be successfully simulated considering the coarse database available for the parameterization of ACRU.

As the lapse rates for the study area were calibrated to match the observed ELA of Peyto Glacier, it is important to show that the calibrated temperatures and the glacial melt factors used in the model did indeed model the average glacial melt output, and the average ELA on an annual basis based on mass balance data from Peyto Glacier (Demuth and Keller, 2009; Comeau et al., 2009). Glacial mass balance varies annually for glaciers, and can vary for different glaciers in the same region. The average glacial melt contributions to streamflows and the average ELA for Peyto glacier were successfully modelled by ACRU, and verified using observed data sources.

The objective of this research was not to simulate a perfect fitting hydrograph to the observed, but rather to accurately simulate mean annual water yields, as well as variance, magnitude and seasonality of streamflows to replicate the general hydrological behavior of the study watersheds under historical and future climate conditions. The process for verifying streamflow as described in Section 3.5.5.1 of this chapter was adopted after initial runs for all the watersheds in the UNSRB were largely over-simulating water yields. Watershed 1 was the exception to this which was under-simulating water yields during initial model runs, until glacier melt was properly simulated. Statistical comparison of simulated against observed streamflow from Watershed 1 and 2 are very acceptable for both daily and monthly time series as well as for both the 1981-92 calibration period and the 1961-90 verification time series. The Nash-Sutcliff

coefficient is also high for both watersheds, with daily values around 0.82 for both watersheds, and monthly values of 0.99, indicating a strong overall fit with the observed streamflow data. Mean annual water yields were either slightly under- or over-simulated for both watersheds and for all time series, but well within the initial simulation objective of being within 5% (Schulze et al., 2004). The simulated streamflow regime compares favorably with the observed for both watersheds. For Watershed 1, simulated mean monthly flows were simulated well when compared to the observed, with slight over-simulations in June, and under-simulations in August. Simulated mean monthly streamflows for Watershed 2 were also simulated well when compared to the observed, with slight over-simulations in August, October, and November. Differences between simulated and observed variances were below 4% for both watersheds, strongly showing that, in general, peak and low flows are realistically simulated.

A number of observed runoff events in Watersheds 1 and 2 do not correspond adequately to the precipitation data used to drive the model. Deviations of simulated values from observed streamflows are mostly related to inadequate precipitation data representation, both in terms of timing and amount, as daily data are extrapolated from a climate base station. However, the annual water yields and periods of low flow, which are critical to the water resource planning, are simulated accurately. Improved results can be expected when locally measured precipitation time series become available. Extensive field studies to investigate soils and land cover are required to improve the local parameterization.

3.7.3 Limitations and assumptions

Data needed to properly model hydrological processes were limited in the UNSRB. Key model inputs, including land cover and soils, are generalized, and some variables, such as plant transpiration coefficients (PTCs), were nonexistent and needed to be determined. In general mountain areas have poor representative climate data, typically captured at lower elevation sites,

which is the case in this study. Some climate data do exist at higher elevations, but these records are short, often seasonal, and inadequate for long-term climate studies (Luckman, 1998).

These limitations in data availability and spatial and temporal representation are problematic when setting up a model for a large, heterogeneous and spatial complex area such as the UNSRB. PRISM climate surfaces (Daly, 2006) were used to provide a spatial reference source for interpolated climate surfaces to calculate a number of critical parameters required for the ACRU model. Although not perfect, the PRISM surfaces were used to calculate initial precipitation and temperature based correction factors in ACRU to account for differences between the interpolated PRISM surface, base station values, and the highly spatially complex terrain of the study area. However, for some watersheds and some months, the PRISM derived correction factors required further adjustment, as became evident after comparing the perceived precipitation regime against the observed streamflow regime. As the UNSRBs western border is along the continental divide, potential influences associated with the divide on local climate are a relatively unknown factor due to the sparse climate station network.

Many generalizations had to be made with the soils data. A sound method was developed considering the poorly mapped soils data in the mountain areas, and having only generalized soils data for only approximately 10% of the study area. Based on analysis of available soils data, it was established that there was no statistically significant relationship between soil properties, such as texture or organic carbon content, and terrain attributes, such as elevation, slope, or aspect. This is in agreement with the findings by Rahman et al. (1996), who found in a study of Rocky Mountain forest soils that relationships among soils properties and terrain attributes were statistically non-significant. Due to a lack of data broad and uniform assumptions over the large study area needed to be made based on sparsely observed data, which may limit interpretations of and introduces uncertainty into the simulated data (Grayson and Bloeschl, 2000).

3.7.4 Recommendations and Final Remarks

The UNSRB is an important watershed as it provides water for two reservoirs that are important for hydroelectric power generation in Alberta. The objective of this chapter was to present the parameterization and verification procedure and results for key watersheds in the UNSRB. ACRU was parameterized for the UNSRB using available data or were estimated within a physically acceptable range from available data and literature sources. Several important hydrological variables including temperatures, PET, SWE, glacial mass balance, and streamflow were verified from ACRU output.

This research has highlighted several data gaps that need to be filled to produce better results from hydrological models in the UNSRB. Critical watershed data including detailed soils data, a broad array of climate variables at different elevations, and several land cover variables such as forest densities could be measured and used to improve modelling capabilities in this region. With limited data available for parameterization of ACRU, adequately simulating overall average conditions and hydrological variables in the UNSRB can be expected until improved data for this region are made available or measured.

The primary objective of this chapter was to accurately simulate mean annual water yields, variance, and seasonality of flows in a key watershed in the UNSRB to build the basis for the investigation of impacts of various climate change scenarios on future. With the parameterization and verification of ACRU complete, ACRU is well suited to investigate impacts of various climate change scenarios on future streamflows in the UNSRB.

CHAPTER 4

Analysis of five GCM derived climate scenarios to examine potential impacts on streamflow in the upper North Saskatchewan River basin, Alberta, Canada.

4.1 Introduction

Throughout the province of Alberta there is increasing demand for water due to population growth, and an increasing demand from agriculture and industry. In contrast, availability of future water resources is uncertain due to climate change, as several studies have shown that declining streamflows are expected to reduce water availability for irrigation, industrial and domestic use, as well as hydroelectric power generation (Gan, 1998; Rood et al., 2005; Byrne and Kienzle, 2008; Sauchyn and Kulshreshtha, 2008). Therefore, the understanding of watershed balances is essential for current and future water resources planning. This research focuses on the estimation of the impacts of climate change on streamflows in the upper North Saskatchewan River basin (UNSRB).

It is widely acknowledged that global warming has, and will, greatly impact regions where winter snowpack and glacier melt are the major sources of the total annual streamflow (Burn, 1994; Jasper et al., 2004). It is suggested that observed changes in streamflow, such as an earlier peak in spring streamflow and often lower streamflow rates in the late summer, are related to climatic changes, with even moderate increases in temperature expected to affect snowmelt dominated watersheds (Stewart et al., 2005). Global Climate Models (GCMs) are large-scale mathematical models which represent the physical processes and known feedbacks between the atmosphere, ocean, cryosphere, and land. They are used for the simulation of future climates (Barrow et al., 2005). Output from a climate model, often referred to as a climate projection, provides a description of the response of a climate system to a particular greenhouse gas scenario. To obtain a climate scenario, regionally downscaled output from the GCM is combined with a baseline or historical observed time series, typically 1961-1990 (Barrow et al., 2005; IPCC, 2007). Future forecasts of hydropower generation need to take into consideration decreased

snowpacks, and decreasing spring and summer flows, as in snowmelt dominated watersheds the timing of runoff flowing into reservoirs is expected to change, and subsequent impacts on actual and potential hydroelectric power generation are also probable (Fredericks and Major, 1997; Byrne and Kienzle, 2008). Combining CGM output with a deterministic hydrological model containing physically based equations describing hydrological processes is the most practical and widely used approach to simulating impacts of climate change (Loukas et al., 2002). The ACRU (Agricultural Catchments Research Unit) agro-hydrological modelling system (Schulze, 1995) used in this research has been used extensively in South Africa and abroad for water resources assessments (Kienzle et al., 1997; Everson, 2001; Schulze et al., 2004), and was successfully applied in Canada in a study of climate change impacts on streamflow in the Beaver Creek watershed in southwestern Alberta (Forbes, 2007).

4.2 Study Area

The upper North Saskatchewan River basin (UNSRB) is situated southwest of Edmonton, Alberta, Canada (see Figure 4.1). The UNSRB has an area of a 20,527km^2 and consists of alpine, subalpine, and foothills landscapes located on the eastern slopes of Alberta's Rocky Mountains. The basin ranges in elevation from 793m at the outlet gauging station to just under 3,500m at the Rocky Mountain peaks at the continental divide. Streamflows are dominated by snowmelt, and include glacial melt from the Columbia Ice Fields, Peyto, Athabasca, and Saskatchewan glaciers (NSWA, 2005). In order to facilitate streamflow verification and the estimation of water yield that feeds the hydro power reservoirs, the UNSRB was divided into 12 watersheds, based on either a gauging station or hydroelectric dam location to define the outlet (Figure 4.1).

Based on the subdivision, there are five watersheds in the UNSRB that are important for hydroelectric power generation. Watersheds 8, 9, and 11 are upstream of Alberta's largest hydroelectric facility, the Brazeau Dam, which was built in 1965. Watersheds 1 and 2 are upstream of the Bighorn Dam, which was built in 1971 and created Lake Abraham, one of the

largest reservoirs in Alberta. Here, only Watersheds 1 and 2 will be assessed for impacts of climate change on streamflow regimes and reservoir inflows (Figure 4.1). Watersheds 1 and 2 make up the area known as the Cline River Watershed, and will be referred to as such throughout this paper.

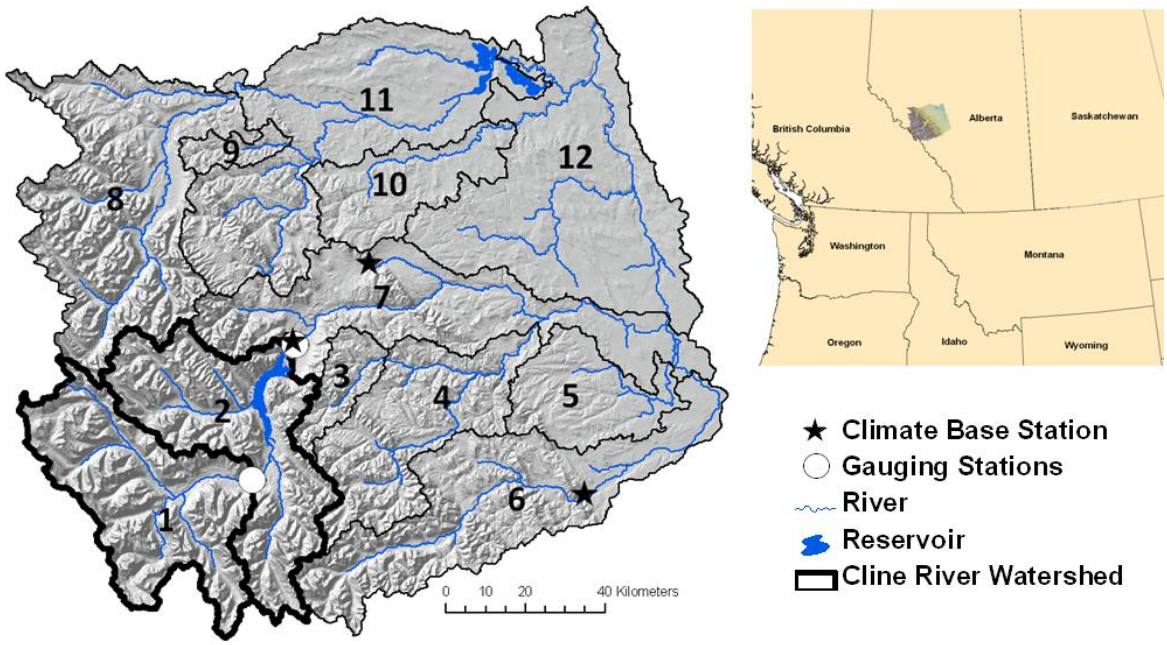

Figure 4.1: UNSRB, with general location in western Canada, with watersheds numbered and location of rivers and reservoirs, with watersheds making up the Cline River Watershed in bold black lines.

4.3 Objectives

The primary objective of this research is to estimate the impacts of climate change on water yield, streamflow extremes, and the streamflow regimes in the UNSRB, and consequently, water availability for hydropower generation in the UNSRB. ACRU was first properly parameterized and several output variables verified with observed data (Chapter 3), for use in estimating impacts of climate change in the Cline River Watershed.

4.4 Methods

4.4.1 The ACRU Agro-Hydrological Modelling System

The ACRU agro-hydrological modelling system has been developed at the Agricultural Catchments Research Unit (ACRU), a research group within the School of Bioresources Engineering and Environmental Hydrology (formerly the Department of Agricultural Engineering at the University of KwaZulu-Natal, Republic of South Africa) since the late 1970s (ACRU, 2007). The ACRU agro-hydrological modelling system from here on is referred to simply as ACRU. ACRU is a multi-purpose, multi-level, integrated physical-conceptual model that can simulate total evaporation, soil water and reservoir storages, land cover, and abstraction impacts on water resources and streamflow at a daily time step. The ACRU model revolves around multi-layer soil water budgeting with specific variables governing the atmosphere-plant-soil water interfaces. Surface runoff and infiltration are simulated using a modified SCS equation (Schmidt and Schulze, 1987), where the daily runoff depth is proportional to the antecedent soil moisture content.

All ACRU variables are estimated from the physical characteristics of the watershed. When not all required variables are available, they are estimated within physically meaningful ranges based either on the literature or local expert knowledge. Spatial variation of rainfall, soils and land cover is facilitated by operating the model in distributed mode, in which case the catchment is subdivided into either sub-watersheds or hydrological response units (HRUs), each representing a relatively homogenous area of hydrological response.

Precipitation is separated into rain or snow using a dynamic temperature based method developed by Kienzle (2008). Subsequent snow processes, such as canopy interception, sublimation, metamorphosis, or changes in albedo and density, are simulated in a physically explicit manner. The snow melt simulation is based on a dynamic degree-day factor, which is determined by the model on a daily basis from incoming radiation and albedo estimates. This

allows the automatic adjustment of the snow melt factor to follow the environmental conditions of climate change.

ACRU has been used extensively for water resource assessments (Kienzle et al., 1997; Everson, 2001; Schulze et al., 2004; Martinez et al., 2008), and climate change impacts (New and Schulze, 1996; New, 2003; Schulze et al., 2004), and often requires extensive GIS pre-processing (Kienzle, 1993; 1996; Schulze et al., 1995). Comprehensive model manuals are available through the internet at the ACRU web page (Schulze, 1995; Smithers and Schulze, 1995; ACRU, 2007). ACRU is well described by Kiker et al. (2006). However, the snow modelling manual is not yet available. The structure of ACRU (Figure 3.2) is conceptual in that it theorizes the processes that govern the hydrological cycle and physical in that the physical laws of hydrology are defined by mathematical equations within the conceptual framework of ACRU (Schulze, 1995; Forbes, 2007).

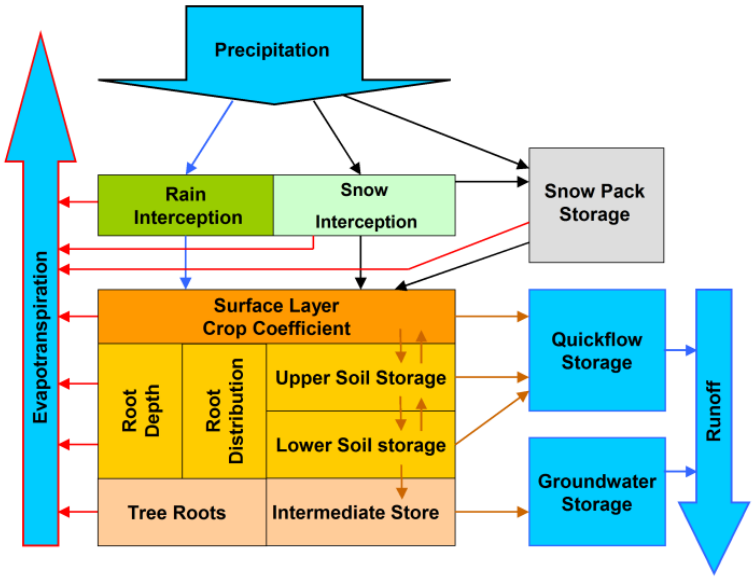

Figure 4.2: Major components of the ACRU agro-hydrological modelling system illustrating the conceptual representation of the water balance (Kienzle and Schmidt, 2008).

4.4.2 Verification of ACRU for the UNSRB

ACRU was parameterized for the UNSRB using available data estimated within a physically acceptable range from available data and literature sources, as some data, such as soils and plant transpiration parameters, were not available for all or only parts of the study area. Whenever possible, simulated output needs to be verified to ensure that it is representative of the physical characteristics of the watershed. ACRU output was calibrated and verified against available observations, which include temperature time series at climate stations, snow course and snow pillow data, glacier melt from Peyto Glacier, potential evapotranspiration using A-pan data, and streamflow time series (Chapter 3). ACRU simulated the mean annual hydrograph well, especially the timing and magnitude of peak flow and baseflow periods. For Watershed 1, annual water yields were very well replicated for the 1961-90 time series, with an over-estimation of less than one percent. The difference between variances of simulated and observed streamflow is also very good for daily (2.33%) and monthly (3.45%) statistics, indicating that simulation of peak and low flows were preserved. Overall correlation statistics are good, with a strong correlation between observed and simulated flows with a coefficient of determination of 0.83 for daily and 0.91 for month statistics. For Watershed 2, annual water yields were also slightly over-simulated for the 1961-90 time series (2.18%). The difference between variances is very good for daily (3.77%) and monthly (0.24%) statistics, indicating that simulation of peak and low flows were preserved. Overall correlation statistics are very good, with a strong correlation between observed and simulated flows with a coefficient of determination of 0.83 for daily and 0.92 for month statistics, and a Nash-Sutcliff coefficient of 0.83 and 0.99 respectively. Thus, annual water yields, and peak and low flow periods were simulated properly as they were well associated to the observed data for the entire Cline River Watershed. Seasonality of the simulated flows also matched well with the observed. After ACRU was properly parameterized and output variables such as daily temperature, snow pack, potential evapotranspiration, and glacier melt were verified

successfully against observed data, ACRU could be set up to estimate impacts of climate change in the Cline River Watershed in the UNSRB.

4.4.3 Global Climate Model (GCM) Scenarios

4.4.3.1 Acquiring GCM Data

Climate change scenarios for this research were derived by Byrne et al. (2010, in prep). Scenarios were downloaded from the Pacific Climate Impacts Consortium (PCIC) for use in estimating climate change impacts on streamflow in the UNSRB. The GCMs available from PCIC are all publically available GCM scenarios covering North America, and prepared from more than 15 GCMs for the IPCC Fourth Assessment (AR4) report (IPCC, 2007). The GCMs and SRES simulations available for this research are listed in Table 4.1. To provide regional estimates of temperature and precipitation changes, and to reduce the influence imposed by a single overlaying 400x400km grid cell, the average of the four GCM grid cells closest to the study area was applied, following the method described by Von Storch et al. (1993). Each of the models selected is driven by one of the emission scenarios for the Special Report on Emissions Scenarios (Nakicenovic et al., 2000). The GCMs and emissions scenarios used in this research were the most up to date, readily available data for climate change impacts research in the UNSRB.

Table 4.1: GCMs and scenarios available from the PCIC

Modelling Center	Country	Model	SRES Simulations
Canadian Center for Climate Modelling and Analysis	Canada	CCCMA_CGCM3	A1B, A2, B1
National Center for Atmospheric Research	USA	NCAR_CCSM30	A1B, B1
Bjerknes Centre for Climate Research	Norway	BCCR-BCM20	A1B, A2, B1
CSIRO Atmospheric Research	Australia	CSIRO-MK30	A1B, A2, B1
NASA/Goddard Institute for Space Studies	USA	GISS_AOM	A1B, B1
Institute for Numerical Mathematics	Russia	INM_CM30	A1B, A2, B1
Center for Climate System Research (The University of Tokyo), National Institute for Environmental Studies, and Frontier Research Center for Global Change (JAMSTEC)	Japan	MIROC32-HIRES and MIROC32-MEDRES	A1B, A2, B1

4.4.3.2 Climate Change Scenario Process and Selections

There are three future time series assessed in this research that are recommended by the IPCC (2007): 2020s (2010-2039), 2050s (2040-2069), and 2080s (2070-2099). Thirty year averaging periods are typically used in scenario construction as a compromise between trying to capture the climate change signal without losing too much of the variability in the model results over time. This also permits the scenarios to better represent the long-term trend than if a shorter period, such as 10 years, was used (IPCC, 2007). For this research, the observed climate data for 1961-90 were used as the baseline period. This period is used instead of the 1971-2000 time period, as it is assumed that it has not been significantly impacted by climate change (Diaz-Nieto and Wilby, 2005).

IPCC (2007) recommended using more than one GCM in an impact assessment to show a range of changes to temperature and precipitation for a study region. From the 42 climate scenarios from eight CGMs, using three different SRES scenarios that were available from PCIC, five scenarios from GCM output were selected. To select the range of GCM scenarios, mean temperature change and percent precipitation change for the 2050 spring (March, April, May or MAM) time period were used. Changes for the 2020s tend to vary the least between individual experimental results than the 2050s or 2080s. The 2050 time period provides more separation in the experimental results, but at the same time contains less uncertainty than the results for the 2080s, and was used for selection of GCM scenarios for this research. This method for selecting climate change scenarios was tailored after the method described by Barrow and Yu (2005), who constructed climate change scenarios for Alberta. This method has also been recently applied for climate impact studies by Forbes (2007) and MacDonald (2008).

Changes in temperature and precipitation were used to create a graph from a plot of possible climate scenario runs from all available models and emission scenarios for the 2050 time period (Figure 4.3). The selection of GCM scenarios is done by creating four quadrants based on

the median temperature change (here: +1.73°C) and the median precipitation changes (here: +13%). Five scenarios from GCM output were selected based on their projection of the range of possible future climates: median, warmer-wetter, warmer-wettest, hotter-wetter, and hotter-wettest. In total, four GCMs following three emissions scenarios, A2, A1B, and B1, were selected for use in estimating impacts of climate change on streamflow in the UNSRB. The A2 emissions scenario is considered to be 'business as usual' in which society continues to burn fossil fuels for most of its energy. The A1B emissions scenario is a balance between fossil intensive and non-fossil energy resources. The other emissions scenario commonly used is B1, which assumes much less greenhouse gas use globally (Nakicenovic et al., 2000). A summary of the selected scenarios used is provided in Table 4.2.

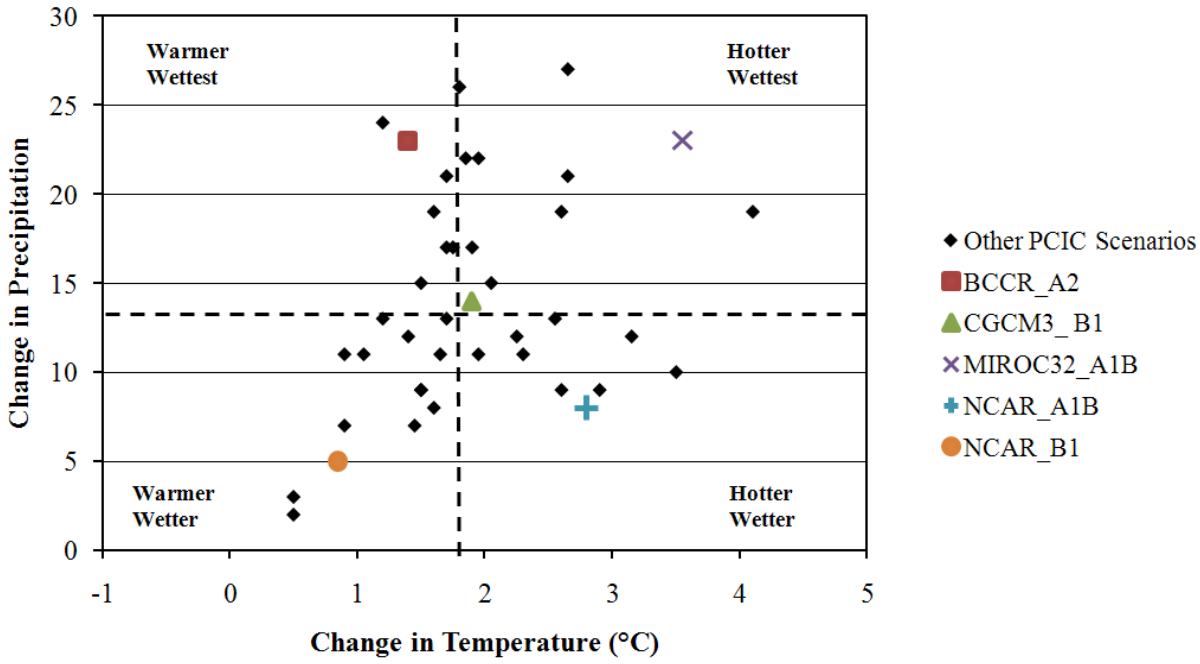

Figure 4.3: Selected GCM runs for the spring 2050 time period from all available PCIC runs that were used for impact assessment of streamflow (after Barrow and Yue, 2005)

Figure 4.3 shows how the estimated changes in temperature and precipitation varied greatly between various GCM scenarios. All model outputs showed an increase based on the 2050 projections for spring temperature (°C) and precipitation changes (%). Projected

temperature changes range in magnitude from 0.5°C to 4.1°C, relative to historical conditions. Projected changes in precipitation showed a consistent increase in precipitation relative to historical conditions, ranging from 2% to 27%.

Table 4.2: Selected GCMs, emissions scenarios and model runs (parenthesis) used to assess climate change impacts in the UNSRB.

Scenario	GCM	Emissions Scenario
Warmer Wetter	NCAR	B1 (6)
Warmer Wettest	BCCR	A2 (1)
Median	CGCM3	B1 (2)
Hotter Wetter	NCAR	A1B (9)
Hotter Wettest	MIROC32	A1B (1)

4.4.3.3 Regional Downscaling

GCMs are assumed to accurately represent climate at a global scale, but are often inaccurate when simulating regional climate (Evans and Schreider, 2002). Therefore, GCM output needs to be downscaled to local or regional climate to evaluate regional climate change impacts. To construct regional climate change scenarios based on GCM output, a widely used procedure called the 'delta method' was applied (Hay et al., 2000; Arnell, 2004). The delta method is commonly used for assessment of climate change impacts, and has been used to downscale CGM output in diverse geographical regions (Wilby et al., 1999; Merritt et al., 2006; Forbes, 2007; Markoff and Cullen, 2007; Nogués-Bravo et al., 2007; MacDonald, 2008; Lui et al., 2009). With this method, monthly temperature and precipitation changes from GCM output are used to perturb the 1961-90 historical record from climate stations in the study area. The delta method applies the climate change signal to the mean of the observed data, but does not account for possible changes to the variability of future climate (Hay et al., 2000).

To model climate impacts on streamflow in the UNSRB, monthly GCM changes for minimum and maximum temperature as well as precipitation were used. For minimum and maximum temperature, monthly regional weighted mean temperature change values (°C) are run

through a Fourier Transformation to result in continuous daily changes, thus avoiding jumps in values from month to month. The daily output from the Fourier Transformation is added to each day of the historical data to give a new 30-year time series for each of the three future time periods. For precipitation, monthly percent change values were used from GCM output. Each day over the entire 1961-1990 baseline time series is multiplied by the monthly percent difference value, and then added to the baseline data to result in a new 30-year time series for each of the three future time periods.

The delta method is limited in that it does not consider changes in the variability of the descriptors (e.g. precipitation regimes) with climate change (Evans and Schreider, 2002). However the delta method is a sound means of selecting a range of plausible estimates of climate change from different GCMs to provide an insight into possible trends associated with climate change, and how they could impact streamflows in the UNSRB (Loukas et al., 2002; Merritt et al., 2006).

4.4.3.4 Projected Climate Changes

Since the future climate cannot be known with a definite certainty, climate change projections are expressed in terms of a range of possible future climates. Table 4.3 shows the monthly forecast changes for each of the scenarios relative to the historical base period. It should be noted that all five climate scenarios were selected based on spring 2050 projections, which does not capture the distribution of projected results seen on a monthly basis.

Table 4.3: Mean monthly GCM projections of temperature and precipitation for 2020, 2050, and 2080 time periods. Changes in temperature (°C) and precipitation (%) are relative to the 1961-90 baseline period.

Scenario	Time Period	Jan	Feb	Mar	Apr	May	Jun	Jul	Aug	Sep	Oct	Nov	Dec
Mean Monthly Minimum Temperature Changes (°C)													
Median	2020	0.7	1.7	0.5	0.4	1.0	1.4	1.4	1.5	1.4	0.9	1.5	2.7
Warmer Wetter	2020	6.1	2.7	1.4	1.2	1.0	1.1	1.5	1.5	1.7	2.6	2.3	2.8
Warmer Wettest	2020	1.6	0.1	-0.4	0.7	0.4	0.3	0.9	0.5	0.6	0.6	2.1	0.1
Hotter Wetter	2020	3.0	1.9	0.7	1.5	1.8	2.1	2.2	1.8	2.4	1.9	1.8	3.9
Hotter Wettest	2020	2.4	2.0	2.3	1.6	2.7	2.1	1.9	2.1	2.0	1.5	1.4	1.8
Median	2050	2.5	2.3	1.4	0.9	1.7	1.8	2.1	2.3	2.3	1.5	2.0	3.0
Warmer Wetter	2050	3.9	2.4	2.0	1.5	1.4	2.5	2.3	2.2	2.0	2.4	2.1	2.4
Warmer Wettest	2050	2.5	-0.2	0.8	1.4	1.0	1.0	1.6	1.2	1.1	0.9	2.2	2.6
Hotter Wetter	2050	5.2	3.6	3.7	2.8	2.4	3.7	3.7	3.1	3.2	2.3	2.8	4.4
Hotter Wettest	2050	3.6	4.7	4.8	3.9	4.9	4.0	3.8	3.8	3.9	2.9	3.2	5.4
Median	2080	2.6	2.2	1.9	1.7	1.9	2.2	2.3	2.6	2.3	1.3	2.7	3.1
Warmer Wetter	2080	6.1	3.4	3.2	2.6	2.0	2.7	2.7	2.5	2.8	2.6	2.6	3.3
Warmer Wettest	2080	3.8	0.5	2.0	1.6	1.5	2.3	3.8	3.1	2.5	1.8	4.6	4.3
Hotter Wetter	2080	7.6	6.3	3.5	3.4	3.3	4.5	4.1	4.5	3.7	3.0	4.4	5.2
Hotter Wettest	2080	6.4	6.2	6.9	6.2	6.4	5.3	5.3	5.8	4.9	4.3	4.7	7.1
Mean Monthly Maximum Temperature Changes (°C)													
Median	2020	0.6	1.3	0.4	0.1	0.6	0.9	1.2	1.3	0.9	0.8	1.2	2.2
Warmer Wetter	2020	4.0	1.6	0.5	0.5	0.9	0.8	1.5	2.6	2.1	2.6	1.4	1.5
Warmer Wettest	2020	1.0	-0.2	-0.5	0.2	1.1	0.5	0.9	0.4	0.9	0.3	1.0	0.2
Hotter Wetter	2020	1.7	1.1	0.5	0.9	2.1	2.4	3.0	2.7	3.5	1.8	1.0	2.1
Hotter Wettest	2020	1.8	1.3	1.4	1.4	2.8	2.3	2.3	2.2	2.3	1.4	1.1	1.1
Median	2050	2.2	1.9	1.1	0.7	1.5	1.3	1.8	2.1	2.0	1.0	1.6	2.5
Warmer Wetter	2050	2.4	1.3	0.7	0.6	0.8	2.3	2.9	2.9	2.3	2.6	1.1	1.3
Warmer Wettest	2050	1.5	-0.4	0.5	0.8	0.9	1.2	2.3	2.2	2.4	1.3	1.2	2.2
Hotter Wetter	2050	3.0	1.9	2.3	1.6	2.5	4.4	4.8	3.9	4.3	1.7	1.7	2.5
Hotter Wettest	2050	2.7	3.0	2.6	3.4	5.0	4.5	4.9	4.4	4.3	3.1	2.7	4.1
Median	2080	2.5	1.6	1.2	0.6	1.4	1.8	2.1	2.5	1.5	0.9	2.1	2.5
Warmer Wetter	2080	4.1	1.9	1.9	2.0	1.4	2.7	3.3	4.0	3.2	2.4	1.4	1.9
Warmer Wettest	2080	3.0	-0.1	0.5	1.0	2.8	2.9	4.0	4.5	3.8	2.1	2.7	3.2
Hotter Wetter	2080	4.5	3.6	2.1	2.0	3.7	5.5	4.5	5.6	4.3	2.3	2.7	3.0
Hotter Wettest	2080	4.7	3.8	4.1	5.9	6.7	5.8	6.6	6.8	5.7	4.4	4.2	5.1
Mean Monthly Precipitation Changes (%)													
Median	2020	6.0	25.0	2.0	8.0	6.0	3.0	13.0	13.0	11.0	17.0	13.0	3.0
Warmer Wetter	2020	24.0	14.0	8.0	5.0	7.0	6.0	10.0	-18.0	-8.0	-1.0	10.0	-5.0
Warmer Wettest	2020	13.0	-4.0	13.0	2.0	7.0	5.0	0.0	2.0	-8.0	15.0	16.0	10.0
Hotter Wetter	2020	9.0	-3.0	-4.0	11.0	2.0	11.0	-12.0	-13.0	-18.0	13.0	6.0	12.0
Hotter Wettest	2020	19.0	10.0	-1.0	10.0	12.0	0.0	-10.0	-1.0	1.0	8.0	16.0	-14.0
Median	2050	6.0	21.0	12.0	9.0	19.0	-1.0	10.0	17.0	10.0	16.0	15.0	16.0
Warmer Wetter	2050	10.0	35.0	5.0	6.0	5.0	24.0	-2.0	-15.0	-6.0	8.0	7.0	-2.0
Warmer Wettest	2050	18.0	15.0	28.0	24.0	17.0	3.0	-5.0	-7.0	-18.0	14.0	10.0	20.0
Hotter Wetter	2050	7.0	23.0	-1.0	17.0	8.0	8.0	7.0	-6.0	-11.0	17.0	21.0	12.0
Hotter Wettest	2050	15.0	3.0	20.0	25.0	23.0	-5.0	-31.0	-11.0	7.0	17.0	25.0	9.0
Median	2080	24.0	31.0	9.0	32.0	18.0	-2.0	10.0	14.0	26.0	39.0	18.0	30.0
Warmer Wetter	2080	21.0	18.0	14.0	11.0	31.0	26.0	-2.0	-21.0	-1.0	0.0	14.0	1.0
Warmer Wettest	2080	5.0	9.0	25.0	24.0	16.0	7.0	0.0	-13.0	-4.0	28.0	39.0	28.0
Hotter Wetter	2080	11.0	18.0	6.0	30.0	12.0	17.0	19.0	6.0	-7.0	21.0	21.0	5.0
Hotter Wettest	2080	35.0	34.0	18.0	40.0	19.0	-4.0	-26.0	-17.0	-11.0	43.0	36.0	19.0

4.5 Results

4.5.1 Modelling with and without glacier contributions

The IPCC Fourth Assessment Report has stated with high confidence that observed evidence suggests there is increased runoff and earlier spring peak discharge in many glacier and snow-fed rivers as a result of climate change (IPCC, 2007). This projection assumes that the increase in volume loss from glaciers is causing an increase in streamflow. This increased runoff from glacier melt can only be short term, because the shrinking of glacier area and volume will eventually limit the volume of melt water produced, even if climate changes sustain greater melt per unit area (Moore and Demuth 2001). In general, basins with significant but rapidly changing glacier cover have exhibited a strong decreasing trend in glacier melt contributions (Demuth and Pietroniro, 2003).

Glaciers comprise 7% of the land area in the Cline River Watershed, and 1.5% of the land area in the whole UNSRB. The glacial melt routine in ACRU currently assumes an endless supply of glaciers to melt out. This assumption was initially made to be able to model glacier melt contributions as part of an initial step in modelling glaciers, and it is assumed to be valid for the glacier melt contributions during the 1961-1990 base period. However, this proves to be a serious deficiency of the current model structure, as glaciers melt out, glacier area and volumes decrease, thereby decreasing the amount of glacial melt produced as the volume of ice in the glacier decreases. With the supply of glaciers in modelled output assumed to be unlimited, future estimates of streamflow when modelling glacier melt for the 2050s and the 2080s are highly questionable. Figure 4.4 shows the modelled glacier contribution for the baseline 1961-1990 time series, and the modelled output for the hotter wettest (MIRO A1B) scenario, when glaciers are modelled (glaciers on) and not modelled (glaciers off). The difference between the curves of 'glaciers on' and 'glaciers off' for each simulation is the glacier contribution to streamflow for that time period. MIRO A1B shows the most extreme changes for the 2080 period, but illustrates

the trend of all scenario output, with simulated very large increases in summer and late season flows when compared to the baseline period. Figure 4.4 clearly shows that the glacier melt contribution for the baseline period is simulated from weeks 27-43 (July to October), and contributions in 2080 from week 22-45 (June to November). It is evident that without modelling future glacier volume losses and subsequent decreases in glacial melt contributions in this region of the UNSRB, projected output for the 2080s and even the 2050s are significantly over-estimated and must be further investigated. For this research, future climate scenarios were modelled with 'glaciers off' to be able to look at impacts on streamflow beyond the 2020 time period until deficiencies in modelling future glacial melt contribution can be corrected.

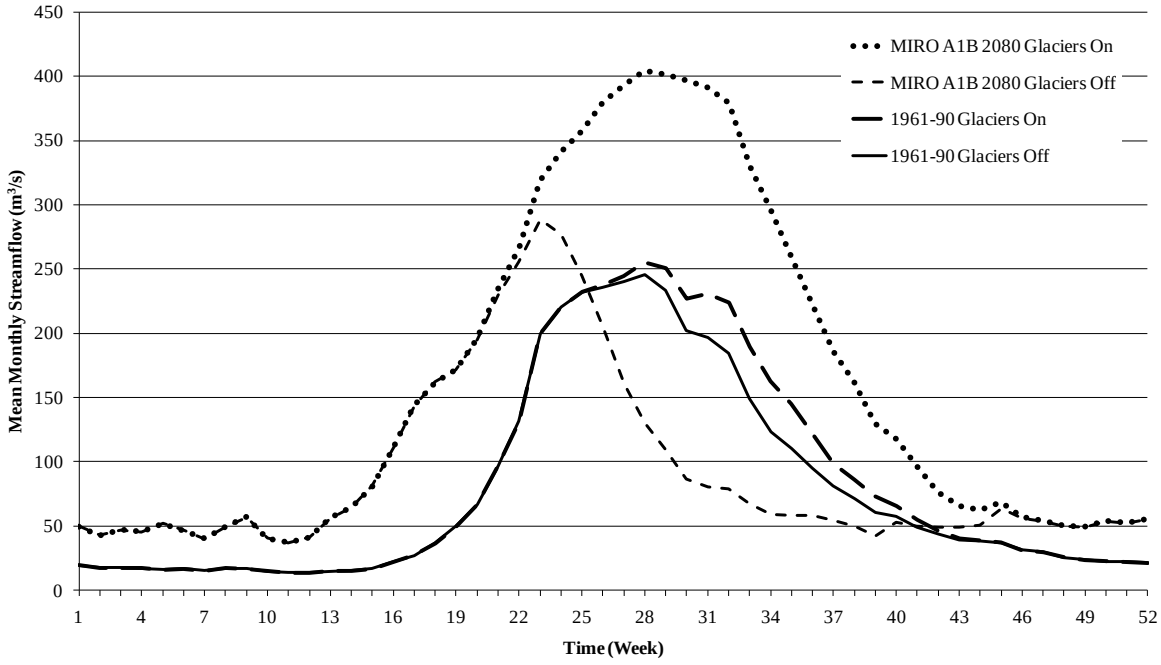

Figure 4.4: Weekly simulated streamflow with (on) and without (off) glaciers being simulated for the baseline period and for the MIRO A1B scenario which showed the greatest contrast in the 2080 time series.

4.5.2 Changes to various hydrologic variables

Results of modelled changes to potential and actual evapotranspiration (PET and AET), soil moisture, ground water (GW) recharge, and snow water equivalent (SWE) were assessed

from climate scenario output for each of the three future time periods. Table 4.4 shows a summary of percent changes to each of these variables relative to the baseline period, based on output from each GCM scenario output for each future time period.

Table 4.4: Change in percentage (%) for potential (PET) and actual (AET) evapotranspiration, soil moisture, ground water (GW) recharge, and snow water equivalent (SWE) relative to the baseline 1961-1990 time period.

	Climate Scenario	PET	AET	Soil Moisture	GW Recharge	SWE
2020	**NCAR B1**	11.9	4.0	0.9	3.6	-49
	BCCR A2	3.4	-0.4	0.8	5.1	-17
	CGCM3 B1	8.2	2.8	1.1	2.4	-40
	NCAR A1B	17.6	2.4	-0.1	-3.0	-65
	MIROC32 A1B	16.6	3.6	0.0	0.1	-63
2050	**NCAR B1**	16.8	5.4	0.8	4.3	-61
	BCCR A2	11.1	2.5	1.0	3.7	-48
	CGCM3 B1	12.3	6.4	3.5	9.4	-49
	NCAR A1B	25.8	7.8	1.5	2.5	-71
	MIROC32 A1B	33.7	6.1	0.5	0.7	-76
2080	**NCAR B1**	21.0	6.9	1.1	4.1	-66
	BCCR A2	20.2	3.9	2.9	7.9	-64
	CGCM3 B1	12.8	8.7	5.3	17.0	-43
	NCAR A1B	33.4	12.5	2.4	2.8	-77
	MIROC32 A1B	47.4	10.7	1.0	8.0	-79

Overall PET, AET, soil moisture, and GW recharge are projected to increase with each successive time period when looking at an average of all the model projections for each of the three future time periods. Projections of future SWE depths are decreasing and show larger decreases into later time periods.

4.5.3 Changes to streamflow

The seasonality of streamflows was calculated on a weekly basis from output for each of the climate scenarios and for each future time period, relative to the observed baseline data (Figure 4.5). Output for all three future time periods show an earlier shift in the annual hydrograph, with an earlier peak flow, and increases in magnitudes of the peak flows. Streamflows in the winter months are higher for the 2020s and 2050s than the baseline period, with larger increases in winter streamflows for the hotter wetter and hotter wettest scenarios, and

even larger winter flows in the 2080s. The largest increases for all time periods relative to the baseline data were in spring and early summer (weeks 17-28). Increases to early spring flows are seen in all time periods, with the most dramatic estimates from the MIRO A1B (hotter wettest) scenario which shows the largest changes to spring streamflow for all future time periods. There is also a decrease in later summer early fall flows from weeks 28-40 relative to the baseline data. This trend of decreased streamflow in this time frame shows increased spread of projections in each of the future time series.

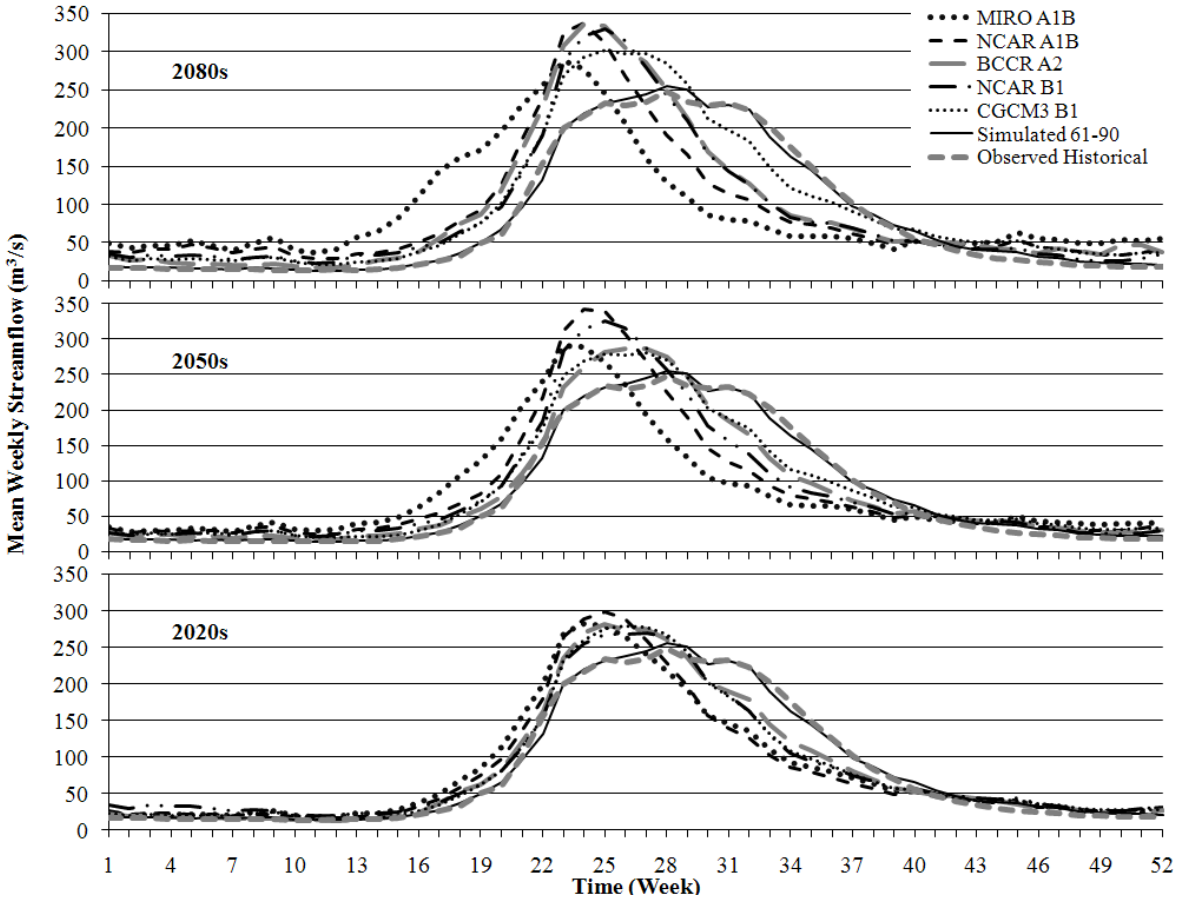

Figure 4.5: Results showing changes in seasonality from all climate scenario output for each of the three future time periods when compared to the historical observed data on a weekly time scale for the 2080s (top), 2050s (middle), and 2020s (bottom).

Figure 4.6 shows the years with the lowest and highest water yields based on the baseline period, and predicted future changes to those years using the two scenarios expected to have the

greatest impacts on the hydrological cycle. The NCAR A1B scenario was selected as it is the "hotter wetter" scenario, with smaller increases in precipitation and larger increases in temperature, thus representing the driest climate change scenario. This scenario would likely see increases in evapotranspiration, decreased soil moisture and more infiltration, and potentially decreases in streamflow when compared to the warmer wettest scenario. The "warmer wettest" scenario (BCCR A2) was selected as the other scenario to evaluate changes to extreme streamflow years as it has the largest increases in precipitation, with only moderate increases in temperature. In terms of minimum flow years, the BCCR A2 scenario shows a lower peak flow for the 2020s and 2050s when compared to the baseline period, and a higher peak flow in the 2080s. All three future time periods show an earlier shift in peak streamflow from July in the baseline data to June for each future time series. There is also a large decrease in flows from July to September for all three future time series relative to the baseline data, with the largest decreases seen in the 2080s. The NCAR A1B scenario output shows lower peak flows in the minimum flow year for the 2020s and 2080s, with a slightly high increase in the 2050s peak flow relative to the observed. The same pattern in terms of an earlier shift in peak flow as well as decreased flows in late summer months are similar to those seen in the BCCR A2 scenarios.

For the maximum flow year, the BCCR A2 scenario results in increased winter and spring flows and decreased summer flows. There is also an increase in the magnitude of all peak flows, and an earlier peak flow for the 2080 time period. The NCAR A1B scenario results in increases in the magnitudes of peak flows, and earlier peak flows for each of the three future time periods. Increases in winter and spring flows are greater than the BCCR A2 projections, as are the decreases to summer flows. In terms of water yields, both scenarios project a decrease in the 2020 and 2050s for the minimum flow year relative to the baseline data, with increased water yields for the 2080s. For the maximum flow year, both scenarios project higher water yields in each of the three future time periods relative to the baseline data.

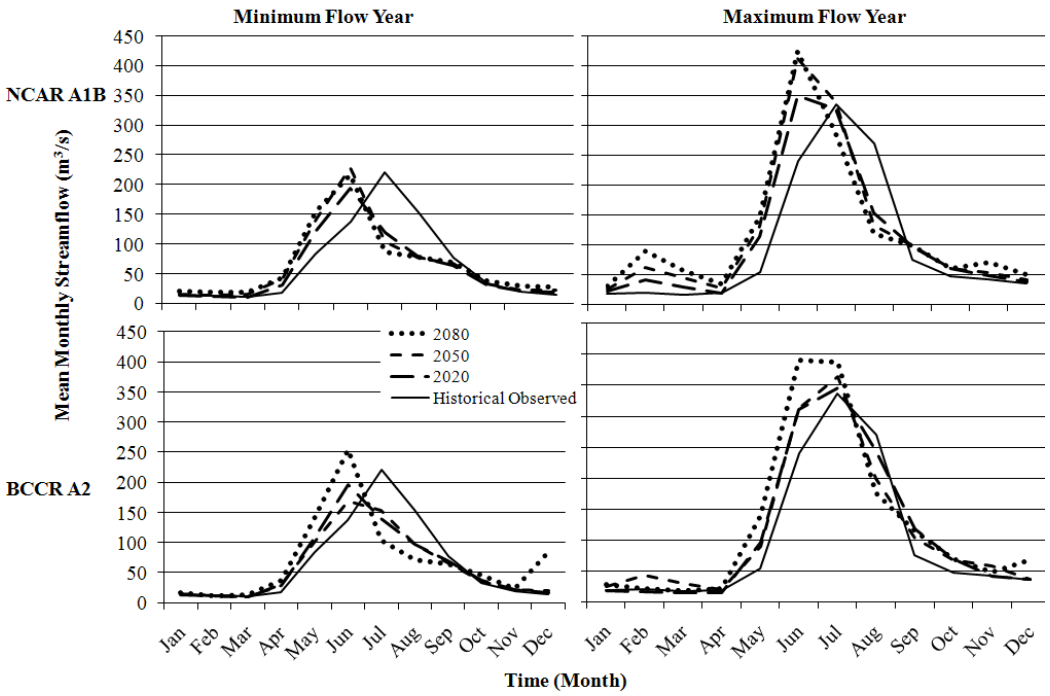

Figure 4.6: Results for years with the lowest and highest water yields based on the historical observed data. Simulated future outputs based on the "hotter wetter" (NCAR A1B) and "warmer wettest" (BCCR A2) scenarios are used to show impacts on change in minimum and maximum flow years in terms of seasonality at a monthly time scale.

Flow duration curves (FDCs) show the percentage of time that streamflow is likely to equal or exceed a given value. Daily streamflow values for the 2020 and 2080 time periods are shown in an FDC in Figure 4.7. This was done to illustrate the projected spread of changes over all time periods. All scenarios in both the 2020s and 2080s show an increase in low flows in terms of frequency and magnitude, relative to the baseline data. The peak flows also show increases in magnitude, however, the higher flows (exceedence probabilities between 11 and 31%) are projected to decrease in magnitude and frequency relative to the baseline data.

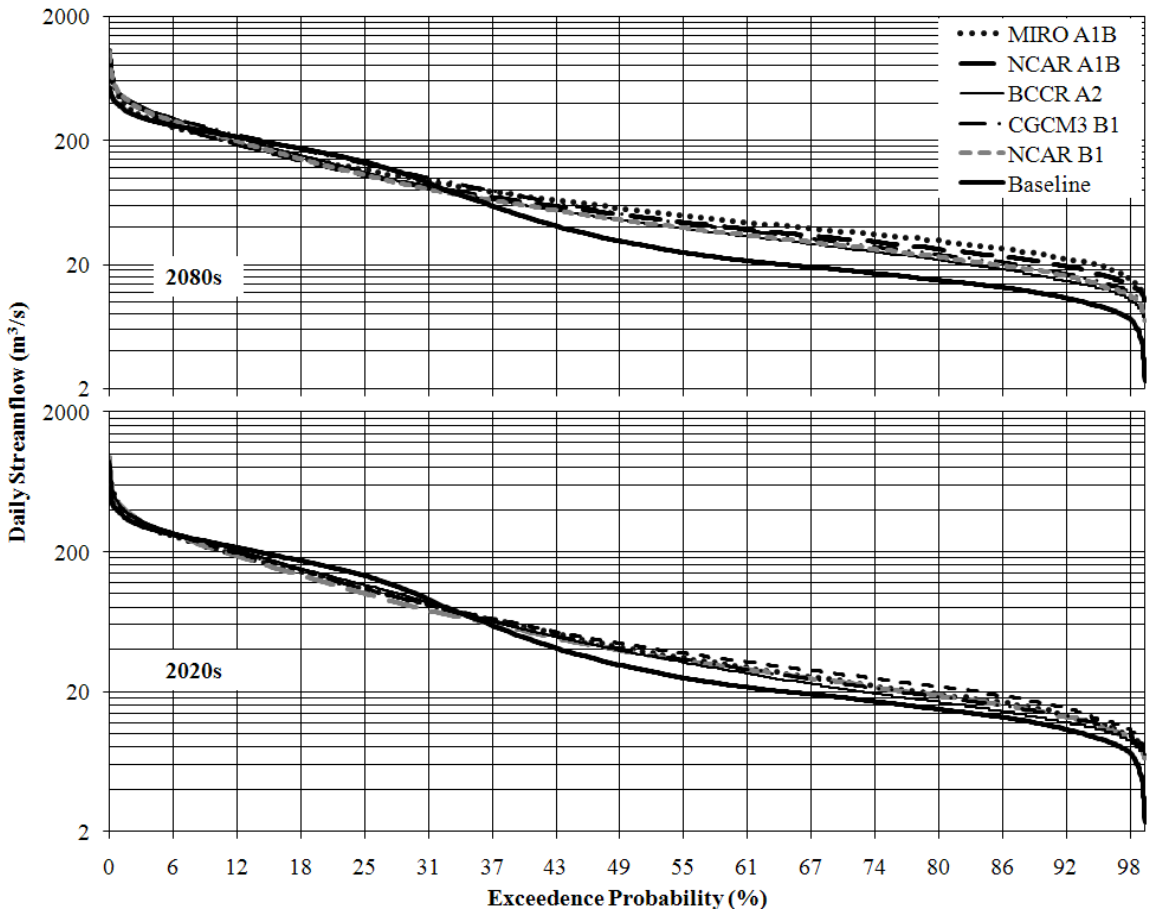

Figure 4.7: FDCs for the 2020 and 2080 time periods relative to the historical observed data from daily data to show the spread of projected changes.

The minimum and maximum flows for each year for output from the 2020 and 2080 time periods were used to create an annual minimum and maximum flow FDC for each scenario, which are compared to the baseline period (Figures 4.8 and 4.9). The 2020s and 2080s were again used to illustrate the spread in terms of projections as the same trend was seen in all future time periods. All of the annual minimum flows in both the 2020s and 2080s for all scenarios are increasing, with the lowest low flows increasing the most in magnitudes and decreasing in frequency (Figure 4.8). For example, the lowest flow in the baseline time period has an exceedence probability of 97%, and a magnitude of 2.3m^3/s. The 97% exceedence probability will have a flow of approximately 7.1m^3/s in the 2020s, and approximately 8.6m^3/s in the 2080s.

Most of the annual maximum flows in the 2020s and 2080s are increasing for all scenarios. The "hotter wettest" scenario output (MIRO A1B) shows lower maximum streamflows when compared to the baseline period at the 61st and 98th exceedence probabilities (Figure 4.9). All of the scenarios for the 2020s and 2080s, except the BCCR A2 scenario, show decreases in frequency and magnitude of lower high flows, with more notable decreases in the 2020s. The frequency and magnitude of maximum peak flows are increasing for all scenarios for each time period, with the highest flows occurring more often compared to the baseline period. For example, the exceedence probability for the base period of the maximum flow of approximately 19m^3/s is about 3%. The average of the same magnitude flow in the 2020 time period is estimated to have an exceedence probability of roughly 23%, and about 30% for the 2080 time period, based on all scenario output for each time period.

Average percent changes in water yields of streamflow, based on comparisons between each future time period and the 1961-1990 baseline data, are shown in Table 4.5. Slight decreases and increases (-2% to +3.6%) in water yields are projected for the 2020s. All model output for the 2050s project 2.3 to 8.3% increases in water yields, and increases in to 2080s from 7 to 15.1%. Monthly average percent changes in water yields of streamflow, based on comparisons between each future time period and the 1961-1990 baseline data, are presented in Table 4.6. Streamflows are simulated to increase the most in the winter and spring (November to May), and showed large decreases in late summer and early fall from July to September (Table 4.6).

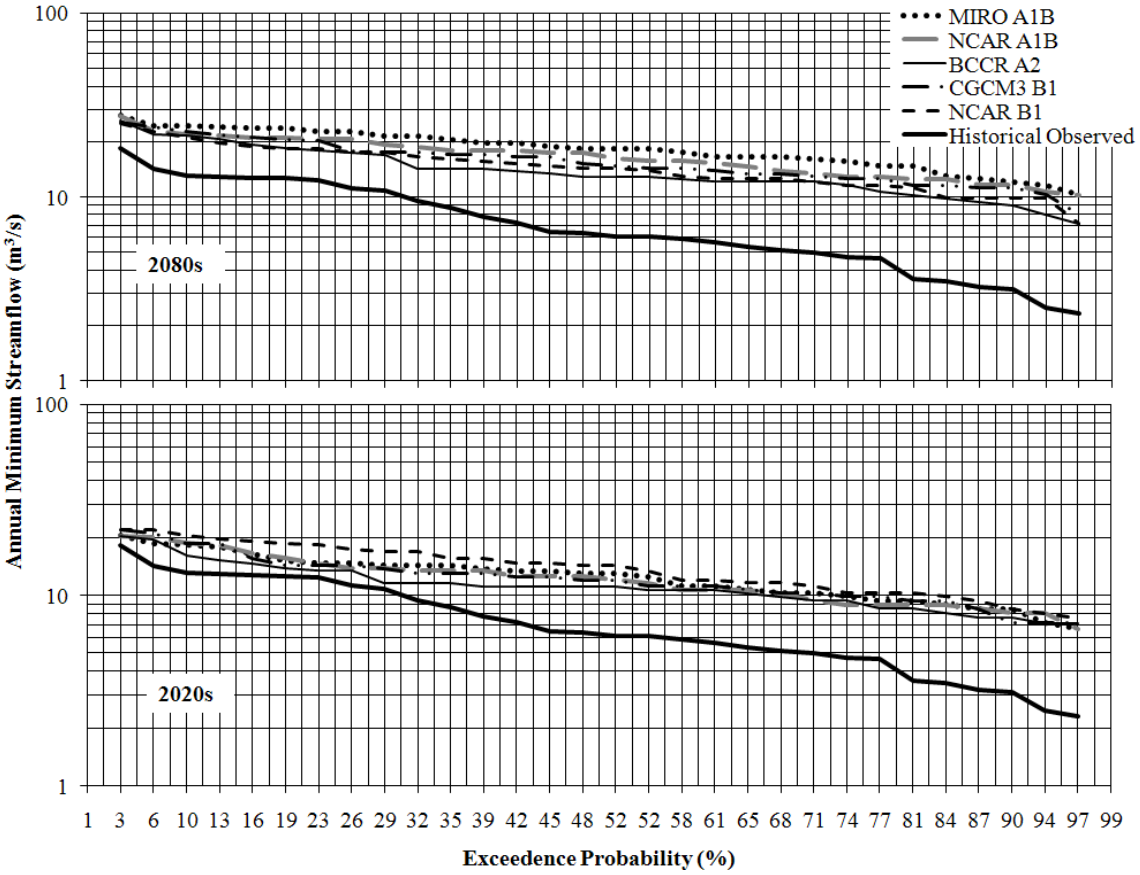

Figure 4.8: FDCs for minimum annual flows from the 2020 and 2080 time series relative to the historical observed data to show the spread of projected changes.

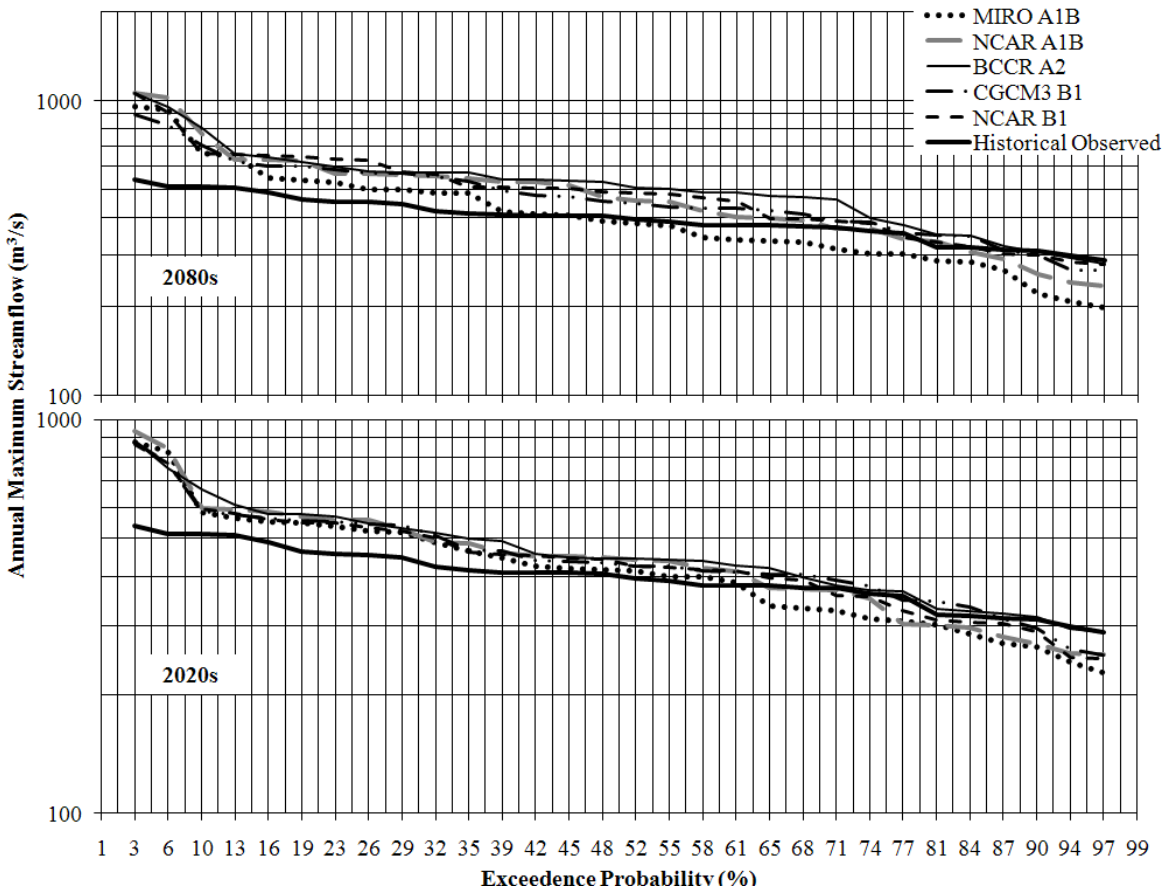

Figure 4.9: FDCs for maximum annual flows from the 2020 and 2080 time series relative to the historical observed data to show the spread of projected changes.

Table 4.5: Average changes of mean annual streamflow (%) based on comparisons between each future time period and the 1961-1990 baseline data.

Scenario	2020	2050	2080
NCAR A1B	-2.0	6.7	8.3
MIRO A1B	-0.1	2.3	11.0
CGCM3 B1	1.5	8.3	15.1
BCCR A2	2.2	2.9	9.7
NCAR B1	3.6	6.2	7.0

Table 4.6: Monthly average streamflow changes (%) based on comparisons between each future time period and the 1961-1990 baseline data.

Scenario	Jan	Feb	Mar	Apr	May	Jun	Jul	Aug	Sep	Oct	Nov	Dec
2020	43	51	30	44	32	21	-4	-35	-28	8	41	46
2050	63	87	77	97	55	31	-8	-42	-31	11	56	72
2080	116	135	107	164	85	36	-15	-47	-33	16	82	112

4.6 Discussion

4.6.1 Projected Changes to PET and AET

Based on output from the selected GCM scenarios, the average increases in PET from all modelled climate scenarios are projected to be 12% for the 2020s, 20% for the 2050s and 27% for the 2080s. Average increases in AET from all scenario output are 3% for the 2020s, 6% for the 2050s, and 9% for the 2080s. These trends in projected increases in PET and AET are consistent with results from a recent study by Zhang et al. (2009), who found positive trends of increased AET in North American boreal regions from 1983-2005 from climate warming. Projected atmospheric warming is expected to increase PET and AET, in part of an overall intensification of the hydrological cycle (Burn, 1994). As the air warms the vapor pressure deficit also increases, resulting in an increase in PET. AET will only increase with PET if increased levels of moisture are available for evapotranspiration. With projected increases in temperature and precipitation in most months for each future time period (Table 4.3), it is reasonable to assume that the large modelled increases in PET are associated with a projected warmer climate. Increases to AET are likely due to the projected increases in precipitation, which would provide the increased moisture levels needed to increase AET. These modelled results do not take into account changes to vegetation canopy and its control on AET.

Some factors that will affect AET in future climate scenarios that are not accounted for in the modelled results are affects increased CO_2 and increases to plant activity and growth. Increased climate warming and CO_2 levels can result in increased AET with an earlier onset and longer growing season, and an increased vegetation structure, causing changes in parameters like LAI (Leaf Area Index) and canopy coverage (Frederick, 1997; Parmesan and Yue, 2003; Zhang et al., 2009). However, observations in laboratory and field studies have shown that increases in concentrations of CO_2 can stimulate net photosynthesis and decrease stomatal conductance, thereby decreasing AET rates as less water is required for a given unit of CO_2 uptake (Rosenberg

et al., 1990; Levis et al., 2000; Long et al., 2004). The overall change on AET that these contrasting statements will have in the future is relatively unknown. However, water use from vegetation in response to CO_2 increases under climate warming is an important factor when assessing the water balance of a watershed, and when applying climate change scenarios in a region.

4.6.2 Projected Changes to soil moisture, ground water recharge, and SWE

Increased temperatures and changes in precipitation regimes could result in changes to soil moisture and evapotranspiration rates, as with increasing temperatures there is a subsequent increase in the potential evapotranspiration (Zhang et al., 2001). Based on simulations from the selected climate scenarios, soil moisture is projected to increase on average annually by 0.5% in the 2020s, 1.5% by the 2050s, and 2.5% by the 2080s. Modelled increases in soil moisture do not take into account the possible increase or decrease plant water use as discussed in Section 4.6.1., and do not incorporate seasonal changes. It has been suggested that an earlier snow melt could result in increased soil moisture earlier in the spring, a time when potential evaporation is low (Barnett, 2005), and that in summer there is likely to be soil moisture deficits (Saunders and Byrne, 1995; Gleick and Chalecki, 1999). Snow is important for water storage and soil moisture recharge, and with projected decreases in SWE (Table 4.4) higher potential vegetation productivity from increased heat and atmospheric CO_2 could be limited due to late summer soil moisture deficits (Eckhardt and Ulbrich, 2003; Sauchyn and Kulshreshtha, 2008).

Based on simulations from the selected climate scenarios, groundwater recharge is projected to increase on average by 2% in the 2020s, 4% by the 2050s, and 8% by the 2080s. Previous studies indicate that the overall rate of groundwater recharge could increase by as much as 53% (e.g. Jyrkama and Sykes, 2007), or decrease as much as 50% (Eckhardt and Ulbrich, 2003) as a result of climate change. Warmer winter temperatures will reduce the extent of ground frost and cause an earlier shift in the spring melt allowing more water to infiltrate into the ground

(Eckhardt and Ulbrich, 2003). Despite groundwater's importance, temporal and spatial changes, and rates of recharge across Canada are unknown, and research on the impacts of climate change remains limited (Hoffman et al., 1998; Jyrkama and Sykes, 2007). Future projected increases in winter flows (Figure 4.5) are likely to be attributed to increased groundwater recharge and possible increases in discharge, assuming an exponential discharge of the groundwater storages.

The Rocky Mountain region in Alberta receives considerable volumes of snow in the winter, with nearly 85% of the area's total annual streamflow derived from this snowpack (Grant and Kahan, 1974). Changes in the snowpack could greatly change the hydrological regime in basins where streamflow is snowmelt dominated. Based on simulations from the selected climate scenarios, depth of SWE is projected to decrease on average by 47% in the 2020s, 61% by the 2050s, and 66% by the 2080s. Reduced winter snowfalls have already been observed in the latter half of the twentieth century (Akinremi et al., 1999). Mote et al (2005) found decreases of 15-30% in snow water equivalent (SWE) in the Canadian Rockies from observed SWE data collected between 1950 and 1997, and expect losses in the snowpack to continue with further increases in temperatures. Increasing winter and spring temperatures would increase the ratio of rain to snow and, thereby, increase winter streamflows and diminish snowpacks (Leung et al., 2004; Lapp et al., 2005; Mote et al., 2005; Byrne and Kienzle, 2008; Sauchyn and Kulshreshtha, 2008). Zhang et al (2000) found that, in the last half of the twentieth century, there was no significant change in spring precipitation amounts, but the ratio of snow to total precipitation significantly decreased. This is confirmed by Akinremi et al (2001) who found that there was a 60% increase in the number of rainfall events in central Alberta during the first four months of the year.

4.6.3 Projected Changes to Streamflow

Climate scenarios project increases in precipitation, and are not forcing changes to evapotranspiration as discussed in Section 4.6.1 of this chapter. According to the basic

hydrological equation, if input (precipitation) is increased and no changes are made to evapotranspiration, it is logical to see increases in streamflow. Table 4.3 shows projected average increases in precipitation for all seasons for all climate scenarios, except for the summer 2050 time period, which projects an overall average decrease in precipitation. These projections are consistent with a study in the headwaters of the UNSRB (Demuth and Pietroniro, 2003) that used five GCMs to project temperature and precipitation centered around the 2050s and projected increased temperatures, particularly for the winter and spring periods. Another study, an evaluation of eleven GCM scenarios for the Canadian Prairie Provinces (Töyrä et al., 2005), also found projected mean annual precipitation increases in both the 2050 and 2080 time periods, with winter precipitation projected to increase, summer and spring precipitation projected to decrease, and annual mean temperatures projected to increase in every season. Increases in spring streamflow yields are likely due to increased precipitation. Increases in winter flows are likely due to increased winter temperatures projected by all of the models in winter (DJF). With projected decreases in SWE and warmer temperatures, increased winter flows are likely the result of an increase of rain on snow events.

Analysis of climate change impacts on hydrological processes, including streamflow, was carried out for the Cline River Watershed, which is a mountainous, heavily glaciated watershed in the UNSRB. Therefore, it does not represent the full extent of potential climate change impacts further downstream of the Cline River Watershed. Of particular interest was how these impacts will affect seasonality of streamflow, variance of annual streamflow, and annual water yields. Interpretations are made in terms of trends rather than absolute changes due to uncertainties associated with the projected changes. Interpretations for all future scenario outputs of streamflow do not include glacial melt contributions. As discussed earlier in this chapter, future declines in volumes of future glacial melt contributions are currently not being modelled in ACRU. Attempts have been made to predict the time in which glaciers will disappear, based on

past and current glacier retreat rates and future climate scenarios. Hopkinson and Young (1998) have proposed that glaciers in the Bow Valley, adjacent to the headwaters of the UNSRB, could disappear in approximately 150 years if they continue to deplete at current rates. Based on this observation, it can be assumed that glacial contributions will occur into the 2080s. Glacial contributions are likely to increase streamflows, particularly evident during low flow years and during low flow periods in late summer and early fall. However, at this time it is not known what magnitude glacier melt contributions will have on future streamflow scenarios. Glacier melt contributions will be modelled when the glacial melt routine in ACRU is updated. Results for all time periods should be updated accordingly, with water yields likely to differ in some months due to un-modelled glacier melt contributions.

4.6.3.1 Seasonality

Output from all scenarios and future time periods show an earlier shift in spring flows, and peak streamflow by almost a month (Figure 4.5). Increases in spring precipitation and warmer temperatures that melt out the snow pack are the main contributions to an early spring runoff and peak flow. Snowpack in the mountain areas would melt out earlier due to warmer spring temperatures, and increases in spring precipitation would add to the melting snowpack or increase runoffs if it fell as rain. An earlier spring melt and increased streamflow in the spring is consistent with other climate change impact studies (Burn, 1994; Barnett et al., 2005; Rood et al., 2008; Sauchyn and Kulshreshtha, 2008). Increases to winter flows, are also evident (Figures 4.5 and 4.6). Projected increases to winter flows are likely due to a higher, and more consistent, baseflow, resulting from modelled increases to soil moisture and groundwater recharge. However, increases to winter flow are fairly minimal until the 2080s (Figure 4.5), making it unclear if increased flows would be due to increased baseflows, warmer temperatures causing winter snow melt, or more rain on snow events, or a combination of those factors. Part of the earlier shift in spring runoff, late summer, and early fall decreases in streamflow are likely over-

estimated due to not modelling glacier melt. It has been shown in parts of the Cline River Watershed that glacial melt runoff can contribute up to 70% of the streamflow in late summer and early fall (Loijens, 1974; Comeau, 2008). Projected warmer temperatures in summer and fall with smaller increases in precipitation are also likely contributing to decreased late summer and fall streamflows relative to the baseline period.

4.6.3.2 Extreme Events

Figures 4.7-4.9 show the estimated changes to flows for the 2020 and 2080 time periods relative to the baseline period. Figure 4.7 highlights an increase in the flows over the entire 30 year period for the 2020s and 2080s. Both time series show the same trend of low, median, and peak flows increasing in magnitude and frequency, with slight decreases in medium high flow relative to the baseline period. These same trends are evident in the 2050s. Figures 4.8 and 4.9 highlight the fact that the minimum and some maximum streamflows are expected to increase in magnitude and frequency. The lowest average low flow in the 2020s and 2080s is estimated to be at least two and a half times the magnitude of the lowest flow in the baseline 1961-90 time period (Figure 4.8) based on modelled climate change output. Low flows associated with the exceedence probability of 42% during the baseline period are simulated to have an exceedence probability of 97% in the 2020s and 2080s (Figure 4.8). This indicates that low flows would be less of an issue than floods for water managers in the UNSRB. The highest estimated peak flows are estimated to increase at least 35% for the 2020s, and as much as 50% for the 2080s when compared to the highest flow from the baseline period (Figure 4.9). Frequency of flood events is also expected to increase as major flood events with an exceedence probability of 3% for the baseline period by the 2020s have an exceedence probability of at least 25%, and at least 20% for the 2080s. Increases to low flows can be the result of no negative changes in baseflows due to increased groundwater recharge (Table 4.4) and an increase in winter runoff. The exclusion of simulating glacial melt contributions likely contributes to future increases in low flows, as glacial

melt contributions are greatest in late summer and early fall with low flows are most common. Increases to peak high flows are likely from an accelerated snowmelt with increases in temperatures and precipitation in the form of rain on snow to accelerate snowmelt and spring runoffs.

4.6.3.3 Water Yields

Water yields were analyzed on a monthly basis for all GCM output and for each time period, and averaged for each time period. Average changes in water yields are projected to be positive, except for small decreases projected by two scenarios in the 2020s (Table 4.5). Changes in monthly streamflow for each time period followed a similar trend, with the largest increases in winter and spring months (November to May), and large decreases in summer (July to September) streamflows (Table 4.6). The largest percent decreases were in August and the greatest increases in April. Increased flows in these winter and spring months are attributed to the warmer projected temperatures and increases to precipitation for these months (Table 4.3), causing earlier snow melt and increases of rain on snow events. Rain on snow events increase the melt rate of snowpacks by increasing sub-snowpack soil temperatures (Putkonen and Roe, 2003). Results showing an increase in winter runoff are consistent with other studies in the region (Stewart et al., 2005; Lapp et al., 2005; Sauchyn and Kulshreshtha, 2008). Demuth and Pietroniro (2003) found that projections for the 2050s indicated increased temperatures, particularly for the winter and spring periods, with increases in precipitation in the winter and spring periods, which would contribute to overall increases in water yields, especially in winter and spring months (Table 4.5). Results from this research are also consistent with many studies that indicate a reduction in summer flows, and overall reduced snowmelt-derived streamflows in the western Rocky Mountains (Rood et al., 2005; Stewart et al., 2005; IPCC, 2007; Byrne and Kienzle, 2008; Sauchyn and Kulshreshtha, 2008). Again, these results exclude glacier melt contributions, which should increase summer and fall streamflows.

Rood et al. (2005) concluded that streamflow has declined in the North American central Rocky Mountains over the past century, and that this region could see streamflows decline by a further 10% by 2050. Results from the output from the selected climate scenarios for a glaciated montane watershed in the UNSRB, streamflows are expected to increase, with water yields flowing into Lake Abraham increasing by 7% on average by the 2050s, based on hydrological simulations excluding glacial melt waters. Clair et al. (1998) found that under a doubling of CO_2, that total annual runoff in the Montane Cordillera and Boreal Plains regions of Canada (making up the UNSRB) is estimated to increase from 12 to 21%, which corresponds to some of the 2080 scenario output for this research.

Glacial melt contributions were not considered in the modelling, however glacial contributions in the Cline River Watershed are significant, and will be modelled when changes are made to glacier melt routines in ACRU. Accumulation and ablation of the snowpack and glaciers in snowmelt dominated watersheds are the most important factors controlling the timing and volumes of water available (Merritt et al., 2006). With glacier melt contributions expected to decline into the future (IPCC, 2007; Sauchyn and Kulshreshtha, 2008), it is critical that glaciers are properly modelled to determine realistic ranges of water yields past the 2020 time period. Demuth and Pietroniro (2003) concluded that, in the UNSRB, hydrological regimes dependent on the timing and magnitude of glacier melt water may already be experiencing the medium to long-term impacts of climate change, which could change future water yield estimates. Results of this research do show that, if glacier melt is neglected (Figure 4.3), the overall volume of water (area under the curves) increases when compared to baseline water simulations. Timing of peak flows is expected to shift with an earlier peak flow, and lower flows starting earlier in the year (Figure 4.3). However, overall water yields, even when glacier melt is neglected, are expected to equal or exceed current water yields based on future climate projections.

4.6.4 Uncertainty in Projections and Modelling

The ability of physically based models to assess the effects of climate change has been recognized (Bathurst and O'Connell, 1992; Barnett et al., 2005; Barrow and Yue, 2005; Forbes, 2007). However, major limitations in the use of physically based distributed models are the availability and quality of watershed and climate data at the spatial and temporal resolution. The selected scenarios produce a wide range of projected changes in the hydrologic regime of the modelled watershed. Output for all selected scenarios indicate an earlier onset of the spring freshet and higher peak flows, with lower late season flows compared to the base scenario. However, there is a large degree of variation between predicted annual and seasonal flow volumes and the scale of the timing shift between all time periods. This can be partly attributed to uncertainty in model outputs due to uncertainties in data, model structure, and projections from the selected scenarios. A brief discussion of uncertainties associated with the model and input data, as well as uncertainties regarding GCM output and the selected scenarios, follows.

4.6.4.1 Data Uncertainty

Data needed to properly model hydrological processes were limited in the UNSRB. Key model inputs, including land cover and soils, are generalized, and some variables, such as plant transpiration coefficients (PTCs), were nonexistent and needed to be determined. In general, mountain areas have poor representative climate data, typically captured at lower elevation sites, which is the case in this study. Some climate data do exist at higher elevations, but these records are short, often seasonal, and inadequate for long-term climate studies (Luckman, 1998).

These limitations in data availability and spatial and temporal representation are problematic when setting up a model for a large, heterogeneous and spatial complex area such as the UNSRB. PRISM climate surfaces (Daly, 2006) were used to provide a spatial reference source for interpolated climate surfaces to calculate a number of critical parameters required for the ACRU model. Although not perfect, the PRISM surfaces were used to calculate initial

precipitation and temperature based correction factors in ACRU for each HRU, to account for differences between the climate base station values and the highly spatially complex terrain of the study area. However, for some watersheds and some months, the PRISM derived correction factors required further adjustment, as became evident after comparing the perceived precipitation regime against the observed streamflow regime. As the UNSRBs western border is along the continental divide, potential influences associated with the divide on local climate are a relatively unknown factor due to the sparse climate station network.

Many generalizations had to be made with the soils data. A method was developed considering the poorly mapped soils data in the mountain areas, and having generalized soils data for only approximately 10% of the study area. Based on the analysis of available soils data, it was established that there was no statistically significant relationship between soil properties, such as texture or organic carbon content, and terrain attributes, such as elevation, slope, or aspect. This is in agreement with the findings by Rahman et al. (1996), who found in a study of Rocky Mountain forest soils that relationships among soils properties and terrain attributes were statistically non-significant. Due to the lack of data, broad and uniform assumptions over the large study area needed to be made, based on sparsely observed data, which cannot be realistic for all HRUs and introduces uncertainty into the simulated results (Grayson and Bloeschl, 2000).

4.6.4.2 Modelling Uncertainty

As discussed in section 4.5.1 of this chapter, current glacier melt routines in ACRU assume an endless supply of glaciers to melt out. This proved to be a serious deficiency of the current model structure, as glaciers melt out, glacier area and volumes decrease, thereby decreasing the amount of glacial melt produced as the volume of ice in the glacier decreases. Attempts have been made to predict the time in which glaciers will disappear based on past and current glacier retreat rates and future climate scenarios. Hopkinson and Young (1998) have proposed that glaciers in the Bow Valley, adjacent to the headwaters of the UNSRB, could

disappear in approximately 150 years if they continue to deplete at current rates. With the supply of glaciers in modelled output assumed to be unlimited, future estimates of streamflow for the 2050s and the 2080s are highly questionable, resulting in future scenarios being assessed without glacier melt as a factor.

As discussed in Section 3.5.3.1 of this thesis, properly modelling SWE as only an open or forested area is problematic when looking at large forested areas with varying degrees of canopy cover and clearings, as seen in the UNSRB. This was dealt with in the verification process by modelling SWE as a forested and open area and taking a percentage of both. Other model deficiencies that add uncertainty into the results are how changes in vegetation cover and plant water use changes over time. ACRU has the ability to manipulate land cover and simulate impacts of changes to it, but was not used in this research to see what impacts changes in vegetation, such as a higher tree-line, would impact streamflow in mountainous areas under climate change.

4.6.4.3 CGM Scenario Uncertainty

The selected climate scenarios for this research do not cover the full spectrum of possible worldwide GCM predictions. Rather, the selected climate change scenarios from the PCIC were selected to provide a basis for sensitivity analysis of the possible impact of changes in climate on streamflow in the UNSRB.

Several factors present uncertainty in using climate models for water resource management including the spatial scale of GCMs, the accuracy of simulated climate in time and space, scenario development based on unknown factors such as population and energy demand growth forecasts, changes in land use or vegetation under different climates, and whether assumptions of parameterization under present climates will hold true for future climates (Lins et al., 1997; Merritt et al., 2006). In GCMs, runoff and evapotranspiration processes tend to be

poorly represented, and precipitation estimates are notoriously uncertain in both magnitude and timing (Merritt et al., 2006). The wide range in the projection of precipitation highlights the uncertainty surrounding future precipitation trends. That being said, all of the selected GCM based climate scenarios estimate mean monthly increases in precipitation and increases in spring precipitation, as discussed in the selection process in Section 4.4.3.2. This indicates a trend of increasing precipitation, regardless of uncertainty in GCM output. Differences between the various GCM based scenarios of future climate are responsible for some of the uncertainty that exists in any attempt to study regional climate change impacts. Uncertainty in the scenarios is due in part to uncertainties in how the natural environment, the economy, and society in general will react to global climate changes (Cohen, 1991).

4.7 Conclusions

Projected increases in temperature and precipitation are projecting average increases in evapotranspiration (potential and actual), groundwater recharge, soil moisture, and streamflow in the Cline River Watershed. Increases in both high and low flow magnitudes and frequencies, and large increases to winter and spring streamflows are projected from all scenario output. Earlier timing of spring runoff, and increased peak flows are estimated to occur up to four weeks earlier than the observed. Output for later time periods show similar trends, with increasing average annual water yields for the 2050s and 2080s, as well as larger increases and decreases in monthly and seasonal water yields. Increased peak and low flow magnitudes and frequencies are also projected to increase into the 2050s and the 2080s. The largest decreases in season flows are projected to be in the summer and early fall months, with estimates of decreasing water yields by over 50% for all three future time periods. With overall water yields projected to increase over time, a large shift in seasonality is likely the biggest impact climate change will have on water resources in the Cline River Watershed.

Current inadequate modelling of future glacial flows by not accounting for possible decreased glacier melt contributions from diminishing glacier volumes in the region over time prevented the modelling of glacier melt contributions to streamflow for this research. Glaciers contribute a significant amount of melt water to streamflow in the Cline River Watershed (Loijens, 1974; Comeau, 2008). On a regional scale, the rate of glacier decline is difficult to project since glacier response to climate variations is individual, depending on many local factors such as glacier shape, size, steepness, and ice depth (Comeau, 2008). For example, glaciers in basins that receive reliable snow input from avalanches or wind-blown snow accumulation may be less susceptible to climate changes (Kuhn 1993). However, glacial retreat rates in the UNSRB need to be integrated in the glacier melt routine in ACRU to be able to properly model melt rates and impacts on streamflow, especially in later time periods. When glaciers are properly modelled climate scenario output for future time periods can be viewed with a greater degree of confidence. Modelled changes on streamflow from this research for the next few decades are of most value to water managers, and should be viewed as conservative or under-estimates as they do not include glacial melt contributions. Once these model deficiencies are dealt with, impacts of climate change can be looked at in more detail for the Cline River Watershed, and will be used by water managers to make informed decisions on possible impacts on future hydropower generation in this area.

Chapter 5

Summary, Conclusions, and Recommendations

5.1 Research Summary and Conclusions

The ACRU agro-hydrological modelling system (Schulze, 1995) was used in this research to establish a fundamental basis to estimate the impacts of climate change on water yield, streamflow extremes, and the streamflow regimes in the upper North Saskatchewan River basin (UNSRB), and consequently, water availability for hydropower generation in the Cline River Watershed.

In order to allow for streamflow verification and the estimation of water yield that feed the hydropower reservoirs, the UNSRB was divided into 12 watersheds, based on either a gauging station or hydroelectric dam location to define the outlet. Each watershed was further divided into hydrological response units (HRUs) based on elevation, land cover, mean annual radiation, and watershed boundary, which resulted in 1528 HRUs. Each HRU was parameterized individually for input into ACRU from spatial surface and hydrometeorological data. After parameterization of ACRU was complete, ACRU was verified against five observed data sources: air temperature, A-pan potential evapotranspiration, snowpack accumulation and melt from snow pillows and snow courses, melt contributions from Peyto Glacier and its equilibrium line altitude, and daily observed streamflow time series for two gauging stations in the Cline River watershed.

Monthly and daily temperatures are slightly over-simulated, with monthly mean temperatures being statistically not different ($p=0.46$) and daily temperatures statistically different ($p=0.00$) based on P-values from the two-tailed t-tests. Simulated PET was under-simulated, but considered not statistically different ($p=0.14$) based on the P-value from a two-tailed t-test. Seasonality of A-pan was properly simulated, however magnitudes were consistently under-simulated, which could be due to known problems with A-pan measurements (Bosman, 1987).

When compared to all observed snow water equivalent (SWE) values, daily SWE depths were slightly under-simulated, with daily SWE depths not statistically different for the snow courses ($p=0.45$), and considered statistically different for the snow pillows ($p=0.01$) based on the P-value of the two-tailed t-test. Overall simulation of peak SWE and timing of the snow melt was good. SWE was sometimes over- and sometimes under-simulated, while some years are well simulated. Correlation statistics were good when all observed SWE data were compared with simulated values, and relatively good correlation between observed and simulated SWE depths for snow courses, snow pillows, and all combined SWE data. When simulated output was compared to observed glacier mass balance data, the average equilibrium line altitude (ELA) was simulated at approximately 2600masl, which is consistent with the literature in the region (Demuth and Keller, 2009; WGMS, 2009). This glacier melt is simulated to result, on average, in a situation where HRUs below the ELA contribute about 85-90% of the glacial melt, while 10-15% occurs above the ELA. The glacial melt factor was also calibrated from almost 30 years of annual glacier melt to ensure that melt contributions closely matched average observed glacial melt in the UNSRB.

Simulated streamflow for the Cline River Watershed compared well with the observed data just downstream of Bighorn Dam. Total water yields were slightly over-simulated for the 1961-90 time series (2.18%). Mean flows were simulated well as simulated means were not statistically different ($p>0.05$) from the observed, based on the P-values of the two-tailed t-tests. The difference between variances is very good for daily and monthly statistics, indicating that simulation of peak and low flows were preserved. Overall correlation statistics are good, with a strong correlation between observed and simulated flows for daily ($r^2= 0.96$) and monthly ($r^2= 0.92$) time series. The regression coefficient is less than unity indicating a slight under-simulation of high flows. Generally, ACRU simulated the behavior of the watershed well, as the timing of peak and baseflows are well simulated. Seasonality of observed and simulated was also well simulated, with slight over-simulations in August, October, and November.

Climate change scenarios for this research were downloaded from the Pacific Climate Impacts Consortium (PCIC) for use in estimating climate change impacts on streamflow in the UNSRB. Five GCM climate scenarios were selected and regionally downscaled using the delta method. Selection was made based on temperature and precipitation changes for the spring (MAM) 2050 time period relative to the 1961-90 baseline period. There were three future time series assessed in this research that are recommended by the IPCC (2007); 2020s (2010-2039), 2050s (2040-2069), and 2080s (2070-2099).

Projected increases in temperature and precipitation are projecting overall increases in evapotranspiration (potential and actual), groundwater recharge, soil moisture, and streamflow. Output for the nearest time period (2020s) projects overall and monthly decreases and increases in water yields. Increases in both high and low flow magnitudes and frequencies, and large increases to winter and spring streamflows are also projected. Earlier timing of spring runoff, and increased peak flows are estimated to occur up to four weeks earlier than the observed. Output for later time periods show similar trends, with increasing overall annual water yields for the 2050s and 2080s, as well as larger increases and decreases in monthly and seasonal water yields. Peak and low flow magnitudes and frequencies are also projected to increase into the 2050s and the 2080s. The largest decreases in seasonal flows are projected to be in the summer and early fall months, with estimates of decreasing water yields by over 50% for all three future time periods. With overall water yields projected to increase over time, a large shift in seasonality is likely the biggest impact climate change will have on water resources in the Cline River Watershed.

Current inadequate modelling of future glacial flows by not accounting for possible decreased glacier melt contributions from diminishing glacier volumes in the region over time prevented the modelling of glacier melt contributions to streamflow for this research. Glaciers contribute a significant amount of melt water to streamflow in the Cline River Watershed

(Loijens, 1974; Comeau, 2008). On a regional scale, the rate of glacier decline is difficult to project since glacier response to climate variations is individual, depending on many local factors such as glacier shape, size, steepness, and ice depth (Comeau, 2008). For example, glaciers in basins that receive reliable snow input from avalanches or wind-blown snow accumulation may be less susceptible to climate changes (Kuhn 1993). However, glacial retreat rates in the UNSRB need to be integrated in the glacier melt routine in ACRU to be able to properly model melt rates and impacts on streamflow, especially in later time periods. When glaciers are properly modelled climate scenario output for future time periods can be viewed with a greater degree of confidence. Modelled changes on streamflow from this research for the next few decades are of most value to water managers, and should be viewed as conservative or under-estimates as they do not include glacial melt contributions. Once these model deficiencies are dealt with, impacts of climate change can be simulated in more detail for the Cline River Watershed, and will be used by water managers to make informed decisions on possible impacts on future hydropower generation in this area.

The results from this research indicate an increase in winter runoffs, which is consistent with other studies in the region (Stewart et al., 2005; Lapp et al., 2005; Sauchyn and Kulshreshtha, 2008), but also contradicts a projected reduction in winter flows by the IPCC (2007). These results are also consistent with many studies that indicate a reduction in summer flows, and overall reduced snowmelt-derived streamflows in the western Rocky Mountains (Rood et al., 2005; Stewart et al., 2005; IPCC, 2007; Byrne and Kienzle, 2008; Sauchyn and Kulshreshtha, 2008).

5.2 Recommendations

5.2.1 Improvements to Present Research

Data needed to properly model hydrological processes were limited in the UNSRB. Key model inputs, including land cover and soils, are generalized, and some variables, such as plant

transpiration coefficients (PTCs), were nonexistent and needed to be determined. PRISM climate surfaces (Daly, 2006) were used to provide a spatial reference source for interpolated climate surfaces to calculate a number of critical parameters required for the ACRU model. Although not perfect, the PRISM surfaces were used to calculate initial precipitation and temperature based correction factors in ACRU to account for differences between the interpolated PRISM surface, base station values, and the highly spatially complex terrain of the study area. Lack of representative long term climate data, combined with unknowns such as influences associated with the continental divide on local climate made modelling in this area very challenging. High elevation climate stations throughout the mountainous regions of the watershed are needed in order to better simulate hydrological processes at higher elevations. Many generalizations had to be made with the soils data. An initial soil parameter estimation method was developed, based on poorly mapped soils data in the mountain areas, and on generalized soils data available for approximately 10% of the study area. Due to a lack of data, broad and uniform assumptions over the large study area needed to be made. To improve modelling capabilities and confidence in the results, field work is required to improve the quality of results for this project.

5.2.2 Future Research in the UNSRB

There is uncertainty in the estimated impacts on streamflows in the Cline River Watershed based on the future climate change scenarios. Streamflows are expected to increase due to predicted higher precipitation rates. However, the true streamflow volumes are likely to be lower than simulated here. This is due to several key factors not addressed in this research: 1) effects of decreasing glacier area and volumes which decreases glacial melt volumes, and 2) a higher tree line in the mountains, likely to result in less runoff due to increased evapotranspiration and increased losses from interception and infiltration processes. In the ACRU version used, glacier melt is simulated as if there was an unlimited supply of glacier ice. Another problem with the estimated streamflows is that the precipitation and temperature patterns used in the 2020,

2050, and 2080 time series are simply perturbed 30-year daily baseline time series from 1961-1990, which may not reflect probable future changes in precipitation patterns, such as an increase or decrease in precipitation days, or changes in rainfall intensities. Any future climate change impact studies on water resources in this region must be able to simulate glacial melt flows under current and predicted future conditions, changes in vegetation such as a higher tree line, and use of longer historical time series, such as using climate trends from tree ring data (Lapp et al., 2009). Five GCM scenarios were selected from 42 possible GCM scenarios from the PCIC to assess climate change impacts on streamflows. To provide a more comprehensive range of plausible climate impacts on water resources in the UNSRB, a larger number of GCM scenarios could also be considered. Selecting a larger number of scenarios to encompass a greater range in terms of overall projected temperature and precipitation changes in the region would also be beneficial for future water management.

REFERENCES

Abbott, M. B., Bathurst, J. C., Cunge, J. A., O'Connell, P. E., & Rasmussen, J. (1986). An introduction to the European Hydrological System - Système Hydrologique Européen, "SHE". 1: History and philosophy of a physically-based distributed modelling system. *Journal of Hydrology*, **87**, 45-59.

ACRU 2007: The ACRU Model: Home Page. http://www.beeh.unp.ac.za/acru/. Last accessed November 11, 2007.

Adams, R.S., Spittlehouse, D.L. and Winkler, R.D. (1998). The snow melt energy balance of a clearcut, forest and juvenile pine stand. Pages In*: Proceedings 23rd Conference on Agricultural and Forest Meteorology*, American Meteorological Society, Boston, Massachusetts, 54-57.

Ahrens, C. D. (2006). Meteorology Today. An Introduction to Weather, Climate, and the Environment. Eighth Edition. Thompson, Brooks/Cole. United States, pp. 537.

Akinremi, O.O., McGinn, S.M., & Cutforth, H.W. (1999). Precipitation Trends on the Canadian Prairies. *Journal of Climate*, **12**(10), 2996-3006.

Akinremi, O.O., McGinn, S.M., & Cutforth, H.W. (2001). Seasonal and Spatial Patterns of Rainfall Trends on the Canadian Prairies. *Journal of Climate*, **14**(9), 2177-2183.

Andréasson, J., Lindström, G., Grahn, G., & Johansson, B. (2004). Runoff in Sweden – Mapping of climate change impacts on hydrology. In: Proceedings, XXIII Nordic Hydrological Conference, Tallinn, Estonia, 8-12 August 2004, pp. 625-632.

Arnell, N.W. (2004). Climate change and global water resources. *Global Environmental Change*, **9**, 31-49.

Bathurst, J. C., & O'Connell, P. E. (1992). Future of distributed modelling: The Systeme Hydrologique Europeen. *Hydrological Processes*, **6**, 265–277.

Barnett, T.P., Adam, J.C., & Lettenmaier, D.P. (2005). Potential impacts of a warming climate on water availability in snow dominated regions. *Nature*, **438**, 303-309.

Barrow, E., & Yu, G. (2005). Climate scenarios for Alberta: A report prepared for the Prairie Adaptation Research Collaborative (PARC) in co-operation with Alberta Environment. Pgs 1-73.

Beven, K. (1989). Changing ideas in hydrology- the case of physically based models. *Journal of Hydrology*, **105**, 157-172.

Beven, K. (2001). How far can we go in distributed hydrological modelling?. Hydrology and Earth System Science, **5**(1), 1-12.

Bitz, C.M. & Liscomb, W.H. (1999). An energy-conserving thermodynamic model of sea ice. *Journal of Geophysical Research*, **104**, 15669–15677.

Bonsal, B.R., Prowse, T.D., & Pietroniro, A. (2003). An assessment of global climate model-simulated climate for the western cordillera of Canada (1961–90). *Hydrological Processes*, **17**(18), 3703-3716.

Bosman, H.H. (1987). The influence of installation practices on evaporation from Symon's tank and American Class A-pan evaporimeters. *Agricultural and Forest Meteorology*, **41**, 307-323.

Bruce, J.P., Martin, H., & Colucci, P. (2003). Climate change impacts on boundary and transboundary water management. A Climate Change Action Fund Project A458/402, Natural Resources Canada. 161 pages.

Brutsaert, W. (1981). Evaporation into the atmosphere: theory, history, and applications. D. Reidel Publishing Company, Dordrecht, Holland, p. 299.

Brooks, E.S., Boll, J., & McDaniel, P. (2007). Distributed and integrated response of a geographic information system-based hydrological model in the eastern Palouse region, Idaho. *Hydrological Processes*, **21**, 110–122.

Burn, D.H. (1994). Hydrologic effects of climatic-change in West-Central Canada. *Journal of Hydrology*, **160**(1-4), 53-70.

Byrne, J. & Kienzle, S.W. (2008). The Prairies. In: Lemmon, D, Warren, F., Bush, E. and Lacroix, J. (Eds.): From Impacts to Adaptation: Canada in a Changing Climate 2007. Report to the Government of Canada, Chapter 7.

Byrne, J., MacDonald, R.J., Kienzle, S.W., & Boon, S. (2010). Modelling the potential impacts of climate change on snowpack in the North Saskatchewan River watershed, Alberta. *In prep*.

Canadell, J, Jackson, R.B., Ehleringer, J.R., Mooney, H.A., Sala, O.E., and Schulze, E.D. (1996). Maximum rooting depth of vegetation types at the global scale. *Oecologia*, **108**, 583-595.

Cayan, D.R., Kammerdiener, S., Dettinger, M.D., Caprio, J.M., Peterson, D.H. (2001). Changes in the onset of spring in the western United States. *Bulletin of the American Meteorological Society*, **82**(3), 399–415.

Chen, J.M., & Black, T.A. (1992). Defining leaf area index for non-flat leaves. *Plant, Cell and Environment*, **15**, 421-429.

Chiew, F.H.S., & McMahon, T.A. (1992). An Australian comparison of Penman's potential evapotranspiration estimates and class A evaporation pan data. *Australian Journal of Soil Research*, **30**(1), 101-112.

Clair, T.A., Ehrman, J., & Higuchi, K. (1998). Changes to the runoff of Canadian ecozones under a doubled CO_2 atmosphere. *Journal of Fisheries and Aquatic Sciences*, **55**(11), 2464-2477.

Cohen, S.J. (1991). Possible impacts of climatic warming scenarios on water resources in the Saskatchewan River sub-basin, Canada. *Climate Change*,**19**, 291–318.

Comeau, L.E.L. (2008). Glacier Contribution to the North and South Saskatchewan Rivers. M.Sc. Thesis. University of Saskatchewan, Saskatoon, Saskatchewan, Canada.

Comeau, L.E.L., Pietroniro, A., & Demuth, M.N. (2009). Glacier Contribution to the North and South Saskatchewan Rivers. *Hydrological Processes*, **23**, 2640-2653.

Daly, C., Neilson, R.P., Philips, D.L. (1994). A statistical-topographic model for mapping climatological precipitation over mountainous terrain. *Journal of Applied Meteorology*, **33**, 140-158.

Daly, C., Gibson, W.P., Taylor, G.H., Johnson, G.L., & Pasteris, P. (2002). A knowledge-based approach to the statistical mapping of climate. *Climate Research*, **22**, 99-113.

Daly, C. (2006). Guidelines for assessing the suitability of spatial climate data sets. *International Journal of Climatology*, **26**, 707-721.

Daly, C., Smith, J.W., & Smith, J.I. (2007). High-Resolution Spatial Modeling of Daily Weather Elements for a Catchment in the Oregon Cascade Mountains, United States. *Journal of Applied Meteorology and Climatology*, **46**, 1565-1586.

Daly, C., Halbleib, M., Smith, J. I., Gibson, W. P., Doggett, M. K., Taylor, G. H., Curtis, J., & Pasteris, P. A. (2008). Physiographically sensitive mapping of temperature and precipitation across the conterminous United States. *International Journal of Climatology*, **28**, 2031–2064.

Demuth, M.N., & Pietroniro, A. (2003). The impact of climate change on the glaciers of the Canadian Rocky Mountain eastern slopes and implications for water resource-related adaptation in the Canadian Prairies: Phase I- Headwaters for the North Saskatchewan River Basin. Report for the Climate Change Action Fund- Prairie Adaptation Research Collaborative, 1-111.

Demuth, M.N., & Keller, R. (2009). An assessment of the mass balance of Peyto Glacier (1966–1995) and its relation to recent and past century climate variability. In: Demuth, M.N., Munro, D.S., Young, G.J. (Eds.), Peyto Glacier: One Century of Science, National Hydrology Research Institute Science Report No. 8, pp. 83–132.

Diaz-Nieto, J., & Wilby, R.L. (2005). A comparison of statistical downscaling and climate change factor methods: impacts on low flows in the River Thames, United Kingdom, *Climatic Change*, **69**(2-3), 245-268. doi: 10.1007/s10584-005-1157-6.

Dingman, S.L. (2002). Physical Hydrology, 2nd Ed. Prentice-Hall: Upper Saddle River, NJ, USA.

Eckhardt, K., & Ulbrich, U. (2003). Potential impacts of climate change on groundwater recharge and streamflow in a central European low mountain range. *Journal of Hydrology*, **284**(1-4), 244-252.

ESRI (Environmental Systems Research Institute, Inc). (2008). ArcInfo (Version 9.3) [Computer software].

Evans, J., & Schreider, S. (2002). Hydrological impacts of climate change on inflows to Perth, Australia. *Climate Change*, **55**(3), 361-393.

Everson, C.S. (2001). The water balance of a first order catchment in the montane grasslands of South Africa. *Journal of Hydrology*, **241**, 110-123.

Field, C. B., Jackson, R. B., & Mooney, H. A. (1995). Stomatal Responses to Increased CO2: Implications from the Plant to the Global Scale. *Plant Cell & Environment*, **18**, 1214–1225.

Flügel, W.A. (1995). Delineating hydrological response units by geographical information-system analyses for regional hydrological modelling using PRMS/MMS in the drainage-basin of the River Brol, Germany. *Hydrological Processes*, **9**(3-4), 423-436.

Flügel, W.A. (1997). Combining GIS with regional hydrological modelling using hydrological response units (HRUs): An application from Germany. *Mathematics and Computers in Simulation*, **43**(3-6), 297-304.

Forbes, K.A. (2007). Simulating the hydrological response to climate change in a southern Alberta watershed. M.Sc. Thesis. University of Lethbridge, Lethbridge, Alberta, Canada.

Frederick, K.D., & Major, D.C. (1997). Climate change and water resources. *Climatic Change*, **37**: 7-24.

Frederick, K. (1997). Water Resources and Climate change. *Resources for the Future, Climatic Issues Brief No. 3, June 1997*, Washington, DC, pp. 16.

Gan, T.Y. (1998). Hydroclimatic trends and possible climatic warming in the Canadian Prairies. *Water Resources Research, American Geophysical Union*, **34**(11), 3009–3015.

Gerrard, J. (1990). Mountain environments: an examination of the physical geography of mountains, MIT Press, Cambridge Massachusetts, p. 298.

Gleick, P.H., & Chalecki, E.L. (1999). The impacts of climatic changes for water resources of the Colorado and Sacramento-San Joaquin River Basins. *Journal of the American Water Resources Association*, **35**(6), 1429-1441.

Government of Alberta: Sustainable Resource Development. (2009). *Forest and Vegetation Inventories: Alberta Vegetation Inventory*. Retrieved Oct 19, 2009 from http://www.srd.alberta.ca/MapsFormsPublications/Maps/ResourceDataProductCatalogue/ForestVegetationInventories.aspx.

Government of Canada: Agriculture and Rural Development. (2001). *Agricultural Region of Alberta Soil Inventory Database*. Retrieved January 16, 2009 from http://www1.agric.gov.ab.ca/$department/deptdocs.nsf/all/sag3249.

Government of Canada: Agriculture and Rural Development. (2003). *Agroclimatic Atlas of Alberta: Maps*. Retrieved April 16, 2009 from http://www1.agric.gov.ab.ca/$department/deptdocs.nsf/all/sag7019.

Grant, L.O., & Kahan, A.M. (1974). Weather modification for augmenting orographic precipitation. W*eather and Climate Modification*, Hess WN (ed.). John Wiley and Sons: 282–317.

Grayson, R. & Blöschl, G. (Eds). (2000). Spatial Patterns in Catchment Hydrology: Observations and Modelling, Cambridge University Press, Cambridge, p. 404.

Gregory J.M., & Mitchell, J.F.B. (1997). The climate response to CO2 of the Hadley Centre coupled AOGCM with and without flux adjustment. *Geophysical Research Letters*, 15, 1943-1946

Hamlet, A.F., & Lettenmaier, D.P. (1999). Effects of climate change on hydrology and water resources in the Columbia Basin. *Journal of the American Water Resources Association*, **35**(6), 1597-1623.

Hay, L.E., Wilby, R.L., & Leavesley, G.H. (2000). A comparison of delta change and downscaled GCM scenario for three mountainous basins in the United States. *Journal of the American Water Resources Association*, **36**(2), 387-397.

Hay, L.E., & Clark, M.P. (2003). Use of statistically and dynamically downscaled atmospheric model output for hydrologic simulations in three mountainous basins in the western United States. *Journal of Hydrology*, **282**(1-4), 56-75.

Hennessy, K. J., Gregory, J. M., & Mitchell, J. F. B. (1997). Changes in Daily Precipitation under Enhanced Greenhouse Conditions. *Climate Dynamics*, **13**, 667–680.

Hock, R., Jansson, P., & Braun, L.N. (2005). Modelling the response of mountain glacier discharge to climate warming. *Global Change and Mountain Regions*, **23**, 243-252.

Hofmann, N., Mortsch, L., Donner, S., Duncan, K., Kreutzwiser, R., Kulshreshtha, S., Piggott, A., Schellenberg, S., Schertzerand, B., & Slivitzky, M. (1998). Climate change and variability: impacts on Canadian water in Responding to Global Climate Change. *National Sectoral Issue, Environment Canada, Canada Country Study: Climate Impacts and Adaptation*, **7**, 1-120.

Hopkinson, C., & Young, G.J. (1998). The effect of glacier wastage on the flow of the Bow River at Banff, Alberta, 1951-1993. *Hydrological Processes*, **12**, 1745-1762.

Hornberger, G.M., Raffensperger, J.P., Wiberg, P.L., & Eshleman, K.N. (1998). *Elements of Physical Hydrology*. The John Hopkins University Press, Baltimore, USA.

IPCC (2001). Climate Change 2001: The Scientific Basis. Contributions of Working Group I to the Third Assessment Report of the Intergovernmental Panel on Climate Change, J.T. Houghton et al., Cambridge University Press, Cambridge, 881pp.

IPCC (2007). Climate Change 2007: Synthesis Report. Contribution of Working Groups I, II and III to the Fourth Assessment Report of the Intergovernmental Panel on Climate Change. [Core Writing Team, Pachauri, R. K. and Reisinger, A. (eds.)]. IPCC, Geneva, Switzerland, 104pp. Available at http://www.ipcc.ch/pdf/assessment-report/ar4/syr/ar4_syr_spm.pdf.

Jackson, R.B., Canadell, J., Ehleringer, J.R., Mooney, H.A., Sala, O.E., and Schulze, E.D. (1996). A global analysis of root distributions for terrestrial biomes. *Oecologia*, **108**, 389-411.

Jansson, P., Hock, P., & Schneider, T. (2003). The concept of glacier storage: a review. *Journal of Hydrology*. **210**(1-4), 116-129.

Jasper, K., Calanca, P., Gyalistras, D., Fuhrer, J. (2004). Differential impacts of climate change on hydrology of two river basins. *Climate Research*, **26**, 113-129.

Jewitt, G.P.W., & Schulze, R.E. (1999). Verification of the ACRU model for forest hydrology applications. *Water, South Africa*, **25**, 483-489.

Jewitt, G.P.W., Garratt, J.A., Calder, I.R., & Fuller, L. (2004). Water resources planning and modelling tools for the assessment of land use change in the Luvuvhu Catchment, South Africa. *Physics and Chemistry of the Earth*, **29**(15-18), 1233-1241.

Jyrkama, M.I., & Sykes, J.F. (2007). The impact of climate change on spatially varying groundwater recharge in the grand river watershed (Ontario). *Journal of Hydrology*, **338**(3-4), 237-250.

Kienzle, S.W. (1993). Application of a GIS for simulating hydrological responses in developing regions. In: HydroGIS 93: Application of Geographical Information Systems in Hydrology and Water Resources Management (Proc. of the Vienna Conference, Austria, April 1993). IAHS Publications no. 211: 309-318.

Kienzle, S.W. (1996). Using DTMs and GIS to define input variables for hydrological and geomorphological analysis. In: HydroGIS 96: Application of Geographical Information Systems in Hydrology and Water Resources Management (Proc. of the Vienna Conference, Austria, April 1996). IAHS Publications no. 235: 183-190.

Kienzle, S.W., Lorenz, S.A., & Schulze, R.E. (1997). Hydrology and Water Quality of the Mgeni Catchment. *Water Resources Commission*, Pretoria, Report TT87/97, 1-88.

Kienzle, S.W. (2008). A new temperature based method to separate rain and snow. *Hydrological Processes*, **22**(26), 5067-5085.

Kienzle, S.W., & Schmidt, J. (2008). Hydrological impacts of irrigated agriculture in the Manuherikia Catchment, Otago, New Zealand. *Journal of Hydrology* (NZ), **47**(2), 67-83.

Kienzle, S.W. (2009). Advances in Spatial Snow Modeling in Mountain Terrain. Pages In : *Proceedings from the Western Snow Conference*, Canmore, Canada, 20-23 April 2004, pp. 57-68.

Kiker, G.A., Clark, D.J., Martinez C.J., & Schulze, R.E. (2006). A Java-based, object-oriented modeling system for southern African hydrology. *Transactions of the ASABE*, **49**(5), 1419–1433.

Krogman, K., & Hobbs, H. (1983). Scheduling irrigation to meet crop demands. Agriculture Canada, Research Branch, Technical Bulletin 1983-10E.

Kuhn, M. 1993. Possible future contributions to sea level change from small glaciers. In –*Climate and Sea Level Change: Observations, Projections and Implications*, Warrick, R.A.,Barrow, E.M. and Wigley, T.M.L. (eds.) Cambridge University Press, 134-143.

Lapp, S., Byrne, J., Townshend, I., & Kienzle, S. (2005). Climate warming impacts on snowpack accumulation in an Alpine watershed: a GIS based modeling approach. *International Journal of Climatology*, **25**(3), 521–536.

Lapp, S., Sauchyn, D., & Toth, B. (2009). Constructing scenarios of future climate and water supply for the SSRB: Use and limitations for vulnerability assessment. *Prairie Forum*, **34**(1), 153–180.

Leavesley, G.H. (1994). Modelling the effects of climate change on water resources- A review. *Climatic Change*, **28**, 159-179.

Legates, D.R., & McCabe, G.J. (1999). Evaluating the use of "goodness-of-fit" measures in hydrologic and hydroclimatic model validation. *Water Resources Research*, **35**(1), 233-241.

Leung, L., Qian, Y., Bian, X., Washington, W., Han, J., & Roads, J. (2004). Mid-Century Ensemble Regional Climate Change Scenarios for the Western United States. *Climate Change*, **62**, 75–113.

Levis, S., Foley, J. A., & Pollard, D. (2000). Large-scale vegetation feedbacks on a doubled CO^2 climate. *Journal of Climate*, **13**, 1313-1325.

Lins, H.F., Wolock, D.M., & McCabe, G.J. (1997). Scale and modelling issues in water resources planning. *Climatic Change*, **37**, 63–88.

Liu, Z., Xu, Z., Huang, J., Charles, S.P., & Fu, G. (2009). Impacts of climate change on hydrological processes in the headwater catchment of the Tarim River basin, China. *Hydrological Processes*, 24(2), 196-208.

Loaiciga, H.A., Valdes, J.B., Vogel, R., Garvey, J., & Schwarz, H. (1996). Global Warming and the Hydrological Cycle. *Journal of Hydrology*. **174**(1-2): 83-127.

Loijens, H.S. (1974). Streamflow formation in the Mistaya River Basin, Rocky Mountains, Canada. Western Snow Conference, **43**, 86-95.

Long, S.P., Ainsworth, E.A., Rogers, A., & Ort, D.R. (2004). Rising atmospheric carbon dioxide: plants FACE the future. *Annual Review of Plant Biology*, **55**, 591–628.

Lopez-Moreno, J.I., Beniston, M., & Garcia-Ruiz, J.M. (2008). Environmental change and water management in the Pyrenees: Facts and future perspectives for Mediterranean mountains. *Global & Planetary Change*, **61**(3-4), 300-312.

Loukas, A., Vasiliades, L., & Dalezios, N.R. (2002). Potential climate change impacts on flood producing mechanisms in southern British Columbia, Canada using the CGCMA1 simulation results. *Journal of Hydrology*, **259**, 163-188.

Luckman, B.H. (1998). Landscape and climate change in the central Canadian Rockies during the 20th century. *Canadian Geographer*, **42**(4), 319-337.

MacDonald, R.J. (2008). Climate change impacts on snowpack. M.Sc. Thesis. University of Lethbridge, Lethbridge, Alberta, Canada.

Markoff, M.S. & Cullen, A.C. (2007). Impact of climate change on Pacific Northwest hydropower. *Climatic Change*, **87**(3-4), 451-469.

Marquinez, J., Lastra, J., & Garcia, P. (2003). Estimation models for precipitation in mountainous regions: the use of GIS and multivariate analysis. *Journal of Hydrology*, **270**(1-2), 1-11.

Marsh, J. (2008). *Saskatchewan River*. The Canadian Encyclopedia. Retrieved September 30, 2008 from http://www.thecanadianencyclopedia.com/index.cfm?PgNm=TCE&Params=A1SEC827709.

Martinez, C.J., Campbell, K.L., Annable, M.D., Kiker, G.A. (2008). An object-oriented hydrologic model for humid, shallow water-table environments. *Journal of Hydrology*, **351** (3-4), 368-381.

Mbogga, M., Hamann, A., & Wang, T. (2009). Historical and projected climate data for natural resource management in western Canada. *Agricultural and Forest Meteorology*, **149**(5), 881-890.

McWhoter, D.B., & Sunada, D.K. (1977). Ground-Water Hydrology and Hydraulics. Water Resources Publi, Ft Collins, CO.

Milewska, E.J., Hopkinson, R.F., & Niitsoo, A. (2005). Evaluation of geo-referenced grids of 1961-1990 Canadian temperature and precipitation normals. *Atmosphere-Ocean*, **43**(1), 49–75.

Moore, R.D., & Demuth, M.N. 2001. Mass balance and streamflow variability at Place Glacier, Canada, in relation to recent climate fluctuations. *Hydrological Processes*, **15**(18), 3473-3486.

Moore, R.D., & Wondzell, S.M. (2007). Physical hydrology and the effects of forest harvesting in the Pacific Northwest: A review. *Journal of the American Water Resources Association*, **41**, 763-784.

Mote, P.W., Hamlet, A.F., Clark, M.P., & Lettenmaier, D.P. (2005). Declining mountain snowpack in western North America. *Bulletin of the American Meteorological Society,* **86**, 39-49.

Muzik, I. (2002). A first-order analysis of the climate change effect on flood frequencies in a subalpine watershed by means of a hydrological rainfall–runoff model. *Journal of Hydrology*, **267**(1-2), 65-74.

Nakicenovic, N., Alcamo, J., Davis, G., de Vries, B., Fenhann, J., & Gaffin, S. (2000). Special Report on Emissions Scenarios: A Special Report of Working Group III of the Intergovernmental Panel on Climate Change, Cambridge University Press, Cambridge, U.K., 599 pp. Available online at: http://www.grida.no/climate/ipcc/emission/index.htm.

National Land and Water Information Service. (2008). *Data*. Retrieved September 10, 2008 from http://www4.agr.gc.ca/AAFC-AAC/display-afficher.do?id=1226330737632&lang=eng

New, M.G., & Schulze, R.E. (1996). Hydrologic sensitivity to climate change in the Langriver catchment, Stellenbosch, South Africa and some implications for geomorphic processes. *Zeitschrift fur Geomorephologie*, **107**, 11-34.

New, M.G. (2002). Climate change and water resources in the southwestern Cape, South Africa. *South African Journal of Science*, **98,** 1-8.

Nogués-Bravo, D., Araujo, M.B., Errea, M.P., Martinez-Rica, J.P. (2007). Exposure of global mountain systems to climate warming during the 21st Century. *Global Environmental Change*, **17**(3-4), 420-428.

North Saskatchewan Watershed Alliance (NSWA). (2005). *State of the North Saskatchewan Watershed Report 2005 - A Foundation for Collaborative Watershed Management*. North Saskatchewan Watershed Alliance, Edmonton, Alberta. 202 pgs.

Parmesan, C., & Yohe, G. (2003). A globally coherent fingerprint of climate change impacts across natural systems. *Nature*, **421**, 37-42.

Penman, H.L. (1948). Natural evaporation from open water, bare soil and grass. *Proceedings of the Royal Society of London. Series A, Mathematical and Physical Sciences*, **193**(1032), 120-145.

Pentland, R. S., W. D. Hogg, George H. Taylor and AMEC, 2002. *Probable Maximum Flood - South Saskatchewan River Project.* Report for Sask Water. Moose Jaw, Saskatchewan.

Peters, T.W., & Bowser, W.E. (1960). Soil Survey Report No. 19: Soil Survey of the Rocky Mountain House Sheet. Canada Department of Agriculture, University of Alberta, Alberta. Pg 1-51.

Peters, T.W. (1981). Soil Survey Report No. 40: Reconnaissance soil survey of the Brazeau Dam area. Agriculture Canada, Land Resource Research Institute Branch, Ottawa, Ontario. Pg 1-68.

Pettapiece, W.W. (1971). Land Classification and soils in the Rocky Mountains of Alberta along the North Saskatchewan River Valley. Alberta Institute of Pedology, University of Alberta. Pg 1-40.

Pomeroy, J.W., & Dion, K. (1996). Winter radiation extinction and reflection in a boreal pine canopy: measurements and modelling. *Hydrological Processes*, **10**, 1591-1608.

Putkonen, J., & Roe, G. (2003). Rain-on-snow events impact soil temperatures and affect ungulate survival. Geophysical Research Letters, 30(4), 1188-1192.

Rahman, S., Munn, C.L., Zhang, R., & Vance, G.F. (1996). Rocky Mountain forest soils: Evaluating spatial variability using conventional statistics and geostatistics. *Canadian Journal of Soil Science*, **76**, 501-507.

Read, K. E., Hedges, P.D., & Fermor, P.M. (2008). Monthly Evapotranspiration Coefficients of Large Reed Bed Habitats in the United Kingdom. Wastewater Treatment, Plant Dynamics and Management in Constucted and Natural Wetlands. Springer Netherlands, 99-109.

Refsgaard, J. C., & Knudsen, J. (1996). Operational Validation and Intercomparison of Different Types of Hydrological Models. *Water Resources Research*, **32**(7), 2189–2202.

Refsgaard, J.C. (1997). Parameterisation, calibration and validation of distributed hydrological models. *Journal of Hydrology*, **198**, 69-97.

Reinelt, E. R. (1970). The role of orography in the precipitation regime of Alberta. *Albertan Geographer*, **6**, 45–58.

Rood, S.B., Samuelson, G.M., Weber, J.K., & Wywrot, K.A. (2005). Twentieth-century decline in streamflows from the hydrographic apex of North America. *Journal of Hydrology*, **306**(1-4), 215-233.

Rood, S.B., Pan, J., Gill, K.M., Franks, C.G., Samuleson, G.M., & Shepherd, A. (2008). Declining summer flows of Rocky Mountain rivers: Changing seasonal hydrology and probable impacts on floodplain forests. *Journal of Hydrology*, **349**(3-4), 397-410.

Rosenberg, N.J., B.A. Kimball, P. Martin, & C.F. Cooper. (1990). From climate and CO_2 enrichment to evapotranspiration. *In* Waggoner, P.E. (ed.) *Climate change and U.S. water resources*. John Wiley & Sons, New York, 151–175.

Rosso, R. (1994). An introduction to spatially distributed modelling of basin response. In: Rosso, R., Peano, A., Becchil, I., Bemporad, G.A. (Eds.), Advances in Distributed Hydrology. Water Resources Publications, pp. 3-30.

Sauchyn, D. & Kulshreshtha, S. (2008) Climate change impacts on Canada's Prairie Provinces: A summary of our state of knowledge, from "Prairies" in *From Impacts to Adaptation: Canada in a Changing Climate 2007*, edited by D. Lemmen et al., Government of Canada, Ottawa.

Saunders, I.R., & Byrne, J.M. (1995). Seasonal climate and climatic changes in the Canadian Prairies simulated by the CCC GCM. *Atmosphere-Ocean*, **33**(3), 621-641.

Schmidli, J., Goodess, C.M., Frei, C., Haylock, M.R., Hundacha, Y., Ribalaygua, J., & Schmith, T. (2007). Statistical and dynamical downscaling of precipitation: an evaluation and comparison of scenarios for the European Alps. Journal of Geophysical Research, **112**:D04105.

Schmidt, E.J., & Schulze, R.E. (1987). Flood volume and peak discharge from small catchments in southern Africa, based on the SCS technique. *Water Resource Commission*, Pretoria, *Technical Transfer Report* TT/3/87. pp. 164.

Schulze, R.E. (1995). *Hydrology and Agrohydrology: a text to accompany the ACRU 3.00 agrohydrological modelling system*. Report TT69/95. Water Research Commission, Pretoria, RSA.

Schulze, R.E., Smithers, J.C., Lynch, S.D., & Lecler, N.L. (1995). Obtaining and interpreting output from ACRU. In: Smithers, J.C. and Schulze, R.E. *ACRU Agrohydrological Modelling System: User Manual Version 3.00*. Water Research Commission, Pretoria, Report TT70/95. Pp AM7-1 to AM7-21.

Schulze, R.E. (2000). Modelling hydrological responses to land use and climate change: a South African perspective. *AMBI*, 29(1), 12-22.

Schulze, R.E., Lorentz, S., Kienzle, S.W., & Perks, L. (2004). Modelling the impacts of land-use and climate change on hydrological responses in the mixed underdeveloped / developed Mgeni catchment, South Africa. In: Kabat, P. et al. (Eds.): Vegetation, Water, Humans and the Climate A New Perspective on an Interactive System. BAHC-IGBP Publication, Springer, 17pp, with 14 Figures and 2 tables.

Shea, J.M., & Marshall, S.J. (2007). Atmospheric flow indices, regional climate, and glacier mass balance in the Canadian Rocky Mountains. *International Journal of Climatology*, **27**(2), 233-247.

Shea, J. M., Moore, R. D., & Stahl, K. (2009). Derivation of melt factors from glacier mass balance records in western Canada. *Journal of Glaciology*, **55**(189), 123-130.

Smith, C. D. (2009). The relationship between monthly precipitation and evelvation in the Canadian Rocky Mountain Foothills. Pages In: *Proceedings from the Western Snow Conference*, Canmore, Canada, 20-23 April 2004, pp. 37-46.

Stanhill, G. (2002). Is the Class A evaporation pan still the most practical and accurate meteorological method for determining irrigation water requirements? *Agriculture and Forest Meteorology*, **112**(3-4), 233-236.

Stewart, I.T., Cayan, D.R., & Dettinger, M.D. (2005). Changes toward earlier streamflow timing across western North America. *Journal of Climate*, **18**, 1136-1155.

Strong, W.L., & La Roi, G.H. (1983). Root-system morphology of common boreal forest trees in Alberta, Canada. *Canadian Journal of Forest Research*, **13**, 1164-1173.

Storck, P., Lettenmaier, D.P. & Bolton, S.M. (2002). Measurement of snow interception and canopy effects on snow accumulation and melt in a mountainous maritime climate, Oregon, United States. *Water Resources Research*, **38**, 1223-1231.

Tetens, O. (1930). Über einige meteorologische Begriffe. *Z. Geophys.*, **6**, 297-309.

Töyrä, J., Pietroniro, A., & Bonsal, B. (2005). Evaluation of GCM simulated climate over the Canadian Prairie Provinces. *Canadian Water Resources Journal*, **30**(3), 245-262.

TransAlta. (2009). Our Plants. Retrieved April 25, 2009, from http://www.transalta.com

United States Department of Agriculture. (1985). National Engineering Handbook, Section 4, Hydrology. USDA Soil Conservation Service, Washington DC, USA.

Van Zyl, W.H., De Jager, J.M., & Maree, C.J. (1989). Correction factors for evaporimeter coefficients used for scheduling irrigation of wheat. *Water Research Commission*, Pretoria. *Report* 151/1/89. pp 155

Visscher, D., Frair, J., Fortin, D., Beyer, H., & Merrill, E. (2004). Spatial-temporal dynamics of elk forages in the central east slopes elk study area. In: Beyer, H., Frair, J., Visscher, D., Fortin, D., Merrill, E., Boyce, M., Allen, J. eds. , Vegetation map and dynamics of elk forage for the central east slopes elk and wolf study, Department of Biological Sciences, University of Alberta, Edmonton, Alberta, Canada, pp 15-60.

Von Storch, H., Zorita, E., Cubasch, U. (1993). Downscaling of global climate change estimates to regions scales: an application to Iberian winter rainfall. *Journal of Climate*, **6**, 1161-1171.

Wilby, R.L., Hay, L.E., & Leavesley, G.H. (1999). A comparison of downscaled and raw GCM output: implications for climate change scenarios in the San Juan River basin, Colorado. *Journal of Hydrology*, **225**(1-2), 67-91.

Winkler, R.D., Spittlehouse, D.L. & Golding, D.L. (2005). Measured differences in snow accumulation and melt among clear-cut, juvenile, and mature forests in southern British Columbia. *Hydrological Processes*, **19**, 51-62.

WGMS. (2009). *Glacier Mass Balance Bulletin* No. 10 (2006-2007). Haeberli, W., Gärtner-Roer, I., Hoelzle, M., Paul, F. and Zemp, M. (eds.), ICSU(WDS)/IUGG(IACS)/UNEP/UNESCO/WMO, World Glacier Monitoring Service, Zurich, 96 pp.

Xu, C.Y. (1999a). From GCMs to river flow: a review of downscaling methods and hydrologic modelling approaches. *Progress in Physical Geography*, **23**(2), 229-249.

Xu, C.Y. (1999b). Operational testing of a water balance model for predicting climate change impacts. *Agriculture and Forest Meteorology*, **98**, 295-304.

Young, G.J. (1991). Hydrological interactions in the Mistaya basin, Alberta, Canada. *Snow, hydrology and Forests in High Alpine Areas (Proceedings of the Vienna Symposium)*. No. 205: 237-244.

Yue, S., Pilon, P., Phinney, B., & Cavadias, G. (2001). Patterns of trend in Canadian streamflow. Pages In: *Proceedings of the 58th Eastern Snow Conference.* Ottawa, Ontario, Canada, May 2001, pp. 1-12.

Zhang, K., Kimball, J.S., Mu, Q., Jones, L.A., Goetz, S.J., & Running, S.W. (2009). Satellite based analysis of northern ET trends and associated changes in the regional water balance from 1983 to 2005. *Journal of Hydrology*, **379**, 92-110.

Zhang, X., Vincent, L.A., Hogg, W.D., & Niitsoo, A. (2000). Temperature and precipitation trends in Canada during the 20th century. *Atmosphere-Ocean*, **38**, 395-429.

Zhang, X.B., Harvey, K.D., Hogg, W.D., & Yuzyk, T.R. (2001). Trends in Canadian streamflow. *WaterResources Research,* **37**(4), 987-998.